

UNIVERSITY OF NAPLES FEDERICO II



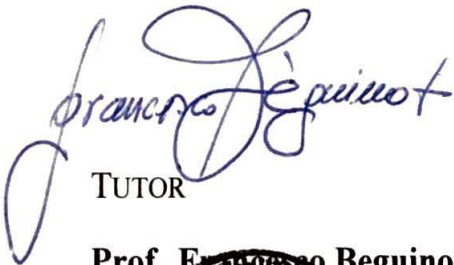
PH.D. PROGRAM IN
CLINICAL AND EXPERIMENTAL MEDICINE
CURRICULUM IN TRANSLATIONAL MEDICAL SCIENCES

XXX Cycle
(Years 2014-2017)

Chairman: Prof. Gianni Marone

PH.D. THESIS

EPIGENETIC SILENCING OF *ANKRD26* GENE
CONTRIBUTES TO ADIPOSE TISSUE INFLAMMATION
IN OBESITY


TUTOR

Prof. Francesco Beguinot



PH.D. STUDENT

Dr. Rosa Spinelli

**Epigenetic Silencing of *Ankrd26* Gene Contributes to
Adipose Tissue Inflammation in Obesity**

TABLE OF CONTENTS

	Page
LIST OF PUBLICATIONS	1
ABSTRACT	3
1 BACKGROUND	4
1.1 Obesity	4
1.2 Biology and pathophysiology of obesity	7
1.2.1 Adipose Tissue	7
1.2.2 Genetic of obesity	12
1.2.3 Epigenetics: gene-environment interactions in obesity	15
1.3 Epigenetics	19
1.3.1 Epigenetic modifications	20
1.3.2 DNA Methylation	22
1.3.3 DNA Methylation and obesity	24
1.4 <i>ANKRD26</i> gene	27
1.4.1 <i>ANKRD26</i> as a candidate (<i>epi</i>)gene for obesity	29
2 AIMS OF THE STUDY	32
3 MATERIALS AND METHODS	33
3.1 Animal study, diet protocols and metabolic tests	33
3.2 Western blotting analysis	33
3.3 Real Time PCR (qPCR)	34
3.4 Methylated DNA Immunoprecipitation (MeDIP)	34
3.5 Bisulfite sequencing	35
3.6 Cloning strategy, site-direct mutagenesis and <i>in vitro</i> methylation	35
3.7 Luciferase assay	35
3.8 Chromatin Immunoprecipitation and Micrococcal Nuclease assays	36
3.9 Electrophoretic mobility shift assay (EMSA)	36
3.10 Primer sequences	37

3.11 Cell culture and transfection	38
3.12 Fatty Acid/BSA complex solution preparation	39
3.13 Patient enrollment and tests	39
3.14 Statistical analysis	40
4 RESULTS	41
4.1 Animal study design	41
4.2 Metabolic characteristics of standard and high fat diet mice	41
4.3 Effect of HFD on Ankrd26 gene expression in visceral adipose tissue	42
4.4 Effect of HFD on DNA methylation at Ankrd26 promoter	45
4.5 Role of free fatty acids on epigenetic regulation of Ankrd26 gene	47
4.6 Methylation of specific CpG sites controls Ankrd26 gene expression	48
4.7 DNA methylation suppresses Ankrd26 promoter activity by impairing the binding of co-activator/acetyltransferase p300	49
4.8 HFD-induced differential recruitment of DNMTs and MBD2 initiates the repression and silencing of Ankrd26 gene	52
4.9 HFD increases nucleosome occupancy at the Ankrd26 promoter	53
4.10 HFD changes histone acetylation and RNA Pol II binding at the Ankrd26 promoter	54
4.11 <i>Ankrd26</i> silencing induces a pro-inflammatory cytokine profile in cultured adipocytes	55
4.12 <i>ANKRD26</i> expression negatively correlates with BMI and inflammatory markers in obese subjects	57
5 DISCUSSION	59
6 CONCLUSION	62
7 REFERENCES	63
ACKNOWLEDGEMENTS	71

LIST OF PUBLICATIONS

(Years 2014-2017)

The Thesis is based on the following publications:

1. Raciti GA*, **Spinelli R***, Desiderio A, Longo M, Parrillo L, Nigro C, D'Esposito V, Mirra P, Fiory F, Pilone V, Forestieri P, Formisano P, Pastan I, Miele C, Beguinot F. Specific CpG hyper-methylation leads to Ankrd26 gene down-regulation in white adipose tissue of a mouse model of diet-induced obesity. *Sci Rep*. 2017 Mar 7;7:43526. doi: 10.1038/srep43526. ***The authors These authors contributed equally to this work.**

2. Desiderio A, **Spinelli R**, Ciccarelli M, Nigro C, Miele C, Beguinot F, Raciti GA. Epigenetics: spotlight on type 2 diabetes and obesity. *J Endocrinol Invest*. 2016 Oct;39(10):1095-103. doi: 10.1007/s40618-016-0473-1.

3. Parrillo L, Costa V, Raciti GA, Longo M, **Spinelli R**, Esposito R, Nigro C, Vastolo V, Desiderio A, Zatterale F, Ciccodicola A, Formisano P, Miele C, Beguinot F. Hoxa5 undergoes dynamic DNA methylation and transcriptional repression in the adipose tissue of mice exposed to high-fat diet. *Int J Obes (Lond)*. 2016 Jun;40(6):929-37. doi: 10.1038/ijo.2016.36.

Other publications:

4. Longo M, Raciti GA, Zatterale F, Parrillo L, Desiderio A, **Spinelli R**, Hammarstedt A, Hedjazifar S, Hoffmann JM, Nigro C, Mirra P, Fiory F, Formisano P, Miele C, Smith U, Beguinot F. Epigenetic modifications of the *ZNF423* gene control adipogenic commitment and are dysregulated in murine adipocytes and human hypertrophic obesity.

5. Fiory F, **Spinelli R**, Raciti GA, Parrillo L, D'Esposito V, Formisano P, Miele C, Beguinot F. Targeting PED/PEA-15 for diabetes treatment. *Expert Opin Ther Targets*. 2017 Jun;21(6):571-581. doi: 10.1080/14728222.2017.1317749. Epub 2017 Apr 21. Review. PubMed PMID: 28395542. Accepted for publication in *Diabetologia*.

6. Longo M*, **Spinelli R***, D'Esposito V, Zatterale F, Fiory F, Nigro C, Raciti GA, Miele C, Formisano P, Beguinot F, Di Jeso B. Pathologic endoplasmic reticulum stress induced by glucotoxic insults inhibits adipocyte differentiation and induces an inflammatory phenotype. *Biochim Biophys Acta*. 2016 Jun;1863(6 PtA):1146-56. doi: 10.1016/j.bbamcr.2016.02.019. ***The authors These authors contributed equally to this work.**

7. D'Esposito V, Liguoro D, Ambrosio MR, Collina F, Cantile M, **Spinelli R**, Raciti GA, Miele C, Valentino R, Campiglia P, De Laurentiis M, Di Bonito M, Botti G, Franco R, Beguinot F, Formisano P. Adipose microenvironment promotes triple negative breast cancer cell invasiveness and dissemination by producing CCL5. *Oncotarget*. 2016 Apr 26;7(17):24495-509. doi: 10.18632/oncotarget.8336.

8. Borriello F, Longo M, **Spinelli R**, Pecoraro A, Granata F, Staiano RI, Loffredo S, Spadaro G, Beguinot F, Schroeder J, Marone G. IL-3 synergises with basophil-derived IL-4 and IL-13 to promote the alternative activation of human monocytes. *Eur J Immunol*. 2015 Jul;45(7):2042-51. doi: 10.1002/eji.201445303.

ABSTRACT

Environmental factors interact with the genome to influence gene expression, tissue function and also disease risk. External stimuli may affect the phenotype through epigenetic mechanisms that provide an interface with the genome. Indeed, epigenetic modifications represent a mechanism through which both genetic and environmental cues, including dietary factors, are integrated at specific genomic loci and affect individual phenotypes, contributing to susceptibility to obesity and type 2 diabetes. Recently, alterations of *Ankyrin repeat domain 26* (*Ankrd26*) gene expression and function have been associated with the onset of these metabolic disorders. However, whether external cues can affect its expression remains unclear. Therefore, the aim of this study is to evaluate whether the administration of a high fat diet (HFD) in mice could affect *Ankrd26* expression and function, and whether chromatin remodeling and epigenetic modifications take part in this regulation. Particularly, I examined the correlation between obesity and inflammation with defective regulation of *Ankrd26* gene in visceral adipose tissue (VAT) depots, aiming at identifying epigenetic mechanism that might underpin the development of VAT dysfunctions induced by overnutrition. Using the HFD-induced obesity mouse model, I reported evidence of detailed epigenetic changes of *Ankrd26* promoter. Indeed, I demonstrated that the HFD-induced *Ankrd26* down-regulation in VAT was directly caused by specific hyper-methylation of -436 and -431 cytosine residues at its promoter region, that was followed by chromatin reorganization. Indeed, DNA methylation of these specific CpG sites impaired binding of the histone acetyltransferase/transcriptional coactivator p300 to this region, both *in vitro* and *in vivo*, causing hypo-acetylation of histone H4 at the *Ankrd26* promoter and loss of binding of RNA Pol II at the *Ankrd26* Transcription Start Site in obese mice. Furthermore, the HFD treatment increased binding of DNA methyl-transferases 3a and 3b and methyl-CpG-binding domain protein 2 to the *Ankrd26* promoter. To evaluate the functional consequences of these changes, the HFD-induced *Ankrd26* down-regulation was mimicked by silencing *Ankrd26* gene expression *in vitro* in 3T3-L1 adipocytes. This silencing caused enhanced secretion of the pro-inflammatory chemokines KC/IL-8, Eotaxin, MCP1 and Rantes. The relevance of these observations to humans is supported by other findings in obese individuals, revealing that the reduction of *ANKRD26* expression in VAT negatively correlates with serum concentrations of inflammatory markers. Taken together, my data provide evidence for environmentally induced DNA changes at *Ankrd26* promoter and, for the first time, highlight a role for *Ankrd26* epigenetic silencing in raising and/or sustaining VAT inflammation following unhealthy dieting and in development of obesity-related insulin resistance. Since direct evidence linking specific environmental cues and metabolic disorders are still limited, addressing this issue will provide new insight into the molecular basis of obesity as well as create novel translational perspective.

1. BACKGROUND

1.1 Obesity

Obesity, considered by the World Health Organization (WHO) as a 21st century global epidemic [1], is defined as excessive adiposity in relation to lean mass throughout the body, that is usually accompanied by mild, chronic, systemic inflammation [2]. The current classification of overweight and obesity in adults is based on the body mass index (BMI) [3,4]. BMI is an indirect measure of body fat, equals an individual's weight in kilograms, divided by the square of height in meters (kg/m^2). According to WHO classification [3], overweight is defined as a BMI of 25 or more, and includes pre-obesity (25-29.9), and obesity that is divided into three categories: Class I (30–34.9), Class II (35–39.9) and Class III (>40) [5]. High BMI is an important risk factor for cardiovascular and kidney diseases, diabetes, some cancers, and musculoskeletal disorders. Concerns about the health and economic burden of increasing BMI have led to adiposity being included among the global non-communicable diseases, with a target of halting, by 2025, the rise in the prevalence of obesity at its 2010 level [1].

Increased fat deposition, according to a simplistic view based on the first law of thermodynamics, results from an imbalance between the caloric intake and energy expenditure, driven by the consumption of high-energy-yielding foods above the needs of the individual and a sedentary lifestyle [6]. However, the etiology of obesity is more complex. Indeed, circumstances such as socioeconomic status, environment and personal behaviors, and genotype–phenotype interactions have to be taken into account to understand obesity, as all these factors affect food intake, nutrient turnover, thermogenesis, lipid utilization, and also differential fat storage in regional adipose depots versus non-adipose tissues [2]. Multiple and complex mechanisms have evolved to regulate energy intake and expenditure and fat deposition to maintain body weight [7]. Several cues affect these regulatory processes: environmental factors, diet quality, level of physical activity, the gut microbiota, endocrine disruptors, drugs, reproductive factors and assortative mating, intrauterine and epigenetic intergenerational effects (fig. 1) [2]. Another problem concerning the obesity study and management is the marked heterogeneity of individuals with obesity. Examples of obesity types are subcutaneous obesity, in which excess subcutaneous fat is found around the hip and thigh areas, and visceral obesity, in which fat is mainly accumulated in the abdominal region. Visceral obesity is more common in men and tends to be more pernicious in health terms [2]. However, different strategies and treatments at the individual level have been developed and prescribed: dietary education and control, physical activity programs, pharmacological treatments and bariatric surgery.

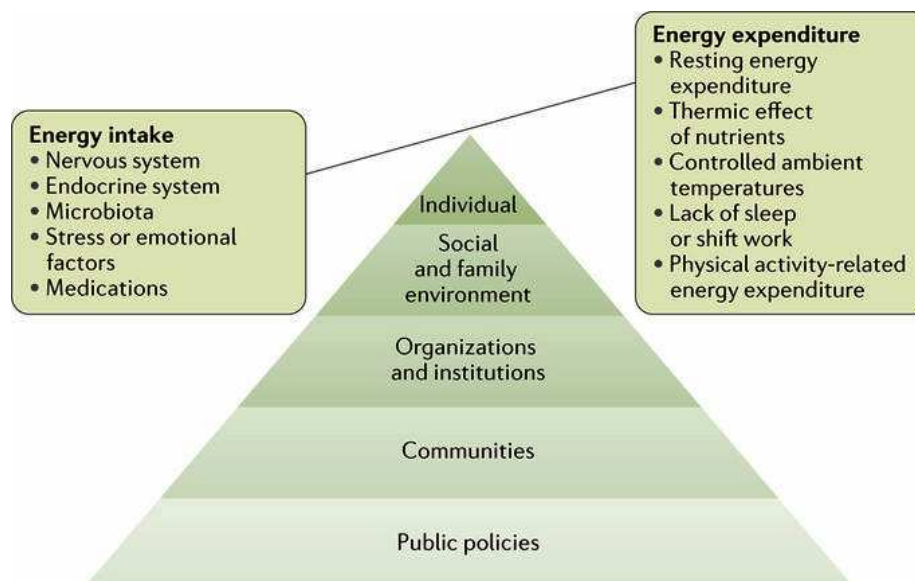


Figure 1. Key factors involved in the regulation of energy balance. The energy balance is influenced by several biological factors. The pyramid holding the balance emphasizes the notion that we need to go beyond individual factors to ultimately have an optimal effect on the energy balance equation. Nat Rev Dis Primers. 2017; 3:17034.

Actually, 39% of the world population is obese or overweight, despite decades of efforts to slow the progress of the epidemic. According to the WHO, >2.1 billion adults were overweight or obese globally in 2014, of which 1.5 billion were overweight and 640 million were obese [3]. In the same year, the age-standardized prevalence of obesity in 2014 was estimated to 10.8% among adult men and 14.9% among adult women. These data suggest that female sex is associated with higher risk of obesity [1]. Furthermore, several studies conducted in the United States, indicate that African Americans exhibited a higher prevalence of extreme obesity than other ethnicities [8]. Asian populations have lower BMI than white individuals, but they have been shown to be prone to visceral fat deposition, making this populations more susceptible to developing T2D at lower BMI than white individuals [9]. Although the prevalence of obesity is likely to increase as the population ages dramatically in coming years [10], in 2013–2014, the worldwide number of children and adolescents with obesity has doubled since 1980 and was estimated to be 110 million [2]. Childhood and adolescence obesity has been associated with metabolic complications and chronic disease in adulthood.

Critical windows in the onset of obesity have been identified in the prenatal period, infancy, childhood and adolescence. The programming of metabolism during the prenatal and neonatal periods at both the genomic and epigenomic level (metabolic imprinting) might permanently influence future disease risk and health, according to the developmental origins of health and disease hypothesis [11,12]. Indeed, it has been shown in literature that the type and amount of energy-yielding nutrients consumed by the mother during pregnancy and lactation, and even by both parents before pregnancy, is associated with the development of metabolic

complications in adulthood [13,14]. Also, an earlier adiposity during childhood has been associated with a high BMI, a high amount of subcutaneous adipose tissue and a high waist circumference in adulthood [15].

State-of-the-art epidemiological approaches, such as integrated bioinformatics system analyses, need to be used to better understand the causes of obesity, including the complex interplay between behavioral, environmental, physiological, genetic, social and economic factors.

Several biological and environmental factors have an effect on energy intake and expenditure (fig. 1). For example, eating behaviors are determined not only by genetic factors and other biological factors but also by the opportunities to eat and food availability. The food choices among energy-yielding food is enormous. Physical activity, another behavioral component, is also conditioned by socioeconomic and cultural factors. An increasing trend toward sedentary lifestyles coupled with increases in energy intake is able to explain the observed enhancement in mean BMI in high-income countries, but also probably in most low- and middle-income countries [16]. In addition to the amount of calories, the type and quality calorie, such as saturated versus non-saturated lipids, as well as the source of fats, carbohydrates and proteins also affects the energy balance and body weight [17]. However, this area is still controversial; indeed, whether the caloric overload with the diet or the impact of a particular nutrient by a direct metabolic effect, is important in obesity development, is unclear [18]. A high-quality dietary intake, defined by a balanced consumption of macronutrients, is inversely associated with weight gain and the risk of developing obesity. Several lines of evidence support the importance and benefits of consuming health meals and high-quality, sustainable dietary regimens in preventing obesity [19,20].

Obesity prevention should focus on maintaining weight loss or controlling excessive weight gain. In general, the preventive strategies are health promotion programs or marketing, addressing lifestyle behaviors and policies that target the environment. At the population level, public policies and economical strategies are needed to improve food and physical environments, the food system and the health system to control the global obesity epidemic. The complexity of obesity requires multilevel approaches by acting on multiple frameworks: in practice, going from the individual, often children or adolescents, schools or occupational environments and the communities. Drugs, such as amphetamines, methamphetamine and phenmetrazine, are approved by the US FDA for short-term treatment (usually <12 weeks) of the patient with obesity for the treatment of obese patients, as adjuncts to diet and exercise [21]. Use of bariatric surgery has become rapidly adopted for the treatment of severe obesity, and this has increased with the reduction of laparoscopic procedure risk [21]. Several studies have reported improvements in biochemical and metabolic outcomes following bariatric surgery. Mortality was reduced by 24%, mainly by reducing the risk of myocardial infarction and, in women, cancer, and many other comorbidities, such as T2D are also ameliorated [22].

To improve prevention and treatment strategies, a better knowledge of factors

contributing to the development of obesity is essential. A deeper understanding of appetite and energy expenditure, as well as the physiopathological role of adipose tissue in the regulation of metabolic function is needed. In this regard, the role of genetics, epigenetics, nutrigenomics or personalized nutrition is crucial to be better understood to improve obesity management.

1.2 Biology and pathophysiology of obesity

Being a complex and heritable disorder, obesity results from the interplay between genetic susceptibility, epigenetics, metagenomics and the environment. These factors act through physiological mediators of food intake and energy expenditure, affecting fat deposition [2].

1.2.1 Adipose Tissue

Adipose tissue is a complex organ with profound effects on physiology and pathophysiology. This tissue has a central role in the regulation of energy balance and nutritional homeostasis, serving as site of calorie storage after feeding and as source of circulating mediators, by which critical metabolic processes are coordinated locally and systemically [23]. The mammalian adipose tissues have been divided into two major types: the white adipose tissue (WAT) and brown adipose tissue (BAT), that are functionally involved in sensing and responding to changes in systemic energy balance [2,23]. Brown adipocytes contribute to energy expenditure via thermogenesis to maintain body temperature. BAT is the site of adaptative thermogenesis, providing extra heat in hibernating animals, cold-exposed mammals and human newborns (cold-induced thermogenesis), as well as maintaining energy balance in response to diet (diet-induced thermogenesis). The brown fat depots are abundant in newborn babies and are located in the interscapular and supraclavicular regions, as well as around the several organs; these depots decrease with age, but can still be found in adults [24,25]. Although BAT has been negatively correlated with the BMI [25], its role in the etiology of obesity is still unclear. White adipocytes are the most abundant adipocytes in humans. The main functions of WAT are: *i.* to store calories as lipid droplets after feeding; *ii.* to release free fatty acids during fasting; and, *iii.* to cushion body parts exposed to high levels of mechanical stress [23]. However, recent research has revealed that white adipocytes synthesize and secrete various bioactive mediators, hormones and cytokines (adipocytokines) such as leptin, interleukin 6 (IL6), adiponectin, monocyte chemoattractant protein 1 (MCP1) and tumor necrosis factor alpha (TNF α), required for the regulation of metabolic processes, such as glucose and lipid metabolism, insulin sensitivity, feeding behavior, inflammation, immunity, angiogenesis and blood pressure (fig. 2) [23,26].

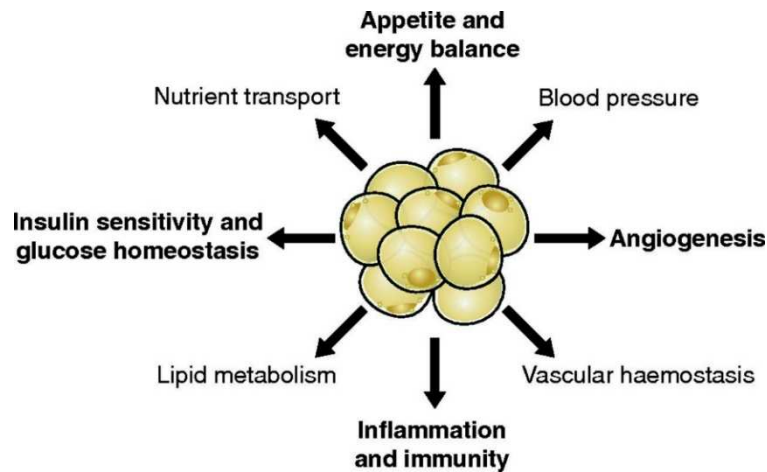


Figure 2. Physiological and metabolic processes regulated by adipocyte-secreted mediators. The interactions may be autocrine, paracrine, or endocrine. *Physiol Rev.* 2013; 93(1):1-21.

Intracellular WAT lipid homeostasis is a key determinant of body weight and insulin sensitivity both in mice and humans. Excessive lipid load causes adipocyte stress, which in turn accounts for many adverse effects of obesity, particularly alterations in adipocytokine release and a low-grade inflammatory response, ultimately leading to the development of metabolic dysfunction such as insulin resistance and glucose intolerance. Due to their critical role in the maintenance of proper adipocyte function, both storage and release of lipids in WAT are physiologically under tight hormonal control [27].

WAT develops in multiple discrete and specific depots [23]. Based on their anatomic locations, the most common classification distinguishes between subcutaneous adipose tissue (SAT) and visceral adipose tissue (VAT) [2,23]. SAT accumulates more than 80% of total body fat in the body and is located beneath the skin. VAT include intra-abdominal (mainly mesenteric adipose tissue), perirenal and pericardial adipose tissue and comprises less than 10% of the total fat mass. However, the visceral versus subcutaneous scheme is oversimplified. In addition, many depots in human have no precise correlation in mice, an vice versa. A large percentage of VAT in humans is contained in the omentum, which is scarcely present in rodents; conversely, the large epididymal adipose tissue (eAT), representative of VAT in mice, does not exist in humans [23].

Subcutaneous and visceral adipose depots are very different in terms of their effects on metabolism [28]. In mice, transplantation of subcutaneous fat into the visceral depot of recipient mice caused improvements in glucose homeostasis as well as decreased body weight and fat mass; conversely, placing visceral fat into a subcutaneous depot of recipient mice, had very little effect [29]. In human, peripheral obesity is characterized by an accumulation of SAT and is more frequent in women. This type of obesity is not associated with an increased risk of related pathologies. However, central or abdominal obesity is more common in men and consists of an accumulation of VAT [28]. This type of obesity has been associated, through epidemiological studies, with a higher risk of diseases such as insulin

resistance, T2D and hypertension [28], and is closely correlates with the development of the various metabolic abnormalities, commonly referred to as the metabolic syndrome [2].

Adipose tissue has the unique attribute of remodeling, by changing its dimensions in response to nutritional demands. Adipose tissue remodeling can be accomplished by increasing the size of cells (hypertrophy) or by recruiting new adipocytes from the resident pool of precursor cells (hyperplasia). In response to caloric overload, adipose depots expand first by hypertrophy until a critical threshold is reached. The hypertrophy is followed by cell death and by secretion of several mediators, that increase the proliferation and/or differentiation of preadipocytes [23]. This cycling between hypertrophy and hyperplasia as obesity progresses is supported by rodent studies indicating that eAT, along with other murine VAT depots, responds to high-fat diet (HFD) feeding through different time-dependent changes, contributing to the inflammatory and metabolic complications in obesity [30,31]. It has been demonstrated that upon short-term HFD exposure (8-12 weeks), the eAT expansion is accompanied by hypertrophy. However, after a more prolonged exposure (20 weeks), the eAT is characterized by an increased rate of adipocyte dying (up to 80%), paralleled by enhanced adipogenesis, so that the fat mass continues to expand as obesity progresses [23,30,31]. Emerging evidence in literature indicates a role for the microenvironment and the transient local inflammation in triggering the adipose tissue remodeling in the context of hyperplastic expansion [30]. Remarkably, the observation that obesity can be associated with adipocyte hyperplasia has been supported by findings showing that manipulation of several genes causes obesity *in vivo* and increases adipogenesis *in vitro*. The increased adipogenesis is not the primer driver of obesity in these *in vivo* models: the overnutrition is the culprit and the adipogenesis is induced by the need to store excess calories (fig.3) [23].

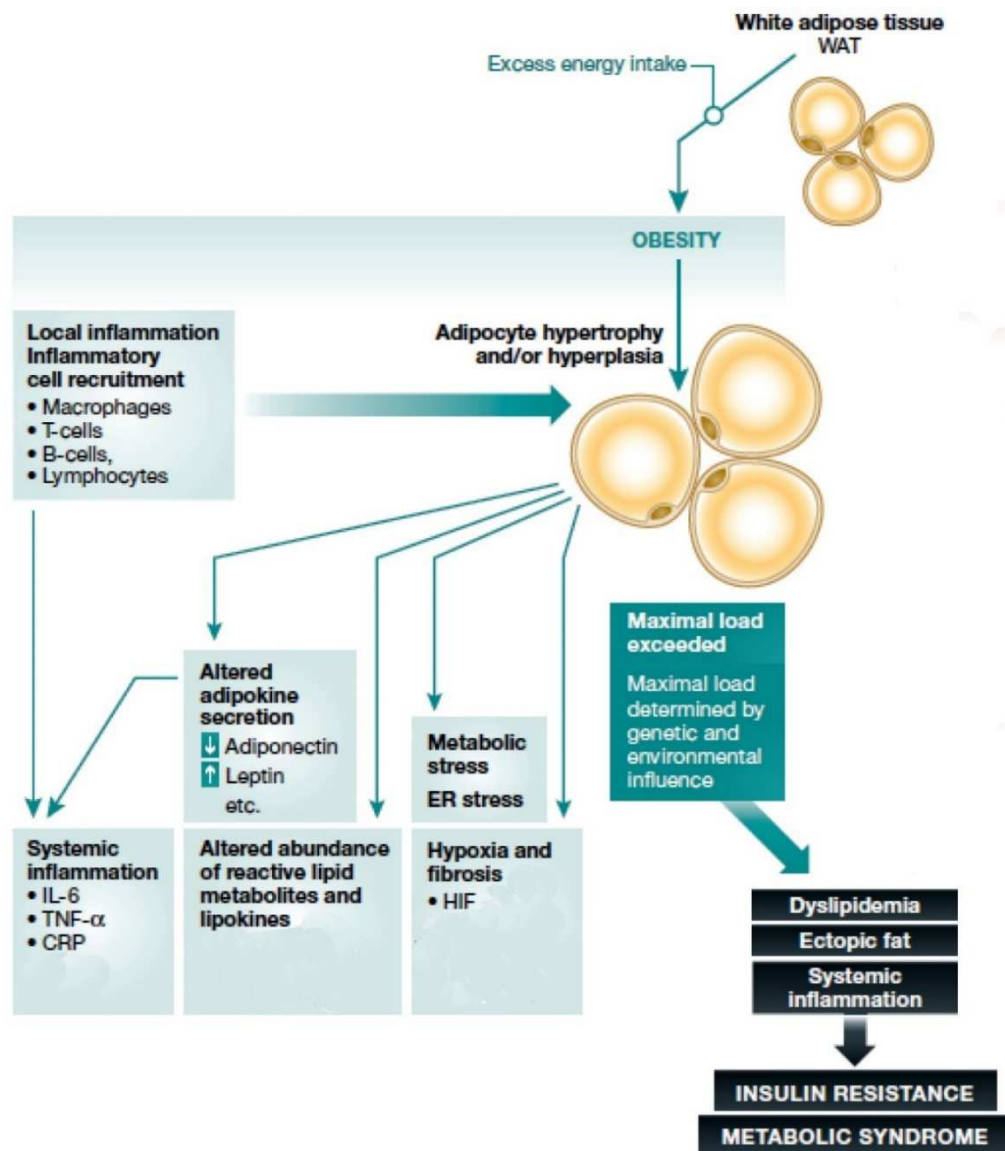


Figure 3. Obesity in light of the adipose tissue expandability hypothesis. Obesity is caused by adipose tissue dysfunction due to insufficient storage capacity, and this results in dyslipidemia, systemic inflammation and altered adipokine profiles. Combination of these factors promotes the development of insulin resistance and the metabolic syndrome, which further impairs adipose tissue function, creating a futile cycle. HIF, hypoxia-inducible factor; IL-6, interleukin-6; TNF- α , tumor necrosis factor- α ; CRP, C-reactive protein. Adapted from EMBO J. 2017; 36(14):1999-2017.

Although it is difficult to translate findings from rodents when examining visceral (epididymal) and subcutaneous (inguinal) fat, consistent evidence in humans shows that the number and severity of health complications, associated with obesity, seem to be dependent on the additional presence of excess fat stored in the VAT depots and in and around lean tissues, such as the heart, the liver and the kidneys (ectopic fat deposition) [23,32]. Also in humans, the number of adipocytes depends on the balance between cell death and adipogenesis. Adipocyte progenitors have been recently identified *in vivo* as immature mesenchymal stromal cells associated with the vasculature. The turnover rate in adult humans

has been estimated at 10% per year and, in any case, the size of fat depots correlates with the number of adipocytes [33]. Importantly, obese individuals have higher total adipocyte numbers, and this becomes evident already in childhood obesity [34]. Human studies focusing on adipose tissue cellularity have demonstrated a marked fat depot-specificity of the hyperplastic response to the diet. Indeed, increased adipocyte number has been detected in the femoral subcutaneous fat depot in humans but not in the upper abdominal subcutaneous depot [35]. As above mentioned, in male mice, higher rate of proliferation/adipogenesis has been shown in the intraabdominal gonadal fat depot but not in the posterior subcutaneous depot [30,31,33]. These differences can have substantial impact on the systemic adaptation of metabolism given the pathophysiological relevance of the individual depots. Accumulation of fat in the intra-abdominal/visceral depots is a central feature of the metabolic syndrome and is associated with insulin resistance and increased risk for diabetes and cardiovascular disease. Conversely, higher subcutaneous fat mass is associated with improved metabolic parameters including insulin sensitivity and blood lipid profiles. Taken together, location specific hyperplastic expansion of adipose tissue can affect body fat distribution, contribute to systemic metabolic homeostasis and influence pathogenesis [33]. Furthermore, *Lotta et al.* [36] have identified a genetic association of 53 loci with traits related to insulin resistance, T2D and coronary heart disease. Remarkably, genetic predisposition for insulin resistance predicted by these loci was associated with reduced fat deposition in peripheral “metabolically safe” depots. Moreover, the same study revealed common links to insulin resistance associated with lipodystrophy, highlighting the importance of adipose tissue function for maintenance of systemic homeostasis [36].

Taken together, these observations emphasize the role of adipose tissue depots as key checkpoints in systemic energy homeostasis. The way by adipose tissue depots manages the excess calories and the oxygen tension generated by the pathological growth of the adipocytes impacts on individual's cardiometabolic risk, insulin sensitivity and dyslipidemia [32,37]. When the SAT responds to energy excess by fat cell hyperplasia, acting as a ‘metabolic sink’, lean tissues are protected against ectopic fat deposition. Conversely, if SAT cannot properly expand through hyperplasia, the stored triglycerides drive adipocyte hypertrophy until these enlarged fat cells become saturated, leading to either death and macrophage invasion and/or increased release of pro-inflammatory adipokines. These phenomena determine a pro-inflammatory and insulin-resistant milieu in inner adipose depots [35]. Furthermore, the excess triglyceride molecules, that have no place in the SAT, will be ectopically stored contributing to an atherogenic, diabetogenic and inflammatory environment in the cell [23,37]. By comparison, increased risk of metabolic dysfunction, as obesity, is associated with expansion of the omentum and increased deposition of fat in the liver, heart and kidneys (fig.4) [38]. However, more complex scenarios are also plausible, because genetic and environmental factors may influence the individual's regional adipose tissue accumulation capacity.

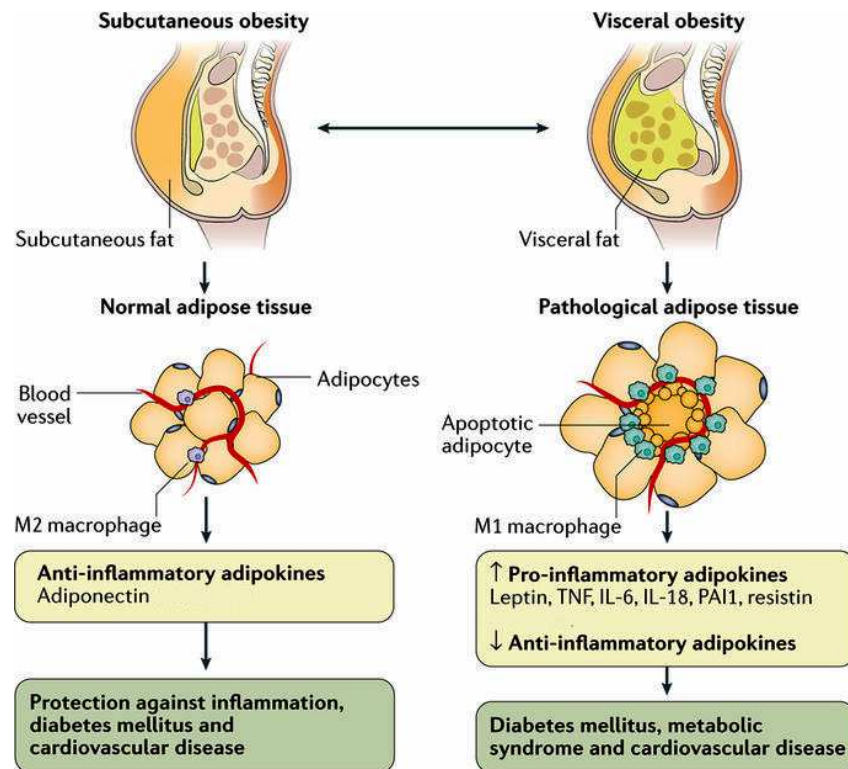


Figure 4. Pathological changes in adipose tissue. The value of visceral fat area correlated with the risk of obesity-associated complications. Adipose tissues in subcutaneous fat obesity might function normally with the expected release of anti-inflammatory adipokines, whereas adipose tissues in visceral fat obesity is increased the secretion of pro-inflammatory adipokines and suppressed the secretion of anti-inflammatory adipocytokines, raising and sustaining the low-grade inflammation, which contributes to obesity-related disorders. Pathological changes in visceral adipose tissue show higher levels of adipocyte necrosis and the recruitment of macrophages with an inflammatory phenotype (M1 macrophages). IL-6, interleukin-6; TNF, tumour necrosis factor; PAI1, prothrombin activator inhibitor 1. Adapted from Nat Rev Dis Primers. 2017; 3:17034.

1.2.2 Genetic of obesity

Genetic factors contribute to obesity-susceptibility, with heritability estimates ranging between 40 and 70% across populations [2,39,40]. The evidence for genetic component of BMI/overall obesity is substantial and come from a variety of population, family and twin-based studies [41]. In 1894, for the first time, Sir Francis Galton reported the familial aggregation of body size [42]. Since then, family history of obesity has become a well-established risk factor for childhood obesity [43]. The ethnic dependent pattern of obesity prevalence further supports an important contribution of genes in obesity heritability [43]. Furthermore, twin studies have shown that monozygotic twins display more similar body fat acquisition in comparison with dizygotic twins, indicating that this trait is highly influenced by the genotype [43,44]. Moreover, adoption studies confirm the genetic component of obesity, as the BMI of adopted children correlates more to the BMI of their biological parents than their adopted parents [43]. Although heritability studies have been important in understanding of the genetics of obesity, interpreting these studies requires attention, because some heritability estimates

may be amplified by unaccounted shared environment [41].

The completion of the human genome sequence, combined with technological and methodological developments has led to the identification of numerous genes associated with syndromic monogenic, non-syndromic monogenic, oligogenic and polygenic obesity [43].

Syndromic monogenic obesity is exceptionally rare and is characterized by mental retardation, dysmorphic features and organ specific abnormalities, in addition to obesity. More than 30 syndromes have been described in literature, but many of these have not been genetically elucidated. The most common forms of early-onset syndromic obesity including Bardet-Biedl, WAGR (Wilm's tumor, aniridia, genitourinary anomalies and mental retardation), Prader-Willi, Alström and Cohen syndromes. The genetic basis of these disorders is extremely heterogeneous [43]. To give an example, the Bardet-Biedl syndrome (BBS) was the first obesity syndrome reported, it is a genetically and clinically heterogeneous ciliopathy with an autosomal recessive inheritance. Clinical features include retinal degeneration, cognitive disability, polydactyly and genital and renal anomalies. Also, the 72–92% of BBS patients are characterized by central and peripheral obesity, appearing due to hyperphagia. To date, 19 BBS genes have been identified to encode the BBS proteins that are implicated in the assembly and function of primary cilia [43]. Due to the physiologic role of primary cilium, the pathogenesis of obesity in BBS is attributed to a defect in the regulation of food intake and adipocyte differentiation [45].

Non-syndromic monogenic obesity refers to a single gene disorder that leads to a highly penetrant form of the disease [43]. More than 200 single-gene mutations have been found to cause autosomal recessive and dominant forms of human obesity. Interestingly, these mutations have been identified in only ten genes and eight of these explain up to 10 % of cases with early-onset extreme obesity [46]. These genes include the leptin (*LEP*) and its receptor (*LEPR*), the melanocortin 4 receptor (*MC4R*) and pro-opiomelanocortin (*POMC*) genes, among others that code for proteins with a central role in the leptin–melanocortin signaling pathway present in the hypothalamus. Mutations in these genes affect body weight through pathways regulating food intake and energy expenditure in the central nervous system [2,46]. Homozygous/compound heterozygous loss-of-function mutations in monogenic obesity genes from the leptin/melanocortin pathway lead to a rare form of fully penetrant obesity in humans. A substantially higher proportion of obesity is observed in subjects carrying heterozygous deleterious coding mutations in these genes, resulting in non-fully penetrant oligogenic obesity [43].

Polygenic obesity is caused by multiple gene defects with modest effects that interact with the environment [43]. Several approaches, such as linkage/positional cloning, candidate gene and genome-wide association study (GWAS) have been used to identify >300 genetic loci for obesity traits [2], providing to better clarify the genetic architecture and pathophysiology of these traits. The first important success of GWAS was the identifications of a cluster of common non-coding variants in obesity-associated (*FTO*) locus showed a highly significant association

with obesity risk in children and adults [2,43]. The biology that underlies this association is only partially described: the *FTO* genotype may contribute to body weight, by regulating appetite, thermogenesis, adipocyte browning and epigenetic mechanisms related to obesity [47,48]. Since the discovery of *FTO*, additional GWAS have identified many other genetic loci associated with BMI, adult obesity, childhood obesity and waist-to hip ratio (WHR) [2,39-41,43,46]. By using different BMI thresholds based on the ethnicity/age group under investigation, GWAS have identified 135 variants associated with BMI level and/or obesity status so far (89 loci associated only with BMI, 21 loci only with obesity, 24 loci with both BMI and obesity) (fig.5). Single nucleotide polymorphisms (SNPs) in most Mendelian non-syndromic genes (*BDNF*, *NTRK2*, *LEPR*, *MC4R*, *PCSK1*, *POMC*, *SH2B1*, *TUB*) and some Mendelian syndromic genes (*SDCCAG8*, *BBS4*) contribute towards polygenic obesity [43].

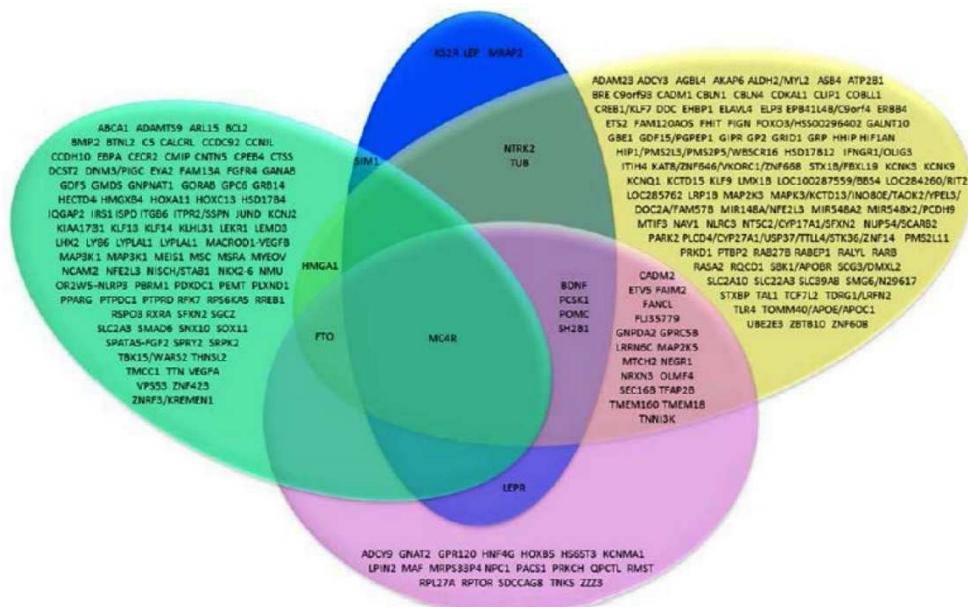


Figure 5: Venn diagram of genes involved in monogenic, oligogenic and polygenic obesity. Monogenic/ oligogenic obesity genes are showed in blue, polygenic BMI-related genes in yellow, overweight or obesity-related genes in purple and fat distribution-related genes in green. Clin Sci (Lond). 2016; 130(12):943-86.

Pathway and tissue enrichment analyses applied to the BMI-associated strengthen the role of the central nervous system in body weight regulation. The pathways are related to synaptic function and neurotransmitter signaling, and the tissues with enriched expression of these genes include the hypothalamus, the pituitary gland and the hippocampus. The same analyses applied to loci associated with the WHR point to pathways regulating adipocyte differentiation, angiogenesis, insulin sensitivity and fat distribution [2]. In particular, the WHR adjusted for BMI (WHRadjBMI) seems to be a highly valuable tool for evaluation of fat distribution, because it combines the negative effects of the abdominal fat and the beneficial effects of gluteal subcutaneous fat, independent of overall

adiposity [43]. Considering the ethnic specificity of body fat distribution, *FTO*, *MC4R* and *CTSS* (Cathepsin S) were identified by a GWAS for fat mass in a multiethnic population [43].

However, some findings from GWASs have to be interpreted with caution. For instance, rare mutations are not detected in GWASs since SNP genotyping arrays are usually designed to capture common SNPs [41]. By using sequencing technologies, it is possible to detect rare variants. Recent advances in next generation sequencing (NGS) technologies are allowing researchers to extend their genome-wide analyses beyond common SNPs to assess the contribution of rare variants in disease predisposition in a fast way. However, population-based approaches to mapping rare variants for complex disease from NGS data require a large number of samples to provide sufficient statistical power for rare variants detection. Moreover, *Hagg et al.* [49] have performed a meta-analysis of GWAS using the 'VERSatile Gene-based Association and adult severe obese patients. These VNTRs account Study' (VEGAS) approach looking for genetic loci that could not be detected by standard single-marker analyses due to allelic heterogeneity, and found six novel loci associated with BMI missed by conventional GWAS [43,49]. For instance, using a variable number tandem repeats (VNTRs) association method, have been identified significant associations between dedicator of cytokinesis 5 (*DOCK5*) VNTRs and childhood for nearly 0.8% of BMI variance [43].

Another source of heritability often missed by GWAS is the contribution of CNVs, that are chromosomal segments encompassing large duplications or deletions in genetic loci, with a size of about 500 kb, present in 5-10% of the population. As many CNVs encompass genes and/or regulatory regions, they may result in alteration of gene dosage and/or disruption of gene structure and/or regulation. Therefore, CNVs may account for significant normal phenotypic variation within a species, susceptibility or resistance to disease, variation in drug response. In relation to obesity, common biallelic CNVs, identified in more than 5% of the population, have been reported in association with BMI and obesity. Similarly to common SNPs, these common CNVs had small effect sizes on obesity risks. However, some CNVs associated with obesity are difficult to replicate across populations, because they can have ethnicity-specific impacts. For example, the *PCSK1* SNP rs6234/rs6235 was found to be associated with obesity in white Caucasian, African and Hispanic ethnic groups, but not in the East Asian populations [43].

1.2.3 Epigenetics: gene-environment interactions in obesity

The threatened recent and rapid increase in the worldwide prevalence of obesity indicates that this disease is becoming the normal metabolic fate of a large fraction of human populations. Genetics alone cannot explain this escalation in frequency, because the emergence over the past 30 years has been too rapid to allow for the appearance of new mutant genes [2,43]. Although considerable efforts have been

made into identifying loci and variants contributing to individual risk of obesity, only a small proportion of observed familial aggregation may be explained by these established loci (~2%) [41]. For instance, *FTO* has the largest, but still small, effect on obesity susceptibility: each risk allele increases the risk of obesity by 1.20–1.32-fold [2]. Moreover, all combined BMI-associated variants account for <5% of BMI variance, and a similar effect sizes has been reported for the variants associated with WHR [2].

The increasing worldwide prevalence of obesity, in particular in developing countries associated with urbanization, and the inverse relationship between this disease and socioeconomic class, provide strong evidence of the environmental influences on weight gain [50]. It has become clear that obesity results from the complex interplay between several susceptibility genes and biological factors, such as age and sex, obesogenic environment and lifestyle factors. The term 'obesogenic' includes major societal and environmental changes as the excessive consumption of energy dense foods, sedentary lifestyles, urbanization and socioeconomic-dependent access to a healthy diet [2]. There is accumulating evidence, for example, that the overall contribution of genes towards the BMI increases from childhood to early adulthood. Moreover, a sexual dimorphism has been identified for half of the WHRadjBMI-associated loci, showing higher effect sizes in women compared to men. Importantly, the genetic influence on BMI and adiposity is significantly increased in an obesogenic environment. and a pre-existent obesity can further amplify the effect of same risk alleles, exacerbating the body weight gain [43]. For instance, obesity genetic variants of *FTO*, *MC4R*, *TMEM18*, *BDNF*, TNNI3 interacting kinase (*TNNI3K*), neurexin 3 (*NRXN3*), *SEC16B* and glucosamine-6-phosphate deaminase 2 (*GNPDA2*) were found to be more strongly associated with increasing BMI in children with higher BMI [51]. In addition, there are increasing data that the susceptibility to obesity in adult life has early development origins and reflects an intergenerational cycle. Indeed, several epidemiological studies have shown that exposure to an adverse nutritional environment during intrauterine development, as a consequence of either an excess or deficient maternal caloric or micronutrient intake, is associated with an increased risk of a range of chronic diseases, including obesity. This evidence has led to the developmental origins of health and disease hypothesis [52]. In 1990, David Barker first proposed that in utero metabolic adaptation defines a trajectory of growth that prepares the fetus for its likely adult environment [53]. The environmental exposures in early life can induce the “metabolic reprogramming” of fetus that depends on the mother's and the father's behaviors before conception and the mother's during pregnancy [41,43,53]. This hypothesis was supported by solid epidemiological data from the Dutch “Hunger Winter”. The offspring of mothers who were exposed to the famine during early gestation have higher rates of subsequent obesity and coronary heart disease were observed, linking early life events (*e.g.*, maternal nutrition) to offspring's disease risk in later life [41,43]. Additional observations results from the follow-up data of members of the Pima Native American community in Arizona, a population with a very high prevalence

of obesity and T2D. There was a higher risk of both obesity (58 vs. 17%) and T2D (45 vs. 1.4%) in the offspring of mothers affected by T2D during pregnancy than in the offspring of women nondiabetic during pregnancy. Moreover, the offspring born after the mother was diagnosed with T2D have higher risk of obesity and T2D than their siblings born while their mother was nondiabetic [41]. Taken together, these observations emphasize the role of intrauterine environment as an important factor in predisposition to obesity and T2D.

The mechanisms underpinning this “nutritional memory response” are not completely clear, but may include alterations of the developmental fate of tissues, reprogramming of stem cells, changes in neural, endocrine and metabolic regulatory circuits. Epigenetic processes, including DNA methylation, histone modification and non-coding RNAs, that change gene expression and cellular phenotype without changing the DNA sequence, are sensitive to external factors (*e.g.*, diet, physical activity) and internal factors (*e.g.*, hormones, genetic factors), are reversible and can be mitotically stable and/or passed on to subsequent generations [2,41,43]. Accordingly to this, epigenetic modifications of gene structure through nutritional and physiological stress provide mechanisms for inducing obesity, that are independent of new mutations to the genome (fig.6). Thus, epigenetics has become a leading candidate for the development and/or progression, and possibly inheritance, of obesity.

The role of epigenetics in obesity has been well demonstrated, largely, in animal models and, only occasionally, in humans; >600 articles have already been published in this area [2]. Animal studies provides experimental support for a causal link between early nutritional status, maternal under- or over-nutrition (*e.g.*, high-fat diet, maternal obesity) and epigenetic changes that can be transmitted through successive generations, predisposing to obesity risk in later life. For instance, the agouti viable yellow (A^{vy}/a) mice, in spite of an identical genotype, exhibit color differences of fur coat, ranging from yellow to brown, that are correlated with adult body weight. The variation in phenotypes is caused by an epigenetic modification of the A^{vy} allele transmitted by the germline from the female (stable intergenerational transmission) [41]. In this model, the maternal diet may affect the methylation status of “metastable” A^{vy} [41], changing the animal's coat color, demonstrating as an environmental factor interacts with a single genotype by epigenetic modifications to produce a different phenotype [54]. Moreover, epigenetic changes have been detected at genes that regulate growth factors, adipogenesis, brain appetite and satiety/reward pathways and glucose homeostasis.

To date, there are relatively few human studies in this area, but one of the most significant was performed on the sons of women exposed to severe undernutrition during the first half of pregnancy, as a result of the Dutch Hunger Winter during World War II. This intergenerational study demonstrated that these individuals as adults showed a reduced DNA methylation of the imprinted gene *IGF2*, associated with an increased risk of obesity or glucose intolerance. Conversely, the later exposure during the pregnancy was not associated with *IGF2* methylation,

demonstrating that the early development period is crucial for establishing and maintaining epigenetic marks [55].

On the other hand, the percentage of phenotypic variance that cannot be explained by inherited epigenetic trans-generational variation, may be due by the impact of acquired epigenetic changes later in life. Analysis of DNA methylation and histone acetylation patterns in a large cohort of monozygotic twin pairs showed that even if twins were epigenetically indistinguishable during the early years of life, older monozygous twins exhibited remarkable differences in their DNA methylation and histone acetylation profile, providing explanations of how different phenotypes, in terms of differences in susceptibilities to disease and a wide range of anthropomorphic features, can be originated from the same genotype [56]. Thus, external and/or internal cues may impact on the individual phenotype by altering the pattern of epigenetic modifications and modulating the genetic and genomic information.

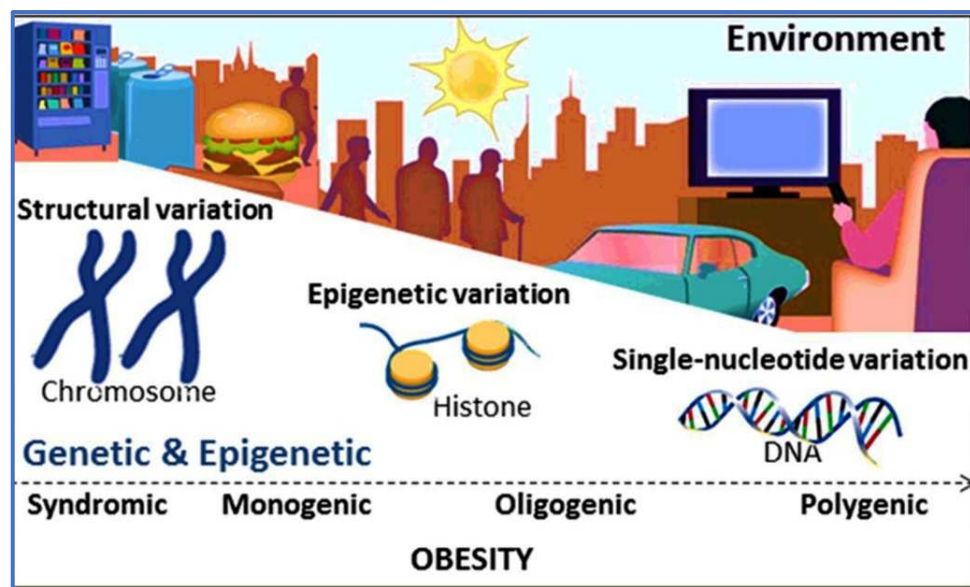


Figure 6. The interplay of genetics, epigenetics and environments. In monogenic and syndromic obesity, a single gene mutation causes severe obesity, regardless of environmental stimuli. In oligogenic and polygenic obesity, environmental factors can exacerbate the progression of obesity in individuals with a genetic predisposition to weight gain by inducing epigenetic modifications. Clin Sci (Lond). 2016; 130(12):943-86.

Several studies have also demonstrated the association between genetic and epigenetic factors. An interesting example came from the obesity risk alleles of *FTO*, representing a good model of haplotype-specific methylation, in which the methylation status of the region is determined directly by the sequence of allelic variants, that create or abrogate methylation sites, exerting their downstream effects through epigenetic mechanisms [41]. Other studies have reported a strong association between obesity-associated SNPs discovered in GWAS and methylation levels at proximal CpG sites. Indeed, several known obesity-associated SNPs are associated with DNA methylation levels at proximal CpG

sites. Interestingly, these SNPs were associated with CpGs that were in the promoters of genes known to take part in the pathogenesis of obesity, such as *POMC*, *BDNF* and *SH2B1*; or were located in regions that interact with such genes. In the paradigm of genetics–epigenetics–environment interplay, it is still unclear whether obesity-associated SNPs directly cause differential DNA methylation at genes or if the observed differential methylation levels are a consequence of a modified gene regulation caused by the presence of a specific risk alleles. It has been proposed that mutations within regulatory regions may affect the binding of transcription factors, which in turn influence DNA methylation. If DNA methylation does not necessarily actively impact on gene expression, it may be considered at least an informative marker of the underlying regulatory activity [57].

As DNA methylation represents a key mechanism to provide a more comprehensive and systemic view of the contribution of epigenetics to obesity risk and/or pathogenesis, several approaches have been developed to study the associations between DNA methylation levels and obesity, including the candidate gene approaches and epigenome-wide association studies (EWAS). Some of these studies are targeting disease-relevant tissues (*e.g.*, VAT, SAT, specific blood-cell components), others focused on whole blood despite the necessity to evaluate the capacity of circulating leukocytes to reflect the DNA methylation status of specific disease-relevant tissues not easy to accessible. The main long-term goals in this field are the identification of epigenetic marks that could be used as early predictors of obesity risk and the development of drugs or diet-related treatments able to delay these epigenetic changes and even reverse them.

To summarize as outlined above, it should be clear that familial aggregation of obesity does not be used as a proxy for overall genetic influences. Indeed, non-genetic familial aggregation may also be explained by the effect of a shared environment resulting from epigenetic influences [41]. Thus, epigenetics conveys specific environmental influences into phenotypic obesity traits through a variety of mechanisms that are often installed in early life and then persist later in the life in differentiated tissues, with the power to modulate the expression of many genes.

1.3 Epigenetics

Genetic information encoded in DNA sequence is largely identical in every cell type of a multicellular eukaryotic organism. However, despite an identical genomic sequence, the cells in different tissues and organs exhibit a substantially different profile of gene expression and specialized functions. Moreover, specific gene expression patterns need to be appropriately induced and maintained and also need to respond to changing developmental and environmental stimuli. Therefore, most of the differences among specialized cells are epigenetic and non-genetic [57].

The term “epigenetics” was coined in the 1940s to describe the events that could not be explained by traditional genetics. Conrad Waddington defined epigenetics

as “the branch of biology which studies the causal interactions between genes and their products which bring the phenotype into being” [58]. The epigenetic field now actively discloses the molecular mechanisms underlying these phenomena. Today, the epigenetics has been defined “the study of changes in gene function that are mitotically and/or meiotically heritable and that do not entail a change in DNA sequence” [59]. In other words, epigenetics is the study of changes in gene expression or phenotype, caused by mechanisms other than changes in the underlying DNA sequence, and some of these epigenetic changes have even been shown to be heritable [60].

1.3.1 Epigenetic modifications

This highlights the role of “epigenetics” and its stable and inheritable information that is distinct from DNA sequence and fostered by specialized mechanisms. These mechanisms include DNA methylation, small interfering RNA (miRNAs), and histone posttranslational modifications (PTMs). To date, however, only DNA methylation has been shown to be stably inherited. While some histone PTMs are expected to contribute to the transmission of epigenetic information, others actively participate within the process of transcription and others are likely to be restricted to “structural functions”, altering chromatin conformation [57].

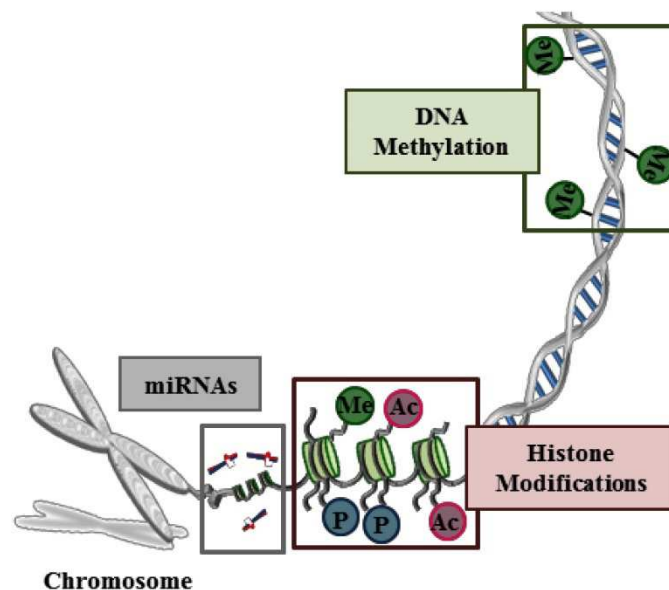


Figure 7. Schematic representation of epigenetic modifications. Epigenetic modifications include DNA methylation, histone modifications and miRNAs. **Ac:** acetylation, **Me:** methylation, **P:** phosphorylation. J Endocrinol Invest. 2016; 39(10):1095-103.

DNA methylation occurs principally at a cytosine residue, mainly the cytosine–guanine nucleotide pair (CpG) sites along the DNA chain in vertebrates. It is a covalent modification, resulting in the attachment of a methyl (CH₃) group at the 5' carbon position of the cytosine ring, and generally contributes to the

transcriptional silencing of genes [61].

Noncoding RNAs (ncRNAs) are another type of epigenetic factors, regulating gene expression by *cis*- and *trans*-acting mechanisms [62]. Some ncRNAs act in concert with components of chromatin and the DNA methylation machinery to establish and/or sustain gene silencing. They can also regulate RNA processing, mRNA stability, translation, protein stability and secretion. Noncoding RNAs include micro-RNAs (21–25 nucleotide, miRNAs) and long noncoding RNAs (lncRNAs). The miRNAs can regulate gene expression by transcriptional regulation and translational inhibition, that are accomplished through direct base pairing with the DNA or RNA target, or by functioning as a component of an RNA-protein complex [63]. The lncRNAs act as tethers and guides to bind proteins responsible for modifying chromatin and mediate their deposition at specific genomic locations [64].

A large number of several PTMs can occur on nucleosomal histone tails. These modifications modify the inter-nucleosomal interactions, altering the overall chromatin architecture. Thus, these modifications contribute to the gene expression control through influencing chromatin compaction or signaling to other protein complexes [65]. Nucleosome is the fundamental unit of chromatin and it is composed of two copies each of the four core histone proteins (H3, H4, H2A, H2B) around which 147 base pairs of DNA are wrapped. Nucleosomes are connected by DNA linker, 10 to 80 base pairs (bp) long. The histone H1 is associated with the DNA linker as well as with the nucleosome core particle itself, thus it plays an important role in the compaction of DNA beyond the nucleosomal level. Indeed, it is well demonstrated that chromatin structure is dynamic and this feature is required to regulate several biological processes essential for normal cellular functions (*e.g.*, gene transcription, DNA replication, repair and recombination) [66]. As histone post-translational modifications can control the packaging of DNA around histone proteins through dynamic modifications of these proteins, they exert an essential role in chromatin structure regulation. The nucleosomal histone tails are unstructured and protrude from nucleosome cores, thus may be targeted by modifying enzymes (epigenetic modifiers), resulting in acetylation, methylation, phosphorylation, sumoylation, ubiquitylation, ADP-ribosylation, deamination and proline isomerization [58]. The combinatorial histone modifications affect the binding of regulatory protein end/or transcription factors to chromatin, thereby influencing gene expression. The most studied histone modifications so far are methylation, acetylation and phosphorylation. Regarding histone acetylation, it is the processes by which the lysine residues on the N-terminal tails protruding from the histone core of the nucleosome are acetylated by the histone acetyltransferases (*e.g.*, p300). This epigenetic modification has the most potential to unfold chromatin since it neutralizes the basic charge of the lysine. As a consequence, histone acetylation alters nucleosomal conformation, promotes the DNA accessibility to the cell transcriptional machinery elements and enhances gene transcription [65].

In this scenario, combinatorial histone modifications function as *codes* in

targeting transcription factors to DNA by recruiting specific adaptors. Therefore, alterations in these epigenetic processes could lead to the deregulation of gene transcription.

1.3.2 DNA Methylation

DNA methylation was the first epigenetic modification to be discovered and it is the most studied so far. In humans, the predominant form of DNA methylation occurs on the 5th carbon of the cytosine in CpGs along the DNA chain [61]. In the human genome, the total number of CpGs is estimated to be around 28 million, and 60–80% of them are generally methylated [67]. Less than 10% of CpGs falls in CG-rich regions, known as CpG islands. The CpG islands characterize the transcription start sites (TSS) of housekeeping and developmental regulator genes, and most of them are unmethylated. On the other hand, CpG sites that exist outside CpG islands are largely methylated [68]. Generally, the hypo-methylated DNA regions are involved in active transcription, while the hyper-methylated DNA regions are involved in gene silencing [67-69]. For example, CpG regions at the promoter regions of tissue-specific genes are usually highly unmethylated in their tissue of expression while they are highly methylated in other tissues where they are not expressed [69]. In accordance, housekeeping genes were found to have constitutively unmethylated CpG islands at their promoters regardless of tissue types [67].

DNA methylation is known to directly repress gene expression by interfering with the binding of transcription factors to their target sequences or by initiating the recruitment of corepressors. However, the effect of DNA methylation may be also mediated by affecting gene accessibility at the level of chromatin structure. Indeed, it has been described that methylated CpGs result in closely packed chromatin and unmethylated CpGs result in more open chromatin structure. For example, the presences of a methyl groups can promote the binding of methyl-binding proteins, as MeCP2 and MBD2 [70], and/or impair the binding of other proteins, as the chromatin proteins CTCF and Cfp1 (fig. 8) [71]. Given its pivotal role in gene regulatory networks, DNA methylation represents a key epigenetic mechanism contributing to normal development, phenotypic variations as well as susceptibility to diseases.

DNA methylation is mainly mediated by two types of DNA methyltransferases (DNMTs): *i*. DNMT1, responsible for maintaining DNA methylation pattern in the newly synthesized DNA strand, after cellular replication cycle; and, *ii*. DNMT3A and DNMT3B, responsible for *de novo* DNA methylation, essential during embryogenesis and other cell differentiation events [72].

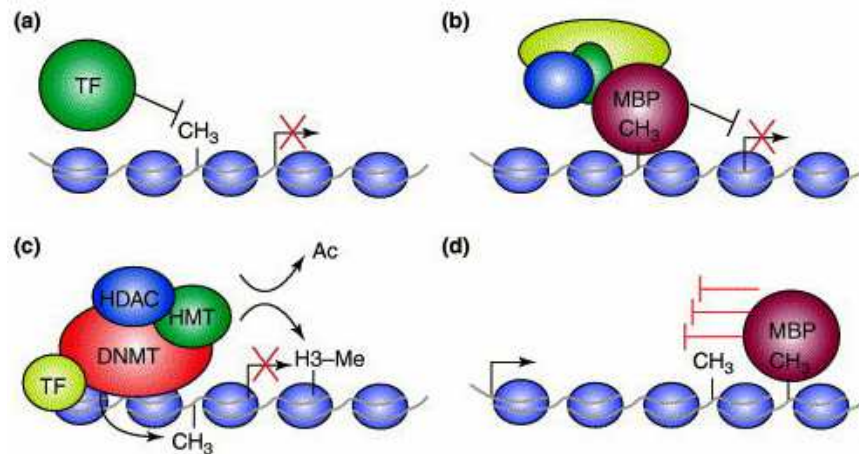


Figure 8. Mechanisms of DNA-methylation-mediated gene silencing. (a) DNA methylation of cytosine residues in DNA-binding sequences of some transcription factors (TF) may directly block transcription factors from binding targets sites, inhibiting transcriptional activation. (b) Methyl-CpG-binding proteins (MBPs) directly recognize methylated DNA and recruit co-repressor factors to modify surrounding chromatin packaging and to silence transcription. (c) DNA methyltransferases may be functionally linked to histone deacetylase (HDAC) and histone methyltransferase (HMT) enzymes. In this case, the transcriptional repression initiated by the addition of methyl groups to DNA is coupled to chromatin modifications. (d) DNA methylation may also have a dampening effect on transcriptional elongation. MBPs may inhibit elongation, either directly or by their effects on the surrounding chromatin structure. Trends Biochem Sci. 2006; 31(2):89-97.

Although the mechanism of DNA methylation is not fully elucidated, data in literature have shown that this modification is typically established during early developmental stages. In the gametes and pre-implantation embryo, almost all methylation modifications are erased, but imprinted regions maintain their methylation status on one allele (also throughout development). Post-implantation, pluripotency genes undergo *de novo* methylation to establish tissue specific DNA methylation patterns. The acquiring of two or more different epigenetic states at a specific genomic locus in different cells or tissues within the same organism is a biological event known as epigenetic mosaicism. This phenomenon adds a further complexity to the field of DNA methylation and contribute to individual phenotypic variation [73]. Global and/or local changes of methylation patterns may also arise in response to environmental exposures or as a function of aging [72,73].

Recent study has shown that methylation patterns at some genomic loci may be inherited through generations [74]. Two principal types of DNA methylation heritability have been identified: *i.* the genetic inheritance of DNA sequence variations within a CpG locus which disrupts the methylation site; and, *ii.* the epigenetic inheritance related to the sequence-independent transmission of epigenetic mark, that may happen through escaping the methylation reprogramming events during development [75]. *Bell et al.* [76] investigated the DNA methylation heritability in twin pairs, by methylation profiling of whole blood-DNA. Their data demonstrated that monozygotic twins shared a significant higher genome-wide methylation profile compared to dizygotic twins, estimating the DNA methylation heritability to be about 18%. Moreover, *McRae et al.* [75]

analyzed the heritability of DNA methylation in whole-blood DNA from multigenerational families, both within and across generations. This study showed that the DNA methylation heritability is mostly driven by the underlying genetic sequence (*i.e.*, genetic inheritance).

1.3.3 DNA Methylation and Obesity

Several findings, mostly derived from animal studies, support the role of DNA methylation as one of the major epigenetic mechanisms responsible for the developmental programming of obesity. Robust data from mouse models have demonstrated that obesity development induced by environmental exposures, such as diet (*e.g.*, the quantity and/or quality of the diet), exercise, epigenetic drugs, parental nutrition, intrauterine environment, is associated with DNA methylation changes at genes involved in the regulation of growth factors, adipogenesis, glucose metabolism, energy homeostasis, appetite and satiety pathways [77-81]. For instance, the administration of a high-fat diet increased DNA methylation of leptin promoter in retroperitoneal adipocytes from obese mice, and this was associated with lower circulating leptin levels, suggesting the DNA methylation impairs its gene expression [82].

Similarly, increasing evidence in humans indicates an association between environmental-induced changes in gene-specific and global DNA methylation and the development of or susceptibility toward obesity. The subtle differences between human and animal findings, may be partly attributed to certain factors, such as sampling tissue, period and duration of exposure and in the case of humans, lifestyle. However, likely animal studies, human data support a role of DNA methylation, either global, gene-specific or genome-wide levels, both in development of obesity and/or its related complications, and in risk of this disease [2,41,43]. Since the blood is easily accessible, peripheral blood cells (PBL) are the principal source of DNA used for epigenetic analyses. On the other hand, metabolically important tissues, as adipose tissue, are of high interest to understand the role of epigenetics in obesity. Adipose tissue includes functionally different cellular types and different depots with specific characteristics depending on their anatomical location. Metabolic alterations are linked to increased fat deposition in visceral depots, whereas storage in subcutaneous depots is considered less detrimental. As DNA methylation has a pivotal role in cell fate and adipocyte differentiation, studying DNA methylation profiles in distinct adipose tissue depots under different metabolic conditions could clarify how epigenetic regulation of adipose tissue is involved in the development of obesity and associated comorbidities, and how this could potentially be manipulated [83].

To date, gene-specific DNA methylation is the epigenetic mark most extensively investigated, in studies regarding the involvement of epigenetics in health outcomes, including obesity. Many of them are cross-sectional analysis, thus, DNA methylation levels and obesity-related traits are assessed at the same time point. A great number of these candidate gene methylation studies have focused

on a range of genes implicated in obesity, cell differentiation, appetite control and/or metabolism, insulin signaling, immunity, growth, circadian clock regulation and imprinted genes [83]. Altogether, these studies have showed the hypomethylation of *TNF α* in PBL, pyruvate dehydrogenase kinase 4 (*PDK4*) in muscle, and *LEP* in whole blood (WB), and hyper-methylation of *POMC* in WB, PPAR γ coactivator 1 alpha (*PGC1 α*) in muscle, and *CLOCK* and aryl hydrocarbon receptor nuclear translocator-like (*BMAL1*) genes in PBL in obese compared with lean individuals. Moreover, associations between BMI, adiposity, and waist circumference, with DNA methylation in *PDK4* in muscle, melanin-concentrating hormone receptor 1 (*MCHRI*) in WB, and the serotonin transporter (*SLC6A4*), the androgen receptor (*AR*), and glucocorticoid receptor (*GR*) in PBL have also been reported. The strongest epigenetic association has been observed between DNA methylation status at the *IGF2/H19* imprinting region in PBL with adiposity measures [83]. In addition, *Kuehnen et al.* [84] have analyzed DNA methylation status at the *POMC* locus, one of the identified monogenic obesity genes which encodes the anorexigenic alpha melanocyte stimulation hormone (α -MSH) produced in the hypothalamic arcuate nucleus, in blood leukocytes of obese children. This study has demonstrated the association between increased DNA methylation in the region adjacent to an intronic Alu element in the *POMC* locus and childhood obesity. Interestingly, the findings showed that the hyper-methylation of this region impaired the binding activity of the histone acetyltransferase/transcriptional coactivator p300, inhibiting the expression of *POMC* gene [84]. Collectively, these studies provide evidence that obesity is associated with modification of DNA methylation status of several metabolically relevant genes.

Additional studies have investigated the relationship of DNA methylation at birth to childhood metabolic outcomes and obesity, also in association with *in utero* exposures [83,85,86]. *Godfrey et al.* [85] have demonstrated that the methylation variation in the promoter of the retinoid X receptor alpha gene (*RXR α*), a nuclear receptor with a known role in adipogenesis, in umbilical cord tissue explain up to 26% of the variation in childhood adiposity and is associated with the onset of obesity in pre-pubertal children. Furthermore, in the same cohort study, it has been demonstrated that this epigenetic mark is also associated with lower maternal carbohydrate intake in the first trimester of pregnancy [85]. *IGF2* is another example of a gene showing loci-specific variation in methylation at birth, and also at childhood, that is associated with obesity in later life. Differences in the DNA methylation levels near *IGF2* locus has been correlated to exposure to a suboptimal environment *in utero* [86]. These findings suggest a critical role of DNA methylation as potential mark to predict the individual's obesity risk, before the phenotype

The development of high-throughput sequencing technologies and genome-wide array-based methods has opened a new window for identifying a large number of differentially methylated genes and CpGs. Overall, obesity-associated differentially methylated sites were enriched both in obesity candidate genes and

in genes regulating adipose tissue functioning, cell differentiation, immune response, and transcription. The majority of EWASs has been performed on blood samples, but adipose tissue, muscle and placenta have also been studied; many of these used BMI and/or body fat percentage to classify obesity [83]. Recently, *Dick et al.* [87] have provided a systematic analysis of the association between variation in DNA methylation and BMI. In particular, it has been used DNA of 479 European individuals and two replication cohorts for a total of 2128 participants to analyze whole blood specific-CpG DNA in relation to BMI. The authors have demonstrated that increased BMI in adults is associated with specific hypermethylation at the hypoxia-inducible factor 3 alpha (*HIF-3α*) locus in blood cells and adipose tissue [87]. The association between *HIF-3α* methylation levels in blood and adiposity has been replicated in independent populations, highlighting the importance of its epigenetic regulation in energy expenditure and obesity [2,43,87]. Another EWAS, using whole-blood DNA from 2377 white adults, CD4⁺ T-cell DNA from 991 white individuals and adipose tissue DNA from 648 white women, has reported the association between the methylation level at 18 CpG sites located in/near the Carnitine Palmitoyltransferase 1A (*CPT1A*), ATP-Binding Cassette, Sub-Family GMember 1 (*ABCG1*), *LYS6GE*, Lysine (K)-Specific Demethylase 2B (*KDM2B*), *RALB*, *PRRL5*, Lectin, Galactoside-Binding, Soluble, 3 Binding Protein (*LGALS3BP*), Chromosome 7 Open Reading Frame 50 (*C7orf50*), Pre-B-Cell Leukaemia Homeobox 1 (*PBX1*), erythrocyte membrane protein band 4.9 (*EPB49*) and *BBS2* genes with BMI in blood and adipose tissue cells [43]. Recently, *Ronn et al.*, by analyzing the whole-genomic DNA methylation and gene expression in human adipose tissue from European individuals (96 males and 94 females), have demonstrated a correlation between age, BMI and/or HbA1c levels and DNA methylation and expression in many genes, that include also the Ankyrin repeat domain 26 (*ANKRD26*) [88]. In order to provide for the first time new and valuable DNA methylation biomarkers of VAT pathogenesis associated with insulin resistance, *Crujeiras et al.* [28] have performed EWAS in VAT from morbidly obese patients, classified based on the insulin sensitivity, evaluated by the clamp technique. This study has identified in 982 CpG sites the specific methylome map associated with insulin-resistant (IR) in VAT. These identified sites represent 538 unique genes, 10% of which are diabetes-associated genes. However, it has been also revealed new IR-related genes, epigenetically regulated in VAT, such as *COL9A1*, *COL11A2*, *CD44*, *MUC4*, *ADAM2*, *IGF2BP1*, *GATA4*, *TET1*, *ZNF714*, *ADCY9*, *TBX5*, and *HDACM*. These data indicate that alteration of epigenetic regulation is involved in the dysregulation of VAT that could predispose patients to insulin resistance and future T2D in morbid obesity, and provide a potential therapeutic target and biomarkers for counteracting obesity-associated diseases [28]. Another study has examined the DNA methylation patterns in adipose tissues from obese women, before and after weight-loss surgery, showing a significant global hypermethylation in subcutaneous and omental adipose tissue, before weight loss through gastric bypass [89]. In particular, relative to promoter regions, this higher

methylation has been discovered in the 3' untranslated region, especially in genes associated with obesity, epigenetic regulation and development, such as, fork head box P2 (*FOXP2*), *DNMT3B* and the *HOX* clusters [89]. Very recently, *Macartney-Coxson et al.* [38], by using novel combinatorial algorithms, have analyzed DNA methylation data previously obtained from obese individuals, before and after gastric bypass [89] to identify specific CpG loci that differentiate between subcutaneous and omental adipose tissue. Significant differential methylation has been observed for 3239 and 7722 CpG sites, between adipose tissue types before and after significant weight loss, respectively. The vast majority of these extended differentially methylated regions are consistent across both time points and enriched for genes with a role in transcriptional regulation and/or development (*e.g.*, *SORBS2*, *HOXC* cluster, *CLD1*), reflecting epigenetic differences critical to the function of these two tissues. Other differentially methylated loci have been observed at one-time point after weight loss (*e.g.*, *WTAPP1*), thus they potentially highlight genes important to adipose tissue dysfunction observed in obesity and/or weight loss. Strong correlations between changes in DNA methylation (subcutaneous adipose vs omentum) and changes in clinical trait, have been particularly identified for CpGs within *PITX2* and fasting glucose and four CpGs within *ISL2* and HDL cholesterol. Only one CpG locus in *ATP2C2* is useful to distinguish between the two tissues in this study cohort, both in lean and obese individuals [38]. The data obtained in the current study illustrate the extreme potential power and the overall utility of DNA methylation as a biomarker, together with other previously reported data in adipose tissue. However, it should be necessary to elucidate the molecular mechanisms involved in adipose tissue dysfunction associated with obesity in an easily accessible biological material, *i.e.*, blood. Consistently with this issue, a study assessing the whole-genomic DNA methylation in PBL from individuals who went from being obese to normal weight on methylation patterns, have reported that peripheral blood mononuclear cell methylation is associated with BMI [90]. Moreover, *Crujeiras et al.*, by using DNA samples isolated from subcutaneous adipose tissue and circulating leukocytes from obese and non-obese patients, have recently identified new DNA methylation biomarkers of obesity-related adipose tissue dysfunction in blood sample, an easily accessible and minimally invasive biological material instead of adipose tissue [91].

Overall, significant progress has been made in the field of epigenetics and obesity, but there is still much to be learned before we fully understand the (causal) role of the epigenetic processes in development of complex diseases such as obesity, and assessing the epigenome at the right time in life and in the relevant tissues is a major barrier for studies in humans.

1.4 *ANKRD26* gene

The *Ankyrin repeat domain 26 (ANKRD26)* gene maps on human chromosome 10p12.1, in a genetic locus that may influence susceptibility to obesity when it is

maternally transmitted, and on chromosome 6 (qF1) in the mouse [92,93]. The gene encodes a ~190 kDa protein that contains ankyrin repeats and spectrin helices. EST database analysis of both the human and mouse genomes shows that ANKRD26 RNA is present in many normal tissues [92]. The protein is highly expressed in neuronal cell bodies and their processes, and in glial cells in feeding centers of the hypothalamus as well as both in areas of the brain that project to these centers and in the ependyma and circumventricular organs, that act as interface between peripheral and central circulation [92-94]. Moreover, it has been identified in other tissues and organs, including liver, skeletal muscle and WAT [93]. The ANKRD26 protein is located in the cytosol close to the inner aspect of the cell membrane, where it could act as scaffold protein regulating the function of signaling proteins and effectors. Indeed, it contains two conserved domains: ankyrin repeats (located from amino acids 74–199) and spectrin regions (743–1538), that are known to mediate protein-protein interactions [95].

Liu et al. [95], by two-hybrid screening, have identified 13 independent interacting partners of ANKRD26. The screening data have showed that only one protein (ANKRD17) interacted with the ankyrin repeat region at the N-terminus of ANKRD26; all the other 12 proteins, including the triple functional domain protein (TRIO), the G protein pathway suppressor 2 (GPS2), the delta-interacting protein A (DIPA) and the hyaluronan-mediated motility receptor (HMMR), bound to region 901–1702 of ANKRD26, containing the coiled-coil domain in the C-terminus [95]. The positive interactions for the above protein was validated in mammalian cells, by immune-precipitation assays. Moreover, to establish the biological relevance of these interacting proteins and whether it may be carried out by their interaction with Ankrd26 protein, knock-down experiments were performed. The specific silencing of ANKRD26, TRIO, GPS2, DIPA or HMMR enhanced adipocyte differentiation upon induction in 3T3-L1 cells, suggesting that ANKRD26 may exert its pro-adipogenic function by modulating the localization and/or function of these interacting partners [95]. These findings indicate that C-terminus domain of ANKRD26 is responsible for its protein-protein interactions and its biological functions, such as the adipogenesis regulation.

In support of this concept, mutant mice in which *Ankrd26* has been inactivated by removing the region encoding amino acids 1212–1710, encompassing all the C-terminus region, have marked hyperphagia, which results in extreme obesity, an increase body size, and insulin resistance and diabetes (fig. 9) [92,93]. In addition, it has been previously demonstrated that partial disruption of the *Ankrd26* gene enhanced adipogenesis, both at level of pre-adipocyte commitment and at early and late differentiation steps, in mouse embryonic fibroblasts from *Ankrd26* mutant mice (MEFs *Ankrd26*^{-/-}) [96].

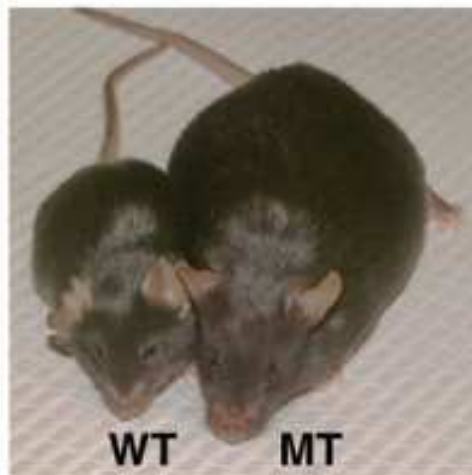


Figure 9. Photomicrograph of a homozygous *Ankrd26* mutant (MT) and wild-type (WT) mice. Adapted from *Proc. Natl. Acad. Sci. U S A.* 2008; 105:270-275.

1.4.1 *ANKRD26* as a candidate (*epi*)gene for obesity

Ankrd26 has been recently identified as a gene involved in the control of the feeding behavior and in the development of both obesity and T2D in mice [92-94]. Indeed, mice with partial inactivation of *Ankrd26* (*Ankrd26*^{-/-}) gene develop marked hyperphagia, without reduction in energy expenditure, severe obesity and diabetes, by impairing both insulin action and secretion, in obesity-dependent manner (tab. 1) [93].

Characteristic	WT male	Mutant male	WT female	Mutant female
Body weight, g	28.4 ± 1.3	40.1 ± 1.2*	23.2 ± 1.6	40.5 ± 3.1*
Fat mass, g	3.6 ± 0.9	9.5 ± 1.5*	3.5 ± 1.2	16.2 ± 2.4*
Fat mass, % body weight	12.2 ± 2.8	23.2 ± 3.3*	14.1 ± 3.8	39.3 ± 2.9*
Lean mass, g	23.7 ± 0.8	29.1 ± 0.7*	18.3 ± 0.5	22.8 ± 1.1*
Lean mass, % body weight	83.5 ± 2.4	72.9 ± 3.2*	79.8 ± 3.5	57.2 ± 2.7*
Length, mm	83 ± 1.2	91 ± 2	80 ± 1	89 ± 2*
Inguinal fat, g	0.4 ± 0.06	1.0 ± 0.23	0.4 ± 0.2	1.4 ± 0.22*
Gonadal fat, g	0.4 ± 0.08	1.1 ± 0.29	0.6 ± 0.3	2.3 ± 0.35*
Brown fat, g	0.1 ± 0.01	0.2 ± 0.04	0.08 ± 0.02	0.3 ± 0.11
Liver, g	1.5 ± 0.1	2.0 ± 0.20	1.1 ± 0.1	1.6 ± 0.22
Kidney, g	0.4 ± 0.01	0.45 ± 0.20	0.3 ± 0.01	0.33 ± 0.01*
Heart, g	0.15 ± 0.01	0.2 ± 0.02*	0.11 ± 0.01	0.15 ± 0.01*
Serum glucose, mg/dl	243 ± 9	248 ± 29	215 ± 17	281 ± 35
Insulin, ng/ml	0.44 ± 0.05	1.4 ± 0.82	0.34 ± 0.07	0.70 ± 0.11
Triglyceride, mg/dl	79 ± 14	76 ± 20	59 ± 21	75 ± 21
Free fatty acids, mM	0.2 ± 0.04	0.23 ± 0.02	0.35 ± 0.06	0.24 ± 0.03
Leptin, ng/ml	8.8 ± 3.8	25.3 ± 9.8	8.3 ± 4.0	49 ± 16*
Adiponectin, µg/ml	8.9 ± 0.4	9.7 ± 1.1	17.6 ± 1.8	29.7 ± 5.0

Table 1. Metabolic characteristics of 4-month-old *Ankrd26* mutant mice (MT). *, $p < 0.05$ versus wild-type (WT) mice of the same sex. *Proc. Natl. Acad. Sci. U S A.* 2008; 105:270-275.

Recently, the phenotyping of the brain regions that control appetite and energy homeostasis from *Ankrd26*^{-/-} mice has demonstrated that these mice exhibit central leptin resistance, the impairment of melanocortin pathway function, caused by

reduced expression of MC4R and resistance to α -MSH, and defects in the expression and subcellular localization of primary specific-cilium proteins [94]. It is known that mutations in genes that directly influence the expression of signaling or structural proteins of the primary cilia induce disturbances in energy homeostasis in both humans and mice, and are responsible for human obesity in Bardet–Biedl syndrome [43,45,94]. Interestingly, *in vivo* data indicate *Ankrd26* as the first example of a non-cilium-specific protein that is necessary to prevent the development of a ciliopathy associated with morbid obesity [94]. This evidence provides a novel mechanism for genetic obesity, in which membrane and/or scaffold proteins are required for the proper primary ciliary function, and broader spectrum of targets, diagnostic and therapeutic approaches to human obesity than previously considered.

Interestingly, earlier findings in humans have showed that individuals homozygous for SNPs in the coding region of the *ANKRD26* gene (rs139049098), among other SNPs with a predicted damaging impact on the protein related to cilia function, develop rare forms of severe obesity [97].

As cilia are relevant for the proper development and physiology of many cell types, tissues and organs, variations of cilia and ciliary genes may contribute to the obesity risk from a broad spectrum of processes, including adipogenesis, hypothalamic food intake regulation and olfactory perception. The evidence that those genes are players in various etiological processes makes them an interesting potential targets for obesity treatment. Indeed, the obesity phenotype in ciliopathies is a consequence of mutations that impair protein function, thus, overexpression of ciliary genes may provide a new way to prevent obesity [97].

However, more knowledge on regulation of cilia and ciliary gene expression and function should be provided to clarify their actual involvement in obesity. In this scenario, assuming that cilia monitor signals from the environment, it would be interesting to know how cilia and ciliary genes respond to changes in energy availability.

Intriguingly, recent data in the literature have identified *ANKRD26* among several genes, of which the changes in gene expression and/or DNA methylation is associate with modifications in calorie intake and body weight. Indeed, gene expression profiles of the hypothalamus and striatum from C57BL/6J mice treated with the anorectic drugs, subutramine, phenimetrazine and methamphetamine, have revealed that the induced reductions of food intake and weight loss were paralleled by the up-regulation of *Ankrd26* gene expression in the above brain regions [98]. These findings not only suggest that *Ankrd26* may account for biological effects of these drugs, but also that this gene may be a target and transcriptional outcome of specific environmental exposure.

In support of this concept, emerging evidence points to alterations in environmental-induced *ANKRD26* epigenetic regulation, in mouse as well as in human obesity. Indeed, the methylome analysis of murine eAT [78], representative VAT depot in rodents [23], has identified promoter hyper-methylation of *Ankrd26* gene in HFD-fed compared to age- and sex-matched chow diet-fed mice,

suggesting that *Ankrd26* gene is amenable to nutritionally-induced epigenetic modifications. Additionally, computational data from the genome-wide analysis of DNA methylation in human adipose tissue have revealed that *ANKRD26* is included in a list of 2825 genes, for which both DNA methylation and mRNA expression levels significantly correlate with age and BMI [88].

Altogether, these observations paved the way to support the hypothesis that the adipose tissue abnormalities may be accompanied by epigenetic changes at the *ANKRD26* gene, in mice as well as in humans, that may represent one of the molecular mechanisms by which environmental cues may generate adipose tissue dysfunction, contributing to development of obesity and associated comorbidities. Interestingly, pleiotropic meta-analyses of genetic variants, across multiple studies, have recently demonstrated that the *ANKRD26* SNP rs7081476, located on 10p12.1, is associated with a variety of obesity- and age-related endophenotypes and diseases, as elevated BMI, systolic blood pressure, triglycerides and blood glucose, reduced HDL cholesterol and increased hazards of diabetes mellitus (DM), heart failure (HF), atrial fibrillation and coronary heart diseases (CHD) [99]. The effects of this *ANKRD26* variant on DM, HF and CHD are mediated through several endophenotypes, among which BMI has the most significant indirect effect [99].

As outlined above, *in vitro* and *in vivo* studies have clearly demonstrated the close relationship between the impairment of *ANKRD26* expression and/or function and development of obesity and associated comorbidities. However, whether these alterations occurring in obese individuals are exclusively determined by genetic mechanisms, and/or non-genetic mechanisms may also contribute to the same, are issues that still remain to be established. Elucidating how the *ANKRD26* gene is regulated could generate further insight into the molecular bases of obesity as well as novel translational perspectives.

2. AIMS OF THE STUDY

Obesity is a complex and multifactorial chronic disease, resulting from the complex interactions between genetic and environmental factors. It is a growing health problem worldwide and genetic models to explain its epidemic are inadequate because its increase has been too rapid to allow for the appearance of new mutant genes. In addition, increasing evidence show that environmental cues, such as fat-enriched diet, strongly contribute to development and progression of multifactorial disease, by altering gene expression through epigenetic modifications.

Ankrd26 gene is widely expressed in metabolically relevant tissues and organs, as hypothalamus, WAT, liver and skeletal muscle. It has emerged as a new important player in the control of the feeding behavior and in the onset of both obesity and T2D. Indeed, *in vitro* and *in vivo* studies, in mice as well as in humans, have clearly demonstrated the close relationship between the impairment of *ANKRD26* expression and/or function and development of obesity and associated comorbidities. However, whether these alterations occurring in obese individuals are exclusively determined by genetic mechanisms, and/or non-genetic mechanisms may also contribute to the same, are issues that still remain to be established.

Based on this knowledge, the aims of this work are: *i.* to clarify whether and how external stimuli, such as the administration of a high fat diet, could impact on *Ankrd26* expression in different adipose tissue depots; and, *ii.* to evaluate whether chromatin remodeling and epigenetic modifications take part in the regulation of this candidate (*epi*)gene, driving the adipose tissue dysfunction that contributes the onset and progression of obesity.

Since the knowledge about the molecular mechanisms linking specific environmental cues and metabolic disorders are still limited, addressing these issues will provide some insights into epigenetic mechanisms associated with obesity.

3. MATERIALS AND METHODS

3.1 Animal study, diet protocols and metabolic test

Six-week-old C57BL/6J male mice (n=48) from Charles River Laboratories International, Inc. (Wilmington, MA) were hosted at the common facility of the University of Naples Medical School. They were housed under the conditions of temperature-controlled (22°C), a light/dark cycle of 12 hours, with free access to food and water. Two weeks after arrival, mice were randomly divided into two groups of 12 mice each and were fed either a HFD (60 kcal% fat content; Research Diets formulas D12331; Research Diets, Inc., New Brunswick, NJ) or a standard chow diet (STD; 11 kcal% fat content; Research Diets formulas D12329; Research Diets, Inc.) for 8 and 22 weeks. The composition of these diets is reported in the Table 2. Body weight was recorded weekly throughout the study.

The glucose tolerance test (GTT) was performed at the beginning and at the 8- and 22-week diet time points. Mice were fasted overnight and then injected with 2g/kg body weight of glucose. Blood samples were obtained from mice tail and glycaemia was measured by using a glucose analyzer (LifeScan) at the following time points, after glucose injection: 0, 15, 30, 45, 60, 90, 120 min.

Similarly, the insulin tolerance test (ITT) was performed at the beginning and at the 8- and 22-week diet time points. Insulin sensitivity was assessed on 5 hours starved mice and then injected with 0,75 U/kg body weight of insulin. Blood samples were obtained from mice tail and glycaemia was analyzed by using a glucose analyzer (LifeScan). Glucose levels were assessed at the following time points: 0, 15, 30, 45, 60, 90, 120 min after insulin injection.

All the experiments performed on mice were conducted in accordance with the Guide for the Care and Use of Laboratory Animals published by the National Institutes of Health (publication no. 85-23, revised 1996). Protocols were approved by the ethics committee of the “Federico II” University of Naples.

3.2 Western blotting analysis

Tissues were weighed and were homogenized in ice-cold T-PER tissue protein extraction reagent (ThermoFisher Scientific), supplemented with the Complete Protease Inhibitor Mixture Tablets (Roche Applied Science). Differently, the cells were homogenized in ice-cold RIPA buffer [25 mM Tris (pH 7.5), 10 mM EDTA, 10 mM EGTA, 1% Nonidet P-40, 10 µg/ml leupeptin, 2 µg/ml aprotinin, 20 µg/ml PMSF, 100 µM NaF, 50 µM NaPPi, 10 µM Na₃VO₄]. The lysates were kept on ice for 15 min and then cleared by centrifugation at 15,000 × g for 20 min. After lysates clarification, protein concentration was determined using Bradford assay (Bio-Rad). Protein extracts (50 µg) were resolved by SDS-PAGE and blotted on nitrocellulose membranes (Millipore, Billerica, MA). Non-specific binding was

blocked with 5% nonfat milk for 1 hour at the room temperature. Bands were revealed by chemio-luminescence (Amersham, Biosciences). The following antibodies were used: antibody against ANKRD26 (#SC-82505, Santa Cruz Biotechnology), and α -Tubulin (#MA1-19162, Sigma-Aldrich), as loading control.

Formula	D12329		D12331	
	g%	kcal%	g%	kcal%
Protein	16.8	16.4	23	16.4
Carbohydrate	74.3	73.1	35.5	25.5
Fat	4.8	10.5	35.8	58

Formula	D12329		D12331	
	g	kcal	g	kcal
Casein, 30 Mesh	228	912	228	912
DL-Methionine	2	0	2	0
Maltodextrin 10	170	680	170	680
Corn Starch	0	0	0	0
Sucrose	835	3340	175	700
Soybean Oil	25	225	25	225
Coconut Oil, Hydrogenated	40	360	333.5	3001.5
Mineral Mix S10001	40	0	40	0
Sodium Bicarbonate	10.5	0	10.5	0
Potassium Citrate, 1 H ₂ O	4	0	4	0
Choline Bitartrate	2	0	2	0
FD&C Blue Dye	0.1	0	0.1	0
Vitamin Mix V10001	10	40	10	40
Total	1366.6	5557	1000.1	5558.5

Table 2. Composition of diets, D12329 and D12331

3.3 Real time PCR (qPCR)

The cDNA synthesis was generated from 1 μ g of total RNA by using Superscript III (Invitrogen, Life Technologies). After cDNA synthesis, Real time PCR was performed on CFX96 (Biorad) in a final volume of 10 μ l containing 20 ng of cDNA, 5 μ l of iTaq Universal SYBR Green Supermix (Biorad) and specific forward and reverse primers (Sigma). For in vivo study, the results of Real time analysis are expressed as the ratio between the copy number variation (CNV) of *Ankrd26* and that of the reference gene.

3.4 Methylated DNA Immunoprecipitation (MeDIP)

DNA methylation enrichment was evaluated on genomic DNA isolated from eAT of STD- and HFD-fed mice and from 3T3-L1 adipocytes. MeDIP assay was performed as described by *Weber et al.* [100]. Sonicated pooled genomic DNA from WAT was immunoprecipitated using anti-5meCpG Q11 (#ab10805, Abcam) or mouse IgG with anti-mouse IgG beads (#10003D, Life Technologies). DNA methylation enrichment on recovered DNA was evaluated by qPCR. Samples were

normalized to their respective input using the $2^{-\Delta CT}$ method.

3.5 Bisulfite sequencing

For bisulfite sequencing analysis, was used genomic DNA isolated from eAT of STD- and HFD-fed mice. Bisulfite conversion of DNA was performed with the EZ DNA Methylation Kit (Zymo Research), following manufacturer's instructions. Converted DNA was amplified by PCR and PCR products were cloned into the pGEM T-Easy vector (Promega). For sequencing analysis, 10 clones for each sample were sequenced on AB 3500 genetic analyzer (Life Technologies). DNA methylation percentage at the -436 and -431 bp CpGs for each mouse was calculated using the formula: DNA methylation % = [methylated CpGs/(methylated CpGs + unmethylated CpGs)]*100.

3.6 Cloning strategy, site-direct mutagenesis and *in vitro* methylation

The *Ankrd26* promoter region encompassing -733 bp to -344 bp flanking TSS, was PCR amplified using murine genomic DNA with primers having restriction sites AvrII and BamHI at 5' and 3' ends respectively. The purified PCR fragment was cloned into the firefly luciferase reporter pCpGfree-promoter-Lucia vector (Invivogen).

The following site-specific mutated constructs were generated by PCR-based mutagenesis: pCpG-*Ankrd26*-436, pCpG-*Ankrd26*-431, pCpG-*Ankrd26*-391. The wild type (Wt) pCpG-*Ankrd26* vector, used as template, was removed from the PCR reaction by DpnI digestion (New England BioLabs). Wt and mutated (mut) vectors were amplified into *E. coli* GT115 cells (Invivogen). Site-specific mutagenesis of each construct was validated by sequencing.

In vitro methylation was performed by using the CpG methyltransferase M.SsI (New England BioLabs). Plasmid DNA (10 µg) was incubated with M.SsI (2 U/µg) in the presence of 640 µM S-Adenosylmethionine (SAM; New England Biolabs) at 37°C for 4 h, with subsequent inactivation of enzyme at 60°C for 20 min. Un-methylated DNA was obtained in the absence of M.SsI (mock-methylated). The methylation was confirmed by resistance to HpyCH4IV digestion (10 U/µg; New England BioLabs).

3.7 Luciferase assay

NIH-3T3 cells were transfected with methylated or un-methylated Wt or mutagenized pCpG-*Ankrd26* vector and Renilla control vector (Promega) by lipofectamine (Life Technologies), following manufacturer's instructions. Where indicated, cells were co-transfected with pCl.p300 expression vector (Promega). Forty-eight hours after transfection, the culture media and the cell lysates were assayed for firefly and renilla luciferase activity. Firefly luciferase activity of each transfection was normalized for transfection efficiency against Renilla luciferase activity.

3.8 Chromatin Immunoprecipitation (ChIP) and Micrococcal Nuclease (MNase) assays

ChIP and MNase assays were performed as described [101,102]. Briefly, 100 mg of eAT were cross-linked with 1% formaldehyde for 15 min at 37°C. The cross-linking reaction was stopped by the addition of glycine 125mM. For ChIP assay, the cross-linked samples were lysed and sonicated to achieve chromatin fragments ranging between 500 and 1000 bp in size. The lysates were incubated at 4°C overnight with the following appropriated antibodies: anti-p300 (#SC-585, Santa Cruz Biotechnology), anti-Ac-H4-K16 (#07-329, Millipore, Temecula, CA), anti-DNMT1 (#NB100-56519) and anti-DNMT3b (#NB300-516) from Novus Biologicals, anti-DNMT3a (#ab2850), anti-MBD2 (#ab38646), and anti-RNA Pol II (#ab5408) from Abcam. Normal anti-rabbit IgG (#I8140) and anti-mouse IgG (#I8765) from Sigma-Aldrich were used as negative control. Immunoprecipitates and INPUT controls were eluted by freshly prepared 1% SDS, 0.1M NaHCO₃ buffer. After reversion cross-linking, DNA was purified by the QIAquick PCR purification kit (Qiagen) followed by qPCR. Samples were normalized to their respective input using the 2^{-ΔCT} method and corrected to negative control.

For MNase assay, the nuclei were isolated from 100 mg of eAT, suspended in wash buffer [100 mmol/L Tris-HCl, 15 mmol/L NaCl, 60 mmol/L KCl, 1 mmol/L CaCl₂] and treated with 200 U of MNase for 20 min at 37°C. Cross-link reversal was performed at 65°C for 16 hours, followed by an RNase treatment and proteinase K digestion. DNA was purified by phenol–chloroform. Samples were then run on 1% agarose gel and the resulting mononucleosomal DNA fragments (~ 150 bp) were gel purified. For both assays, relative protein binding and nucleosome occupancy to the *Ankrd26* promoter region were evaluated on recovered DNA by qPCR. Samples were normalized to their respective input using the 2^{-ΔCT} method.

3.9 Electrophoretic mobility shift assay (EMSA)

Nuclear proteins were extracted from NIH-3T3 cells by NE-PER Nuclear and Cytoplasmic Extraction Kit (ThermoFisher Scientific) according to the manufacturer's protocol. The *Ankrd26* promoter region spanning from -455 bp to -425 bp and including the p300 response element, was used as probe to detect sequence-specific p300 binding *in vitro*. Protein-DNA complexes were detected using unlabeled or biotin end-labeled double-stranded DNA probes by annealing complementary oligonucleotides. Biotin 3'-end oligonucleotides were from Sigma-Aldrich and where indicated were synthesized to incorporate methylated cytosines (meC). The binding reaction was performed using the LightShift kit (ThermoFisher Scientific) as described below. Before the addition of labeled probe, 10 µg of nuclear extracts were incubated for 20 min on ice in 20 µl of reaction buffer, containing 5% glycerol, 1 mM MgCl₂, 50 mM KCl, 0.5 mM EDTA, 50 ng of double-stranded poly (dI-dC). Biotin-labeled probe (20 fmol) was

added and the reaction was allowed to incubate for 20 min at room temperature. In the competition experiments, the nuclear extracts were preincubated with 200 molar excess of unlabeled probes for 20 min on ice. In super-shift experiments, 2 µg of p300 antibody (#SC-585, Santa Cruz Biotechnology) or 2 µg of rabbit IgG (#I8140, Sigma-Aldrich) were preincubated with nuclear extracts for 1 hour on ice. Protein-DNA complexes were separated on native polyacrylamide gel, transferred onto nylon membrane and detected by the LightShift Chemiluminescent EMSA kit (ThermoFisher Scientific) following the manufacturer's procedure.

3.10 Primer Sequences

The oligonucleotides used for PCR, qPCR, MeDIP, bisulfite sequencing, ChIP, MNase, EMSA are listed in the Table 3.

Technique	Gene/Region	Primer sequence
qPCR	<i>Ankrd26</i>	F 5'-CTTTGGACGCGAGAGTGCTA-3' R 5'-AGCAGTCCTGTCTTCTTGTC-3'
	<i>β-Actin</i>	F 5'-AAGATCAAGATCATTGCTCCTCCTG-3' R 5'-AGCTCAGTAACAGTCCGCCT-3'
	<i>ANKRD26</i>	F 5'-GTATGCTAGTAGTGGTCTGC-3' R 5'-GTAGGCCTTCCTTCATCCTCAT-3'
	<i>RPL13A</i>	F 5'-CTTTCCGCTCGGCTGTTTC-3' R 5'-GCCTTACGTCTGCGGATCTT-3'
MeDIP-qPCR	<i>Ankrd26</i> S1	F 5'-CTGCAAGGCTTCAACAGGAA-3' R 5'-ACAAAATCTCTCCCTTACTCTTCC-3'
	<i>Ankrd26</i> S2	F 5'-TGGAACAACACACTGCCCA-3' R 5'-AACGCAGTAGGGCACTTAT-3'
Bisulfite sequencing	<i>Ankrd26</i> Region 1	F 5'-TAAATTATTTAGTTAATAAAATTTTTTTT-3' R 5'-TCTTTACTATTCAAAAAATCAAAAC-3'
	<i>Ankrd26</i> Region 2	F 5'-TTTTGATTTTTTGAATAGTAAAGAAGG-3' R 5'-CCTTATAAATCTTACCCATATCCTTATC-3'
Cloning and mutagenesis	<i>Ankrd26</i> Wild Type	F 5'-GCCCTAGGCCCTTGAGGTGAGTTGTGGCT-3' R 5'-GCGGATCCGGCAGTTAAACCTGTTGGGG-3'
	<i>Ankrd26</i> Mut -436	F 5'-TCCCTTACTCTTCCATGCCACGATTCCATCC-3' R 5'-GGATGGAATCGTGGCATGGAAGAGTAAGGGA-3'
	<i>Ankrd26</i> Mut -431	F 5'-ACTCTCCACGCCATGATTCCATCCATGC-3' R 5'-GCATGGATGGAATCATGGCGTGAAGAGT-3'
	<i>Ankrd26</i> Mut -391	F 5'-GTAGTTTACTTTTTGATTATTGCCTACCTAGAGTCCAATAG-3' R 5'-CTATTGGACTCTAGGTAGGCAATAATCAAAAAGTAAACTAC-3'
ChIP-qPCR and MNase	p300/DNMTs/MBD2	F 5'-ACCTCCCATCAGCTTGTCTAAC-3' R 5'-GCCTTGTTTCAGTGGCAG-3'
	bs <i>Ankrd26</i>	
	-257/-198	F 5'-TCCTGGAGTACTGGGTCTGG-3' R 5'-AGGCTTCAACAGGAATGGGG-3'
	Nuc-2 <i>Ankrd26</i>	
	-84/-25	F 5'-CCTGAACAGCAAAGAAGGCG-3' R 5'-CAGCGACCAAGTGCCAG-3'
	Nuc-1 <i>Ankrd26</i>	
EMSA	+16/+159	F 5'-GTTGCTAGTTTGACAGTCGG-3' R 5'-CAACGTTGGCTGACAACACA-3'
	TSS <i>Ankrd26</i>	
	Labeled <i>Ankrd26</i> probe	F 5'-CTCTTCCCTTACTCTTCCACGCCACGATTCC-3' [Btm] R 5'-GGAATCGTGGCGTGGAAGAGTAAGGGAAGAG-3' [Btm]
	Un-labeled <i>Ankrd26</i> probe	F 5'-CTCTTCCCTTACTCTTCCACGCCACGATTCC-3' R 5'-GGAATCGTGGCGTGGAAGAGTAAGGGAAGAG-3'
	Un-labeled Methy <i>Ankrd26</i> probe	F 5'-CTCTTCCCTTACTCTTCCA ^{me} CGCCA ^{me} CGATTCC-3' R 5'-GGAAT ^{me} CGTGG ^{me} CGTGGAAGAGTAAGGGAAGAG-3'
	Un-labeled Mut <i>Ankrd26</i> probe	F 5'-CTCTTCCCTTACTCTTCCATGCCATGATTCC-3' R 5'-GGAATCATGGCATGGAAGAGTAAGGGAAGAG-3'

Table 3. Oligonucleotide sequences. Methylated CpGs are indicated as meC. Mutated cytosines (C → T) are indicated in bold. F, forward; R, reverse.

3.11 Cell culture and transfection

3T3-L1 preadipocytes were maintained as a subconfluent monolayer culture and differentiation was induced by placing cells in differentiation cocktail (DMEM with 10% FBS, 1 µg/ml bovine insulin, 1 µM dexamethasone and 0.5 mM IBMX) for 48 hours and then changing the medium every two days with DMEM with 10% FBS and 1 µg/ml insulin. The cells were fully differentiated 8 days after induction, as evidenced by observation of lipid droplet formation. The mature adipocytes were *i.* silenced with 25 nmol/l of scrambled-siRNA or *Ankrd26*-siRNA for 48 hours, or *ii.* treated with palmitate (0.250 mM; Sigma-Aldrich), or oleate (0.250 mM; Sigma-Aldrich) or corresponding vehicle (diluent solution with the same

concentrations of BSA and ethanol of the Fatty Acid/BSA complex solution) for 96 hours, or *iii.* treated with leptin (100 nM; R&D Systems) or corresponding vehicle (20 mM Tris-HCl, pH 8.0) for 24 hours. Adipokines were assayed in media from silenced cells by Bio-Plex Pro Mouse Cytokine Immunoassay following the manufacturer's protocol (Bio-Rad). *Ankrd26* promoter methylation and gene expression in cell cultures were analyzed as previously described in this section.

3.12 Fatty Acid/BSA complex solution preparation

Palmitate and oleate have been conjugated to fatty acid-free BSA (2:1 molar ratio Fatty Acid/BSA) as described by [103]. The stock solution of palmitate (100 nM) was dissolved at 70 °C in 50% ethanol in a shaking water bath. In parallel, the fatty acid-free BSA solution was prepared at 55 °C in NaCl in a shaking water bath. Finally, the palmitate and the fatty acid-free BSA solutions were complexed at 55 °C in a shaking water bath, cooled to room temperature and sterile filtered. Oleate was complexed to the fatty acid-free BSA solution following the same protocol. For fatty acid cell treatment, control adipocytes were treated with diluent only, corresponding concentrations of BSA and ethanol.

3.13 Patient enrollment and tests

Abdominal VAT biopsies and serum samples were obtained from patients undergoing bariatric surgery. A cohort of 11 normal glucose tolerance (NGT) obese subjects was selected for *in vivo* human study. The baseline characteristics of the enrolled subjects are reported in the Table 4. Participants with metabolic and endocrine disorders, inflammatory diseases, previous or current malignancies, and/or treated with drugs able to interfere with the epigenome were excluded from the study. Secreted mediators were assayed in serum samples by Bioplex multiplex Human Cytokine, Chemokine and Growth factor kit (Bio-Rad) following manufacturer's protocol. *ANKRD26* gene expression in VAT was analyzed as previously described in this section. This study adhered to the Declaration of Helsinki and has been reviewed and approved by the Ethics Committee of the “Federico II” University of Naples (Ethics Approval Number: No. 225_2013). Informed consent was obtained from all of enrolled individuals.

	Subjects, n=11(5M/6F)	
	Mean \pm SD	Range
General variables		
Age (years)	27.4 \pm 5.6	19.0 - 46.0
BMI (Kg/m ²)	43.6 \pm 9.3	32.6 - 61.0
Fasting glucose (mmol/l)	4.8 \pm 0.4	4.3 - 5.8
Fasting insulin (pmol/l)	105.9 \pm 31.5	63.2 -154.9
HOMA-IR	3.0 \pm 1.2	1.3 - 5.1
OGTT plasma glucose (mmol/l)	6.4 \pm 0.8	5.0 - 7.0

Table 4. Baseline characteristics of the obese subjects with normal glucose tolerance. Data are means \pm SD of determinations. For each variable, the lowest and the higher values are shown. BMI, Body Mass Index; OGTT, Oral Glucose Tolerance Test.

3.14 Statistical analysis

The area under the curve (AUC) was calculated using the trapezoidal rule. Data are expressed as mean \pm SD. Statistical significance of the differences between groups was determined by two-tailed unpaired Student's t test or the one-way analysis of variance, as appropriate, using GraphPad Software (version 6.00 for Windows). Correlation between two variables was calculated using the parametric Pearson *r*-test. $p < 0.05$ was considered statistically significant.

4. RESULTS

4.1 Animal study design

It has been well demonstrated the link between obesity, diet and epigenetic mechanisms both in animal models and in humans. The administration of high fat diet to several animal species leads to obesity and induces disease signs that model human T2D. Moreover, diet-induced obesity (DIO) in the mouse, in the absence of mutation of selected genes, provide a powerful tool for identifying epigenetic and environmental mechanisms potentially involved.

C57BL6/J is a well-established model for studies of metabolic diseases and the most commonly used mouse strain for diet-induced obesity. Indeed, this strain develops severe obesity, hyperglycemia and insulin resistance if weaned onto HFD, and therefore it was used for this study.

Animals were acclimated for 2 weeks before experiments and diet protocol started when mice were 8 week-old. To avoid sex hormone influences, exclusively male mice were used in this study. They were randomly divided into two groups of 12 mice each and were fed either a HFD or a STD. After each time point of diet protocol, mice were sacrificed and tissues collected for further analysis (fig. 10).

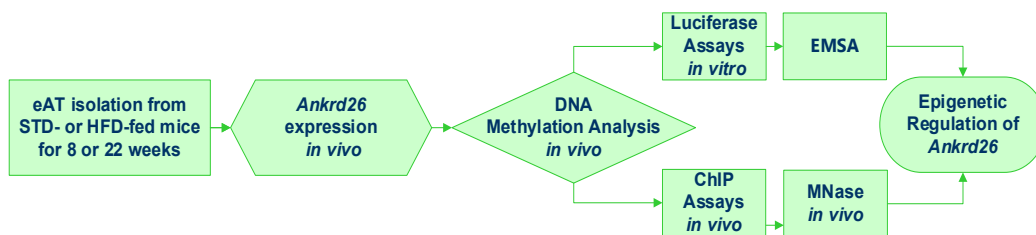


Figure 10. Experimental study design for diet-induced obesity. In the current study, two different diet regimens were used to investigate the potential pathophysiologic effect of epigenetic regulation of *Ankrd26* gene in obesity-related adipose tissue dysfunction.

4.2 Metabolic characteristics of standard and high fat diet mice

Body weight and food intake were weekly evaluated during each diet protocol duration. Table 5 reports the difference in body weight of STD- and HFD-fed mice at 8 and 22 weeks of diet protocol. HFD mice significantly increased their body weight after 8 and 22 weeks of feeding (16-week-old HFD 34.4 ± 3.2 g vs 16-week-old STD 24.7 ± 2.1 g, p -value<0.001; 30-week-old HFD 38.8 ± 3.3 g vs 30-week-old STD 26.4 ± 2.8 g, p -value<0.001). Concomitantly, these obese mice also exhibited an impairment of glucose metabolism (tab. 5). The glucose homeostasis of these mice, was assessed by measuring the blood glucose levels and the glucose tolerance. Fasting blood glucose was significantly increased in HFD group compared to STD mice (16-week-old HFD 7.7 ± 1.7 mmol/l vs 16-week-old STD 5.9 ± 0.9 mmol/l, p -value<0.001; 30-week-old HFD 9.1 ± 1.8 mmol/l vs 30-week-

old STD 5.8 ± 1.2 mmol/l, p -value<0.001). Additionally, during GTT, glucose loading rendered HFD-fed mice significantly more hyperglycemic than control mice during the following 120 min, revealing a strong impairment of glucose tolerance after 8 and 22 weeks of diet regimens. Furthermore, as showed in the Table 5, after intraperitoneal insulin injection HFD mice displayed reduced insulin sensitivity compared to the control mice. Therefore, upon 8 and 22 weeks of high fat diet treatment, mice become both glucose intolerant and insulin resistant.

Variable	16 week-old		30 week-old	
	STD (n=12)	HFD (n=12)	STD (n=12)	HFD (n=12)
Body weight (g)	24.7 ± 2.1	34.4 ± 3.2^a	26.4 ± 2.8	$38.8 \pm 3.3^{b,c}$
Fasting glucose (mmol/l)	5.9 ± 0.9	7.7 ± 1.7^a	5.8 ± 1.2	9.1 ± 1.8^b
GTT AUC (mmol/l 120 min ⁻¹)	725.7 ± 103.3	1290.7 ± 162.4^a	653.6 ± 150.0	1344.2 ± 172.2^b
ITT AUCi (mmol/l 120 min ⁻¹)	741.6 ± 127.0	355.7 ± 132.2^a	681.0 ± 128.9	312.9 ± 117.6^b

Table 5. Effect of HFD on Body weight, fasting blood glucose, glucose tolerance and insulin sensitivity. 8-week-old male C57BL/6J mice were fed a high-fat diet (HFD) or a standard chow diet (STD) for 8 and 22 weeks. Body weight, fasting blood glucose, glucose tolerance test (GTT) Area Under the Curve (AUC) and insulin tolerance test (ITT) AUCi were reported. Data are mean \pm SD of determinations. ^a p <0.001, 16-week-old HFD vs 16-week-old STD; ^b p <0.001, 30-week-old HFD vs 30-week-old STD; and ^c p <0.001, 30-week-old HFD vs 16-week-old HFD.

4.3 Effect of HFD on *Ankrd26* gene expression in visceral adipose tissue

As mentioned before, *Ankrd26* gene is widely expressed in metabolically relevant tissues including WAT, and, both *in vitro* and *in vivo* studies have clearly demonstrated the close relationship between the impairment of *Ankrd26* expression and/or function and development of obesity and associated comorbidities, in mice as well as in humans. In this context, it has been investigated whether *Ankrd26* expression could be affected by external cues, in particular by a high fat diet administration.

Therefore, by immunoblotting analysis it has been compared the *Ankrd26* protein levels in visceral adipose tissues of mice fed with standard or high fat diet for 8 and 22 weeks. The results show that obese mice have higher *Ankrd26* protein levels than lean control mice in eAT after 22 weeks of HFD regimen, but not after 8 weeks of the same obesogenic treatment (fig. 11).

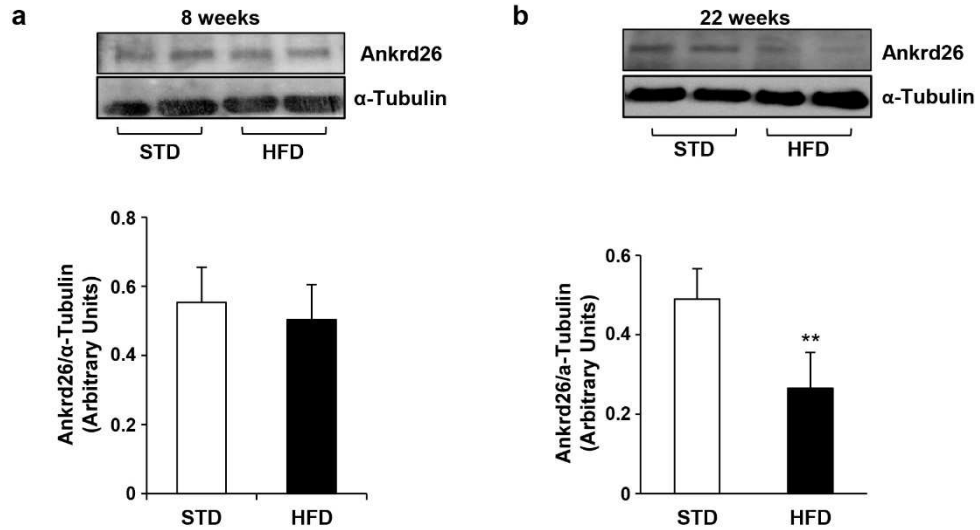


Figure 11. Ankrd26 protein expression in eAT. Western blot analysis of Ankrd26: total protein extracts obtained from eAT (50μg) of C57BL/6J mice fed a standard diet (STD) or high fat diet (HFD) for 8 and 22 weeks were separated by SDS-PAGE followed by immunoblotting with Ankrd26 antibody; alpha-tubulin was used as a loading control. **(a)** Representative western blot for Ankrd26 and α-Tubulin and densitometric analyses of the data from mice upon 8 weeks of STD or HFD treatments. **(b)** Representative western blot for Ankrd26 and α-Tubulin and densitometric analyses of the data from mice upon 22 weeks of STD or HFD treatments. **(a-b)** Bars represent mean ± SD from three independent experiments. **(b)** Asterisks denote statistically significant differences (** $p < 0.01$ vs STD).

Consequently, to further investigate whether the increased Ankrd26 expression, induced by long-term HFD treatment, is linked to a transcriptional regulation of *Ankrd26* gene, its mRNA expression has been evaluated in eAT by performing qPCR (fig. 12). The obtained results confirmed western blot analysis. Indeed, *Ankrd26* mRNA showed no differences between HFD- and STD-fed mice after 8 weeks of diet regimens (fig. 12a). On the other hand, the treatment with HFD for 22 weeks led to a significant decrease in *Ankrd26* mRNA levels ($p < 0.001$) in obese mice compared to lean controls (fig. 12b).

Interestingly, HFD treatment for 4 additional weeks did not elicit any further decrease in *Ankrd26* mRNA expression in the eAT of HFD-fed mice (34 week-old STD, *Ankrd26* mRNA: $2.29 \times 10^{-3} \pm 0.11 \times 10^{-3}$ AU; 34 week-old HFD, *Ankrd26* mRNA: $1.36 \times 10^{-3} \pm 0.19 \times 10^{-3}$ AU; $p < 0.001$), suggesting that the aging does not have a role in mediating the transcriptional regulatory response of *Ankrd26* gene to prolonged obesogenic diet.

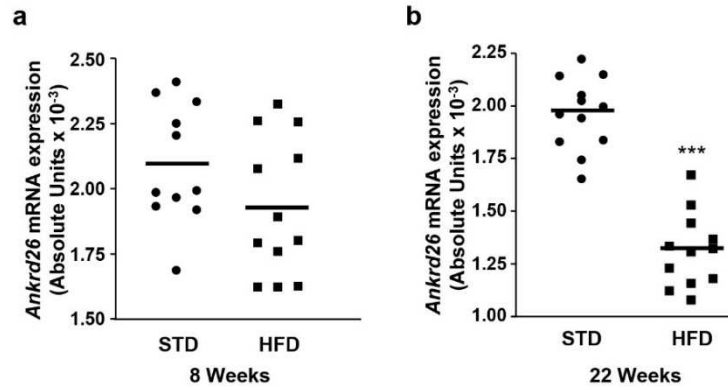


Figure 12. *Ankrd26* mRNA expression levels in eAT. *Ankrd26* mRNA levels were measured performing absolute cDNA quantification by qPCR analysis. Data are shown as copy number variation (CNV) of *Ankrd26* normalized on CNV of a reference gene, and are expressed in absolute units (AU). *Ankrd26* mRNA for standard diet (STD)- (n=12) and high fat diet (HFD)-fed (n=12) mice, upon 8 weeks (a) and 22 weeks (b) of diet regimens. (b) Asterisks denote statistically significant differences (***) $p < 0.001$ vs STD).

To determine whether the down-regulation of *Ankrd26* expression in the eAT during obesity is a depot-specific phenomenon or is feature of VAT dysfunction, the transcript levels of *Ankrd26* gene have been determined in another VAT depot: the mesenteric adipose tissue (mAT). As shown in Figure 13, *Ankrd26* mRNA expression was significantly lowered by long-term HFD treatment also in the mAT of obese mice ($p < 0.01$).

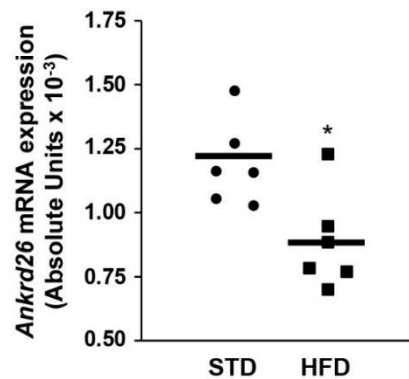


Figure 13. *Ankrd26* mRNA expression levels in mAT. *Ankrd26* mRNA levels were measured performing absolute cDNA quantification by qPCR analysis. Data are shown as copy number variation (CNV) of *Ankrd26* normalized on CNV of a reference gene, and are expressed in absolute units (AU). *Ankrd26* mRNA for standard diet (STD)- (n=6) and high fat diet (HFD)-fed (n=6) mice upon 22 weeks of diet regimens. (b) Asterisks denote statistically significant differences (*) $p < 0.05$ vs STD).

Moreover, real time analysis suggest that *Ankrd26* mRNA levels are higher in the eAT than in the mAT, however the data indicate that high fat diet affects *Ankrd26* expression at transcriptional levels and this regulation seems to be a specific response of VAT depots.

Therefore, for the first time it has been demonstrated that *Ankrd26* can be modulated by environmental cues.

4.4 Effect of HFD on DNA methylation at *Ankrd26* promoter

Among various biological processes, DNA methylation is one of the key transcriptional regulatory mechanisms governing the accessibility of transcription machinery to target sites, through modulation of chromatin structure. Furthermore, recent findings have shown that DNA methylation is an active regulatory mechanism responding to the changes in nutrient cues, with multiple impacts on the regulation of systemic energy homeostasis.

To gain insight into the involvement of DNA methylation in the obesity-induced decrease of *Ankrd26* expression, Methylated DNA Immunoprecipitation (MeDIP) assay has been adopted to investigate the DNA methylation levels of the *Ankrd26* promoter and 5'-untranslated regions (5' UTR) in eAT of STD- and HFD-fed mice, upon 22 weeks of diet regimens. The degree of DNA methylation of *Ankrd26* promoter was examined in a region positioned 500 bp upstream of *Ankrd26* TSS, that has been arbitrarily subdivided in two segments: S1 (from -462 to -193 base pairs) and S2 (from -158 to +140 base pairs) (fig.14). The results obtained showed a 2-fold enrichment in DNA methylation in the promoter region encompassing the positions -462 to -193 base pairs in obese mice compared to lean controls. Conversely, no DNA methylation enrichment was observed in the region located around the TSS, ranging from -158 to +140 base pairs.

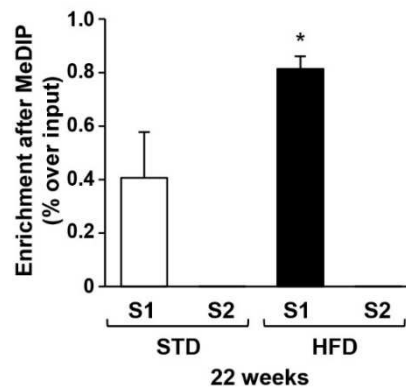


Figure 14. Methylation analysis of the *Ankrd26* gene by MeDIP assay. Relative quantification of *Ankrd26* promoter region DNA immunoprecipitated with anti-5meCpG in eAT of standard diet (STD) and high fat diet (HFD) mice. DNA immunoprecipitation was followed by qPCR amplification with primers spanning the 500 bp upstream the *Ankrd26* TSS. Results are expressed as enrichment relative to input (%) and corrected for IgG control levels both at segment 1 (S1; -462 bp/-193 bp) and segment 2 (S2; -158 bp/+140 bp) of *Ankrd26* promoter region. Data are means \pm SD from three independent experiments. Asterisks denote statistically significant differences (* p <0.05 vs STD).

To further validate the HFD-induced DNA methylation changes occurring at the *Ankrd26* gene and determine the specific methylation profile of 9 CpGs located in the promoter region that showed a more enrichment in the MeDIP signal, the

Ankrd26-associated differentially methylated region (DMR) has been subjected to bisulphite treatment and then directly sequenced. As shown in Figure 15a, this procedure revealed an average 10% increased DNA methylation of this region from HFD compared with STD-exposed mice, validating the MeDIP data. In particular, the DMR featured a significantly higher DNA methylation density in 2 close cytosine residues at -436 and -431 base pairs from the *Ankrd26* TSS in obese mice compared to lean controls (fig. 15b). In addition, plotting the combined percentage of the DNA methylation at these specific cytosine residues versus the amount of *Ankrd26* mRNA revealed a strong inverse correlation ($n=8$, $r=0.952$, $p<0.001$).

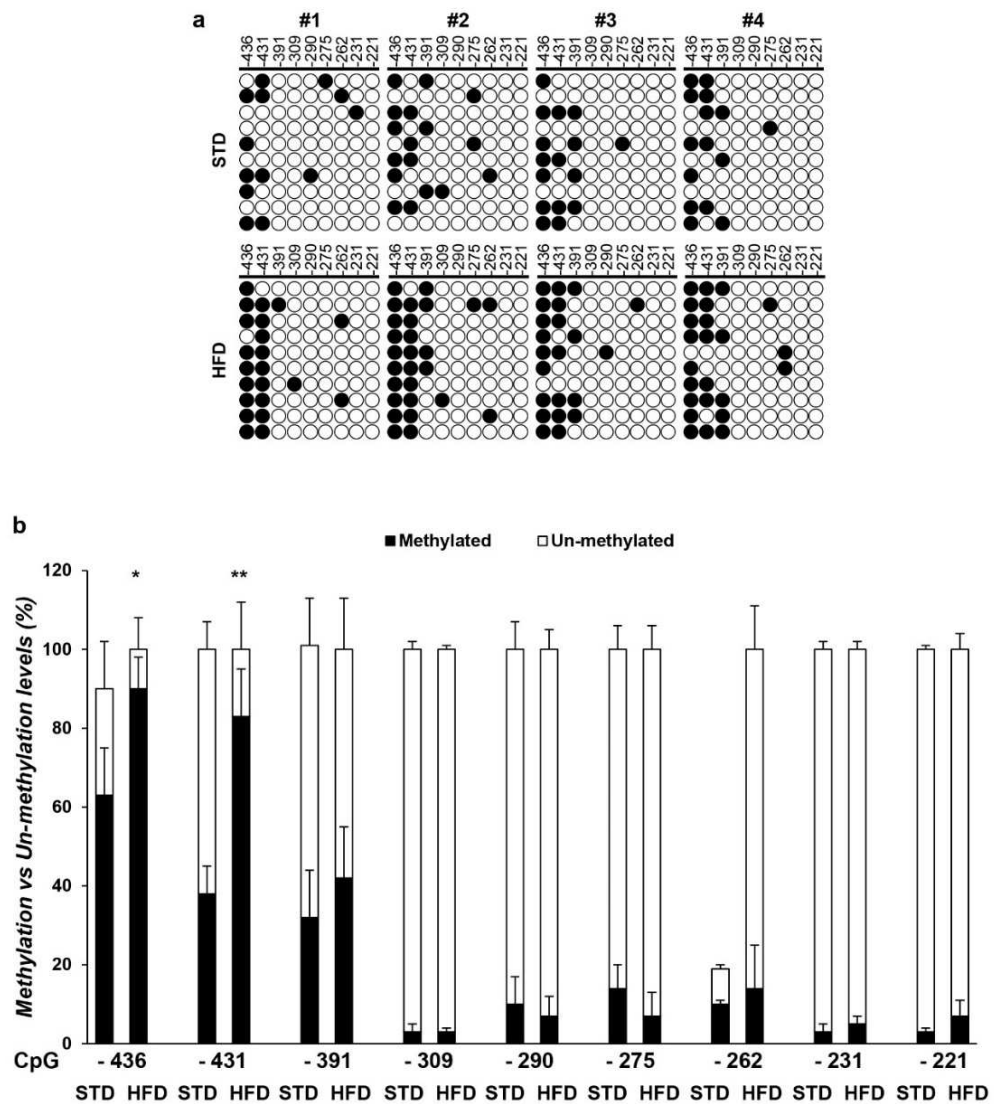


Figure 15. *Ankrd26* promoter is specifically hyper-methylated in obese mice after 22 weeks of high fat diet. Graphic representation and results of the bisulphite-sequenced portion of the DMR relative to the *Ankrd26* locus. **(a)** Bisulfite sequencing of *Ankrd26* promoter region (-462 bp/-193 bp) in standard diet (STD)- ($n=4$) and high fat diet (HFD)-fed ($n=4$) mice. Each horizontal row represents a single independent clone; the methylation percentages of 10 individual clones are indicated, with un-methylated (○) and methylated (●) CpG sites. CpG position relative to *Ankrd26* TSS is shown above each column. **(b)** Bars are means \pm SD of 4 animals/group. Asterisks denote statistically significant differences (* $p<0.05$ vs STD; ** $p<0.01$ vs STD).

These data indicate that HFD-induced *Ankrd26* silencing in eAT of obese mice is accompanied by a specific increase of DNA methylation at its promoter region, suggesting a functional relevance of these epigenetic changes in *Ankrd26* transcriptional regulation in VAT during obesity. To clarify this point, DNA methylation profile of *Ankrd26*-associated DMR has been also analyzed in eAT of STD and HFD mice upon 8 weeks of diet regimens. As shown in Figure 16, not statistically differences were observed between STD- and HFD-fed mice, as expected, supporting the functional relevance of specific CpG methylation in the epigenetic regulation of *Ankrd26* gene in murine VAT.

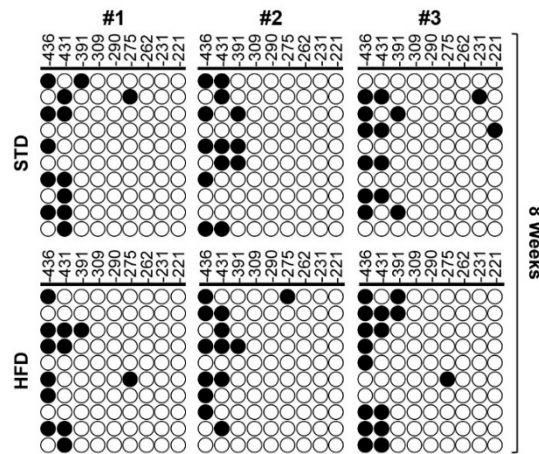


Figure 15. Methylation analysis of *Ankrd26* promoter by bisulfite sequencing in mice upon 8 weeks of diet regimens. Graphic representation of bisulfite sequencing of *Ankrd26* promoter region (-462 bp/-193 bp) in standard diet (STD)- (n=3) and high fat diet (HFD)-fed (n=3) mice. Each horizontal row represents a single independent clone; the methylation percentages of 10 individual clones are indicated, with un-methylated (○) and methylated (●) CpG sites. CpG position relative to *Ankrd26* TSS is shown above each column.

4.5 Role of free fatty acids in epigenetic regulation of *Ankrd26* gene

It has well known that alterations in the extracellular milieu, including elevated free fatty acids and hyperleptinemia, are features of DIO mice, when they are weaned onto HFD [104]. To investigate whether diet-induced obesity or specific fats is responsible for the changes in *Ankrd26* expression and methylation associated to HFD exposure, cultured 3T3-L1 mature adipocytes have been used and screened for putative factors involved in *Ankrd26* methylation. Supplementation of the culture medium with 0.25 mM palmitate, a major component of the HFD, decreased *Ankrd26* expression (fig. 17a) and increased its promoter methylation (fig. 17c) to a similar extent as that observed in eAT from HFD-treated mice. Medium supplementation with 0.25 mM oleate or 100 nM leptin did not elicit any significant effect (fig. 17a-d). These results provide further evidence of high CpG methylation in murine adipocyte fraction and, collectively, demonstrate that the transcriptional repression accompanying the epigenetic dysregulation of *Ankrd26* may have been, at least in part, caused by the saturated fat enrichment of the diet rather than representing a consequence of obesity.

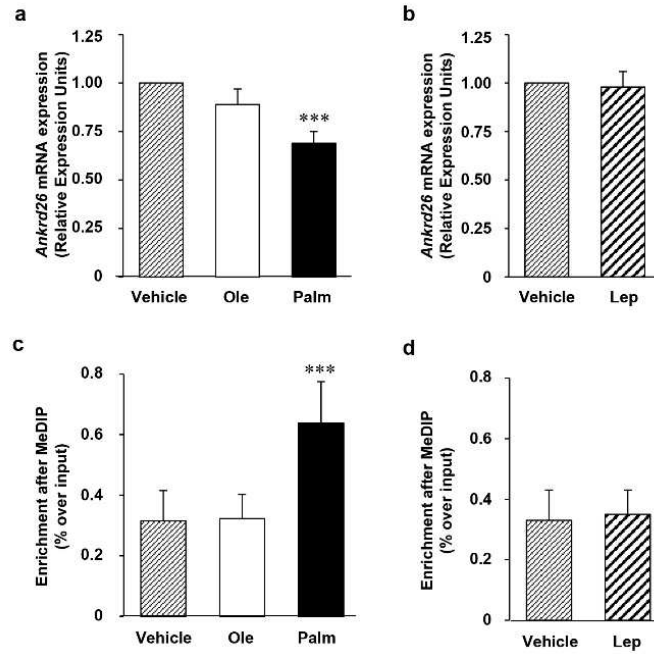


Figure 17. Ankrd26 expression and DNA methylation changes in mature adipocytes upon treatment with palmitate or oleate for 96 h, or leptin for 24 h. 3T3-L1 mature adipocytes were treated with palmitate (0.250 mM; Palm), or oleate (0.250 mM; Ole) or corresponding vehicle (diluent solution with the same concentrations of BSA and ethanol of the Fatty Acid/BSA complex solution; Vehicle) for 96 h, or treated with leptin (100 nM; Lep) or corresponding vehicle (20 mM Tris-HCl, pH 8.0; Vehicle) for 24 h. (a-b) *Ankrd26* mRNA levels were measured performing relative cDNA quantification by qPCR. (c-d) Relative quantification of *Ankrd26* promoter region DNA immunoprecipitated with anti-5meCpG in treated mature adipocytes. DNA immunoprecipitation was followed by qPCR amplification with primers spanning the 500 bp upstream the *Ankrd26* TSS. Results are expressed as enrichment relative to input (%) and corrected for IgG control levels at segment 1 (S1; -462 bp/-193 bp) of *Ankrd26* promoter region. (a-d) Data are means \pm SD from three independent experiments. Asterisks denote statistically significant differences (*** p <0.001 vs Vehicle).

4.6 Methylation of specific CpG sites controls *Ankrd26* gene expression

Given that DNA methylation located within or close to the 5' region of genes has been associated with regulation of gene expression [104], the effect of specific DNA methylation on *Ankrd26* gene activity has been further investigated by using a CpG-free gene reporter assay. The luciferase assay has been performed in NIH-3T3 cells transfected with *in vitro* methylated (me) or un-methylated (unme) pCpG-*Ankrd26* luciferase reporter vectors, in which the selected region of the *Ankrd26* promoter, spanning the -436, -431 and -391 CpG site, was cloned. The un-methylated portion of *Ankrd26* promoter induced a 2.5-fold increase of luciferase activity compared to the empty vector (fig. 18a) demonstrating, for the first time, that the region from -733 to -344 is sufficient to mediate maximal *Ankrd26* promoter activity. In addition, *in vitro*-methylated portion of *Ankrd26* promoter caused a 35% decrease of luciferase activity compared to the same un-methylated construct (fig. 18a) implying the causal relationship between promoter DNA methylation and transcription of *Ankrd26* gene.

Next, to define whether the -436 or -431 CpG site or both is/are responsible for the regulation of the *Ankrd26* gene activity, C→T mutations have been introduced at -436, -431 or -391 CpG sites into the pCpG-*Ankrd26* luciferase reporter vector

by site-specific mutagenesis. The obtained un-methylated mutagenized constructs have been further used to perform luciferase assays in NIH-3T3 cells. The un-methylated *Ankrd26* construct mutagenized at the -436 CpG site (*Ankrd26*-436unme), similarly to *in vitro*-methylated wild type (Wt) *Ankrd26* construct, showed a 40% reduction of the luciferase activity when compared to un-methylated Wt *Ankrd26* construct (fig. 18b). The same data have been obtained by using un-methylated *Ankrd26* construct mutagenized at the -431 CpG site (*Ankrd26*-431unme) (fig. 18b). Conversely, the un-methylated *Ankrd26* construct mutagenized at the -391 CpG site (*Ankrd26*-391unme) did not elicit any significant difference in luciferase activity in comparison to un-methylated Wt *Ankrd26* construct (fig. 18b).

Therefore, it has been demonstrated, for the first time, that DNA methylation influences *Ankrd26* gene activity and that the transcriptional silencing effect of DNA methylation is mediated, at least in part, through the CpG sites located at -436 and -431 base pairs in the promoter region.

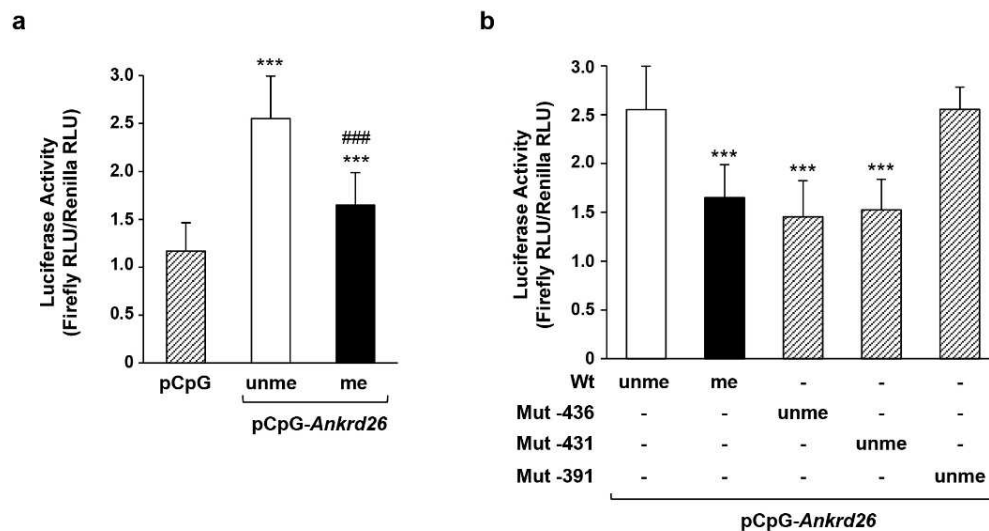


Figure 18. Suppression of the *Ankrd26* promoter activity by specific CpG methylation. (a) Luciferase activity of un-methylated (unme) or *in vitro* methylated (me) or pCpG-*Ankrd26* constructs and of pCpG empty vector. Firefly luciferase activity was normalized to Renilla luciferase activity. Luciferase activity was measured in relative light units (RLU). Data are means \pm SD from three independent experiments. Asterisks denote statistically significant differences *** p <0.001 vs pCpG; ### p <0.001 vs pCpG-*Ankrd26*unme. (b) Luciferase activity of un-methylated mutagenized vectors: pCpG-*Ankrd26*-436, pCpG-*Ankrd26*-431 and pCpG-*Ankrd26*-391. Firefly luciferase activity was normalized to Renilla luciferase activity. Luciferase activity was measured in relative light units (RLU). Data are means \pm SD from three independent experiments. Asterisks denote statistically significant differences *** p <0.001 vs Wt unme.

4.7 DNA methylation suppresses *Ankrd26* promoter activity by impairing the binding of co-activator/acetyltransferase p300

Despite an ongoing debate to what extent CpG methylation is a driver of gene silencing or the consequence thereof, the general view is that methylation has a repressive effect on transcription factor (TF) binding, thus, endogenous methylated motifs containing a CpG at specific sites provide mechanism underlying the epigenetic control of TF binding and gene expression [105].

To test whether methylated -436 and -431 CpG sites impair the binding of transcription factors, TFBIND tools has been used to analyze TF binding motifs in the *Ankrd26* promoter, focusing on nucleotide sequence including these two cytosine residues. The bioinformatics analysis identified a putative binding site for p300, a transcriptional co-activator that acts as histone acetyltransferase and regulates chromatin remodeling [106]. The *Ankrd26* promoter region containing this site spanned nucleotides -442 to -429 upstream the TSS. To examine whether HFD-induced DNA methylation of *Ankrd26* promoter could affect p-300 binding affinity, quantitative Chromatin Immunoprecipitation (ChIP) assay has been performed in eAT of STD- and HFD-fed mice, using p300 antibody. ChIP analysis showed a 40% decrease in p300 binding at *Ankrd26* promoter in obese mice compared to lean controls (fig. 19), indicating that decreasing levels of *Ankrd26* gene in eAT are also accompanied by a lower binding affinity of p300 for the *Ankrd26* promoter.

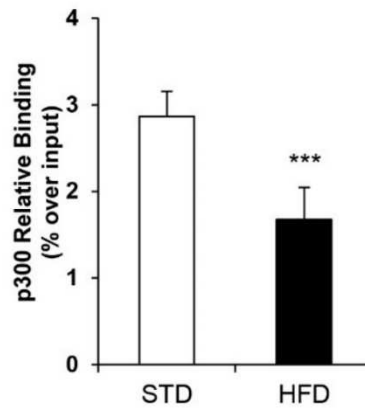


Figure 19. High fat diet impairs the binding of transcriptional co-activator p300 at *Ankrd26* promoter. Relative quantification of *Ankrd26* promoter region DNA immunoprecipitated with anti-p300, in eAT of standard diet (STD) and high fat diet (HFD) mice, upon 22 weeks of diet regimens. Chromatin immunoprecipitation was followed by PCR amplification with primers spanning the *Ankrd26* promoter region containing the putative p300 binding site. Results are expressed as enrichment relative to input (%) and corrected for IgG control levels. Data are means \pm SD of 3 animals/group. Asterisks denote statistically significant differences (** $p < 0.001$ vs STD).

To determine whether p300 directly binds its putative binding site in the *Ankrd26* promoter and the methylation of -436 and -431 CpG sites affects p300-binding affinity, Electrophoretic Mobility Shift Assays (EMSAs) have been performed. For these experiments, it has been necessary to synthesize double-stranded biotinylated probes containing the consensus sequence for p300, with un-methylated, methylated or C→T mutated -436 and -431 CpG sites. Super shift EMSAs with p300 antibody showed that p300 had a strong binding to un-methylated Wt probe, as indicated by the super-shift of one of the complexes formed by the interaction of the probe with the nuclear extract (NE) from NIH-3T3 cells (fig. 20a, lane 3). Moreover, the presence of an un-methylated competitor to the probe/NE mix effectively displaced p300 binding to the probe (fig. 20b, lane 3), while the

probe/p300 complex was not affected by the addition of both a methylated (fig. 19b, lane 4) or a mutagenized competitor (fig. 20b, lane 5). These results indicate that: *i.* p300 binds to its consensus sequence in the *Ankrd26* promoter; and, -436 and -431 cytosine residues have functional significance in p300-binding affinity.

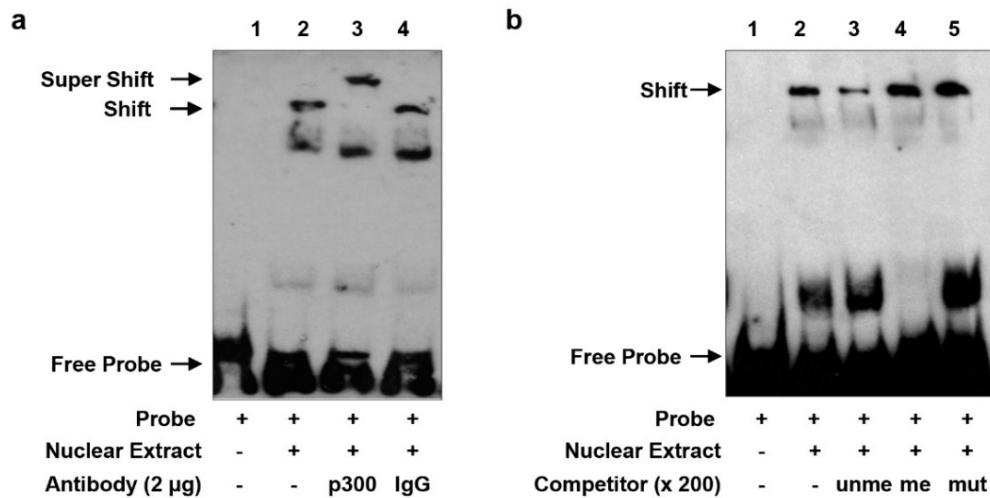


Figure 20. Methylation of -436 and -431 CpG site affects p300-binding affinity to *Ankrd26* promoter. Representative Electrophoretic Mobility Shift Assays (EMSA) for double-stranded biotinylated *Ankrd26* probe with Nuclear Extract (NE) from NIH-3T3 cells. **(a)** Super-shift EMSA with p300 antibody (lane 3) or a rabbit IgG (lane 4). **(b)** Competition EMSAs with 200-fold molar excess of un-labeled un-methylated (unme; lane 3), methylated (me; lane 4) or mutagenized (mut; lane 5) competitor.

To examine whether p300-binding site is crucial for *Ankrd26* promoter activation, a p300 expression vector has been co-transfected into NIH-3T3 cells along with un-methylated or methylated pCpG-*Ankrd26* luciferase reporter vectors. The promoter activity of un-methylated *Ankrd26* construct was increased 3-fold in the presence of p300 (fig. 21). At variance, when p300 was over-expressed, the luciferase activity of the methylated *Ankrd26* construct was 60% lower compared to the un-methylated *Ankrd26* construct (fig. 21).

All together, these data indicate, for the first time, that p300 regulates *Ankrd26* promoter activation and its binding is dependent on the methylation state of the -436 and -431 cytosine residues.

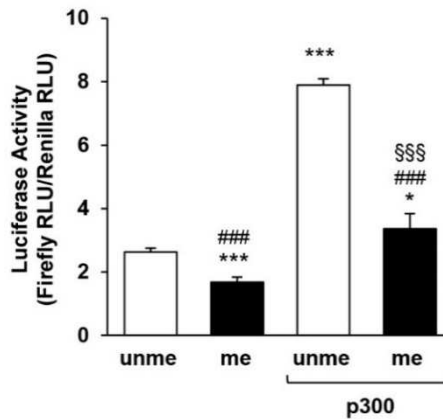


Figure 21. Methylation inhibits *Ankrd26* promoter activity by impairing binding of p300. Luciferase activity of un-methylated (unme) or *in vitro* methylated (me) pCpG-*Ankrd26* construct, in NIH-3T3 cells co-transfected with pCl.p300 vector. Firefly luciferase activity was normalized to Renilla luciferase activity. Luciferase activity was measured in relative light units (RLU). Data are means \pm SD from three independent experiments. Asterisks denote statistically significant differences (***) $p < 0.001$ vs pCpG-*Ankrd26* unme; ### $p < 0.001$ vs pCpG-*Ankrd26* unme+pCl.p300; §§§ $p < 0.001$ vs pCpG-*Ankrd26* me).

4.8 HFD-induced differential recruitment of DNMTs and MBD2 initiates the repression and silencing of *Ankrd26* gene

DNA methylation of *Ankrd26* promoter influences binding of p300 to DNA, both *in vitro* and *in vivo*, potentially leading changes in the occupancy and activity of TFs and/or epigenetic modifying enzymes based on methylation of their recognition motifs. Thus, ChIP assays have been performed to analyze the molecular events upstream the methylation-induced displacement of p300 binding to *Ankrd26* promoter.

First, it has been verified which DNMTs among the three isoforms in mammals, DNMT1, DNMT3a and DNMT3b [72], were responsible for the HFD-induced hyper-methylation of *Ankrd26* promoter. ChIP analysis showed that the levels of DNMT3a and DNMT3b binding observed at the *Ankrd26* promoter was significantly increased in eAT from the obese mice compared to lean controls ($p < 0.001$), whereas no changes were observed in the levels of DNMT1 binding (fig. 22a).

Then, to get further insight into the functional role of the HFD-induced hyper-methylation on TF occupancy at *Ankrd26* promoter, ChIP assay has been performed to identify the enrichment of methylation-dependent transcriptional repressor MBD2 [70]. Interestingly, as shown in Figure 22b, significantly increased levels of MBD2 binding were detected in obese mice compared to control diet group ($p < 0.01$) at the same specific region of *Ankrd26* promoter.

These results imply that the HFD-induced hyper-methylation of *Ankrd26* promoter is mediated, at least in part, by epigenetic targets, such as *de novo* DNMTs and MBD2.

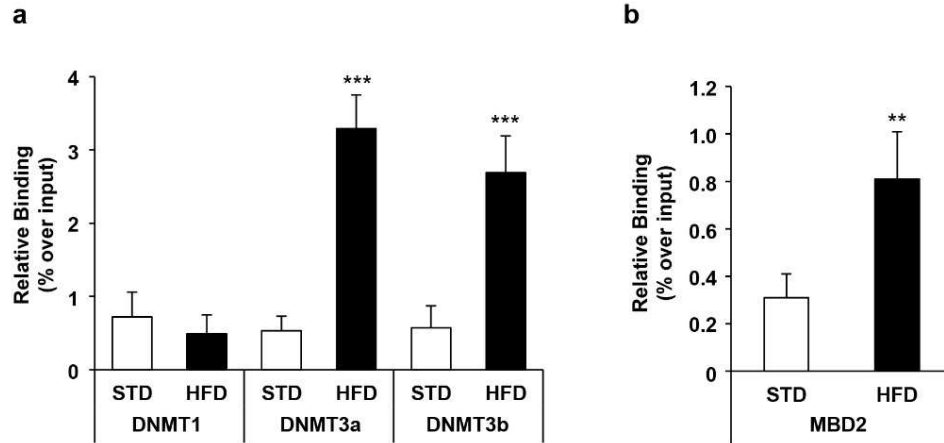


Figure 22. Changes in DNMTs and MBD2 binding at *Ankrd26* promoter in DIO mice. Relative quantification of *Ankrd26* promoter region immunoprecipitated with anti -DNMT1, -DNMT3a, -DNMT3b and -MBD2 antibodies, in eAT of standard diet (STD) and high fat diet (HFD) mice, after 22 weeks of feeding. Chromatin immunoprecipitation was followed by PCR amplification with primers spanning the *Ankrd26* promoter region from -553 to -348 base pairs relative the TSS. Results are expressed as enrichment relative to input (%) and corrected for IgG control levels. Data are means \pm SD of 3 animals/group. Asterisks denote statistically significant differences (*** p <0.001 vs STD; ** p <0.01 vs STD).

4.9 HFD increases nucleosome occupancy at the *Ankrd26* promoter

It is well demonstrated, also here, that methylated CpG dinucleotides can be recognized by methyl-CpG domain-binding proteins, some of which can recruit histone deacetylases and are thought to promote local chromatin condensation [105]. To analyze the dynamics of chromatin organization at *Ankrd26* promoter in eAT, upon HFD administration, Micrococcal Nuclease (MNase) assays have been performed on 300 base pairs upstream *Ankrd26* TSS.

Many studies indicated that nucleosome organization is somewhat non-random and some regions of the genome are more likely to contain nucleosomes than others. Thus, to predict nucleosome occupancy at *Ankrd26* promoter, a further bioinformatics analysis of its nucleotide sequence has been performed, by using the NuPoP software. This tool predicted 2 nucleosomes (Nuc), Nuc-2 (-288 bp/-132 bp) and Nuc-1 (-105 bp/+41 bp), positioned between the p300 consensus sequence and the *Ankrd26* TSS, that were analyzed.

After nuclei isolation and MNase digestion, nucleosome-protected DNA was evaluated by qPCR and the data are represented as the percentage of the loss of amplification following MNase digestion. As shown in Figure 23, in eAT of the HFD-fed mice, the *Ankrd26* promoter region upstream of the TSS showed a reduced MNase sensitivity, reported as a higher nucleosome-bound DNA in the analyzed Nuc-2 and Nuc-1 fragments, thus suggesting a more condensed chromatin conformation compared to their control mice.

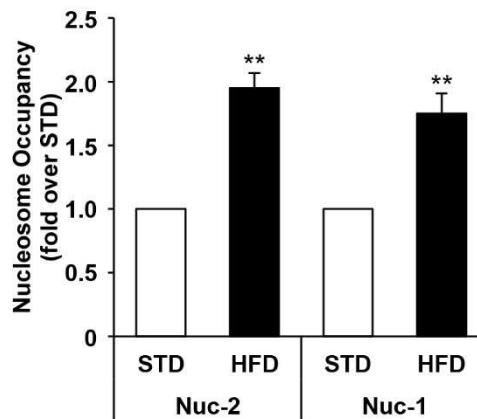


Figure 23. MNase assays upon HFD administration. Micrococcal Nuclease (MNase) analysis was performed in eAT of standard diet (STD) and high fat diet (HFD) mice, after 22 weeks of feeding. After MNase digestion, nucleosome-bound DNA was analyzed by qPCR and normalized to not digested DNA. Nuc-2: from -257 to -198; Nuc-1: from -84 to -25; (distance is relative to *Ankrd26* transcription start site). Data are means \pm SD of 3 animals/group. Asterisks denote statistically significant differences (** $p < 0.01$ vs STD).

4.10 HFD changes histone acetylation and RNA Pol II binding at the *Ankrd26* promoter

Transcriptional repression and gene silencing are dynamic processes involving the conversion of the transcription factor-accessible euchromatin into the closed chromatin [105]. A key role in these processes is played by histone modifications. Their presence or absence may create or disrupt chromatin contacts. Among the modifications of different histones, those on histones H3 and H4 are the most studied and involved in the regulation of gene expression [66,82]. Moreover, regulation of histone modifications has been shown to be influenced by nutrients [82].

Therefore, this evidence suggests that decreased *Ankrd26* expression in eAT of mice exposed to long-term HFD may be the result of specific histone modifications, occurring at its promoter, associated to reduced gene transcription. To test this hypothesis, ChIP assays have been performed to evaluate both the levels of histone 4 acetylation of lysine 16 (AcH4K16) on the regions of *Ankrd26* promoter with reduced MNase sensitivity (Nuc-2 and Nuc-1), and the RNA Pol II binding at the region encompassing the *Ankrd26* TSS (fig. 24). Consistently, ChIP analysis showed that HFD feeding significantly lowered histone H4 acetylation at both nucleosomes ($p < 0.001$; fig. 24a) and RNA Pol II binding to the *Ankrd26* TSS ($p < 0.001$; fig. 24b) in the obese mice compared to lean controls, upon 22 weeks of feeding. Thus, all together these data suggest that, with development of obesity, DNA methylation, through complicated mechanism involving multiple modifications, as the recruitment of HDAC by the bound of MBD2, reduces the acetylation of histone H4 and RNA Pol II binding at the *Ankrd26* promoter and tightly compacts the nucleosomes, leading to a transcriptionally repressed state.

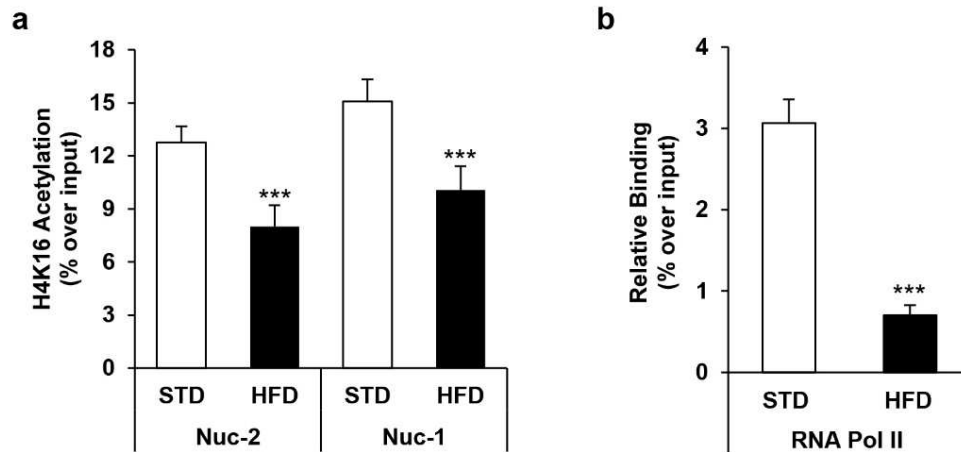


Figure 24. Changes in histone H4 acetylation and RNA Pol II binding at the *Ankrd26* promoter in DIO mice. Relative quantification of *Ankrd26* promoter region immunoprecipitated with anti-AcH4K16 and -RNA Pol II antibodies, in eAT of standard diet (STD) and high fat diet (HFD) mice, after 22 weeks of feeding. **(a)** Chromatin immunoprecipitation with anti-AcH4K16 antibody was followed by PCR amplification with primers spanning the Nuc-2 (-257 bp/-198 bp) and Nuc-1 (-84 bp/-25 bp) fragments. **(b)** Chromatin immunoprecipitation with anti-RNA Pol II antibody was followed by PCR amplification with primers spanning the *Ankrd26* promoter region from +16 to +159 base pairs relative the TSS. **(a-b)** Results are expressed as enrichment relative to input (%) and corrected for IgG control levels. Data are means \pm SD of 3 animals/group. Asterisks denote statistically significant differences (***) $p < 0.001$ vs STD).

4.11 *Ankrd26* silencing induces a pro-inflammatory cytokine profile in cultured adipocytes

Chronic inflammation is a common feature of obesity, and, it has been well demonstrated that inflammatory signals may originate within VAT as this fat depot expands in response to chronic positive energy balance. Both adipocytes and macrophages within fat secrete numerous hormones and cytokines that contribute to local inflammation within adipose tissue and may be the sentinel event that causes systemic insulin resistance and systemic inflammation [107]. A growing body of evidence shows that the inciting event that causes adipose tissue to become inflamed as it expands has a significant epigenetic component, potentially accounting for some of the variance in metabolic risk between equivalently obese individuals.

To examine whether the *Ankrd26* hyper-methylation induced by caloric overload is involved in the obesity-related adipocyte pro-inflammatory response, *Ankrd26* gene has been specifically knockdown in mature adipocytes. In particular, in order to mimic the HFD-induced epigenetic silencing of *Ankrd26* *in vitro*, its expression has been reduced by 35% in the siRNA transfected 3T3-L1 adipocytes. The efficacy of transfection was analyzed by qRT-PC and the data presented in Figure 25a.

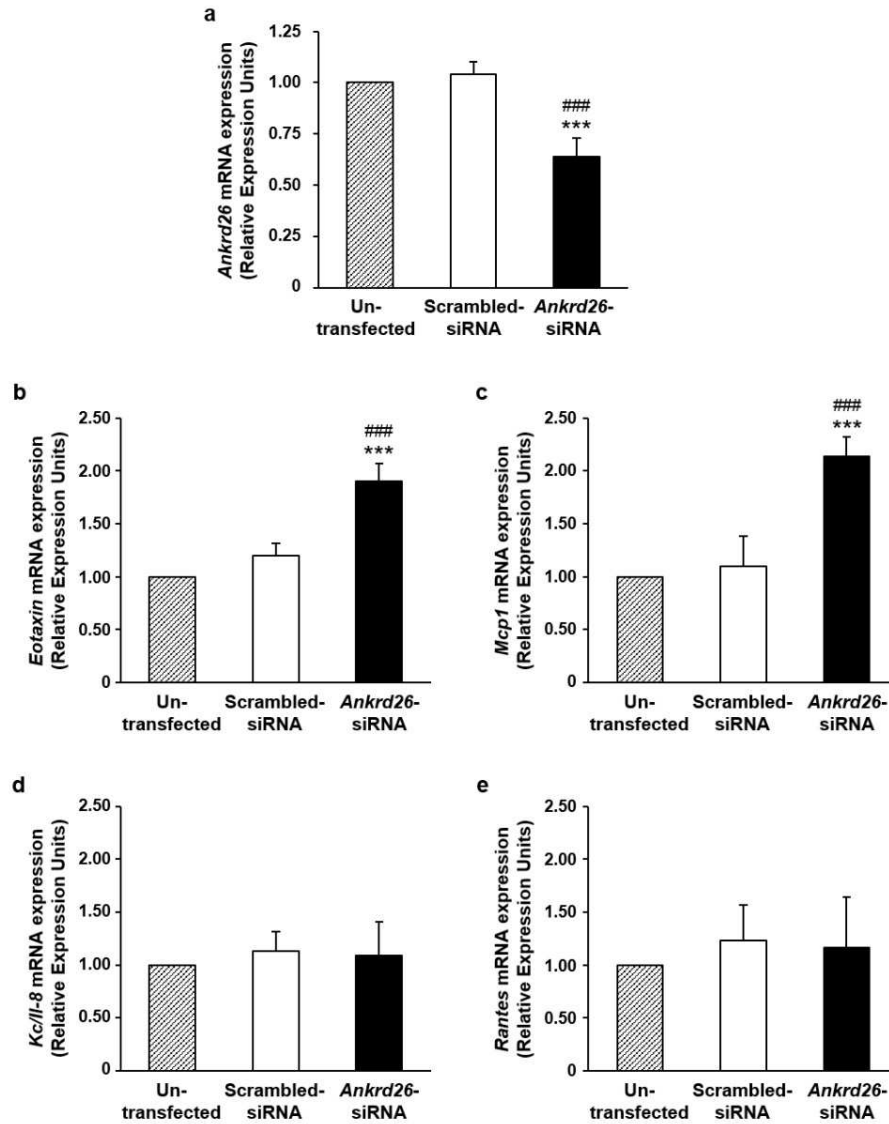


Figure 25. Effect of *Ankrd26* gene silencing on pro-inflammatory mediators mature adipocytes. 3T3-L1 mature adipocytes were silenced with 25 nmol/l of scrambled-siRNA or *Ankrd26*-siRNA for 48 h. Un-transfected cells were used to exclude transfection interference on gene expression. *Ankrd26* (a), *Eotaxin* (b), *Mcp1* (c), *Kc/Il-8* (d) and *Rantes* (e) mRNA levels were evaluated at the end of the experiment and expressed in Relative Expression Units (REU). Data are mean \pm SD of determinations from three independent experiments. *** p <0.001, vs Un-transfected; ^{###} p <0.001, vs Scrambled-siRNA.

Table 6 also shows the effect of *Ankrd26* knockdown on secretion of pro-inflammatory mediators. When compared to Scrambled-siRNA cells, *Ankrd26*-siRNA adipocytes showed significant increase of secretion of pro-inflammatory chemokines, Keratinocyte-derived Cytokine/Interleukine 8 (KC/IL-8), Eotaxin, MCP1 and Rantes. Similarly, mRNA levels of *Eotaxin* and *Mcp1* were also significantly increased in *Ankrd26*-deficient cells; however, the increase of *Kc/Il-8* and *Rantes* mRNA expression just failed to reach significance (fig. 25b-e). These results strongly support the physiopathological role of *Ankrd26* in regulating adipocyte pro-inflammatory secretion profile through effects occurring at different levels.

Variable	3T3-L1 Adipocytes		
	Un-transfected	Scrambled-siRNA	<i>Ankrd26</i> -siRNA
Eotaxin (pg/ml)	514.34 ± 73.25	521.16 ± 82.90	705.92 ± 98.99 ^{b,d}
G-CSF (pg/ml)	6.45 ± 0.96	7.11 ± 0.22	7.14 ± 0.90
IL-4 (pg/ml)	3.41 ± 0.32	3.21 ± 0.44	3.81 ± 0.51
IL-5 (pg/ml)	0.88 ± 0.14	0.79 ± 0.16	0.83 ± 0.33
KC/IL-8 (pg/ml)	565.39 ± 15.32	588.67 ± 30.86	702.58 ± 34.08 ^{a,c}
IL-17 (pg/ml)	1.44 ± 0.62	1.72 ± 0.51	1.56 ± 0.42
MCP1 (pg/ml)	1758.04 ± 72.31	1718.77 ± 248.29	2500.31 ± 225.38 ^{b,d}
MIP1β (pg/ml)	1.32 ± 0.75	1.14 ± 0.52	1.17 ± 0.37
Rantes (pg/ml)	27.95 ± 2.74	33.31 ± 8.88	53.45 ± 2.35 ^{b,d}
TNFα (pg/ml)	4.98 ± 1.46	5.29 ± 1.31	5.57 ± 1.81

Table 6. Effect of *Ankrd26* gene silencing on adipocyte-released chemokines/cytokines. 3T3-L1 mature adipocytes were silenced with 25 nmol/l of Scrambled-siRNA or *Ankrd26*-siRNA for 48 h. Conditioned media were collected for 24 h in Dulbecco's modified Eagle's medium without serum and with 0.5% BSA. Secreted adipokines were then assayed using the Bio-Plex Pro Mouse Cytokine Immunoassay. Un-transfected cells were also used to exclude transfection interference on adipokine secretion. Detectable adipokines are reported. Data are mean ± SD of determinations from three independent experiments. ^a*p*<0.001 and ^b*p*<0.01, vs Un-transfected; ^c*p*<0.001 and ^d*p*<0.01, vs Scrambled-siRNA. Granulocyte-colony stimulating factor, G-CSF; Interleukin, IL; Keratinocyte-derived Cytokine/Interleukine 8, KC/IL-8; Monocyte chemotactic protein 1, MCP1; Macrophage inflammatory protein 1 beta, MIP1β; Tumor necrosis factor alpha, TNFα.

4.12 *ANKRD26* expression negatively correlates with BMI and inflammatory markers in obese subjects

Together, these data along with findings emerging from other studies [88,97,99], led to speculate the possibility of potential role of *ANKRD26* gene for human obesity. To address this hypothesis, the correlation between mRNA expression of *ANKRD26* in VAT and BMI or inflammatory parameters has been examined in normal glucose tolerant (NGT) obese subjects (tab. 4). Interestingly, in human VAT, *ANKRD26* expression was not only negatively correlated with BMI (fig. 26a), but also negatively associated with serum levels of pro-inflammatory chemokines IL-8 and RANTES, as well as of inflammatory markers IL-6 and C-reactive protein (CRP) (fig. 6b-e), findings that further support the potential role of reduced *ANKRD26* gene expression in VAT to mediate the obesity-related inflammatory status.

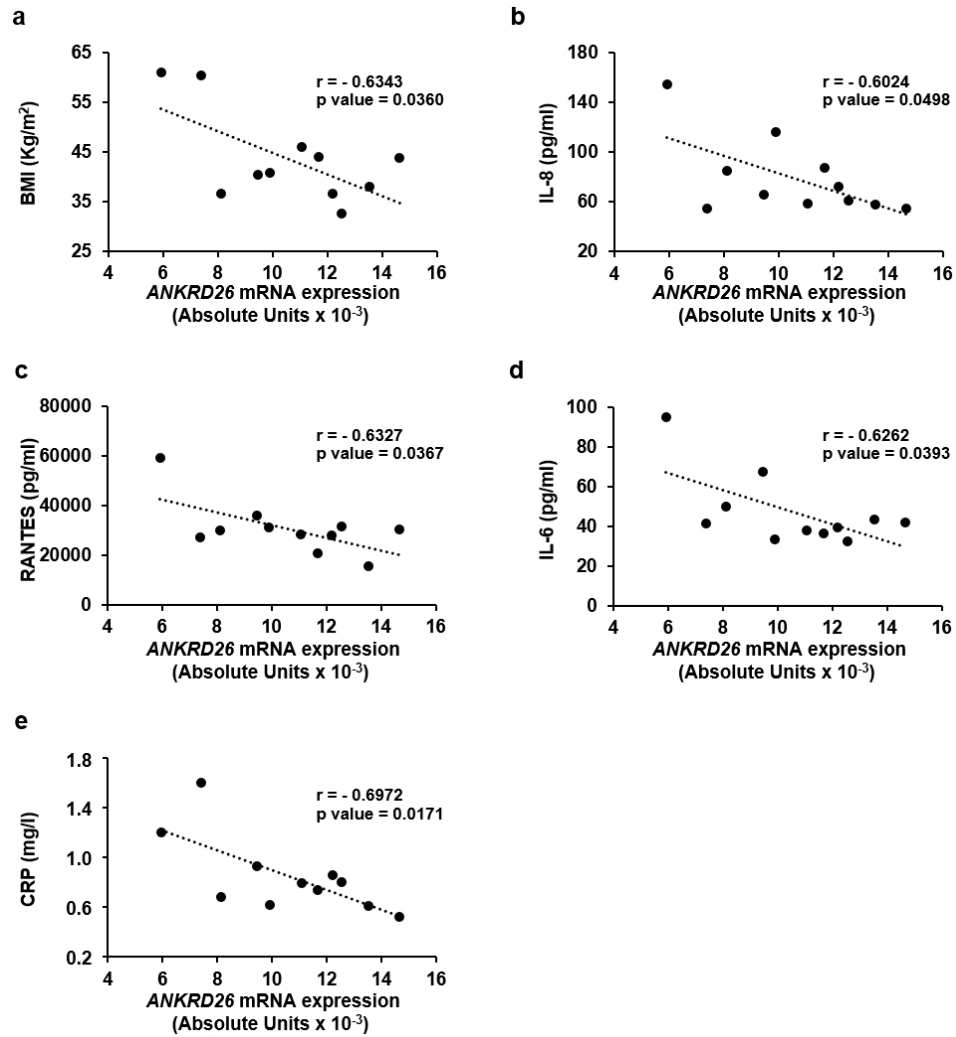


Figure 26. Correlation between VAT *ANKRD26* mRNA expression and BMI or systemic inflammatory markers in obese subjects. Correlations between VAT *ANKRD26* mRNA expression and BMI (a) or serum levels of IL-8 (b), RANTES (c), IL-6 (d) or CRP (e) in normal glucose tolerant obese individuals (n=11; 5M/6F). r , Pearson's coefficient; $p < 0.05$ was considered statistically significant.

5. DISCUSSION

Epigenetic modifications are responsible for chromatin structure and stability as well as the modulation of tissue-specific gene expression, thus, epigenetics may be an important contributor to many chronic diseases including obesity [39-41,82]. The relationship between obesity and the epigenetic regulation of gene expression has been widely reported, and DNA methylation of promoter regions of several genes has been demonstrated to change upon the development of obesity in animal models and humans [58]. Notably, DNA methylation is the only known epigenetic modification that targets DNA itself and is usually associated with gene silencing [82] and appears to be dynamically regulated responding to changes in nutrients cues, such as fat and high-calorie diets, affecting systemic energy homeostasis both in humans and rodents [108].

Interestingly, in this current study, a negative functional relationship has been demonstrated between DNA methylation of the *Ankrd26* promoter and *Ankrd26* gene transcription, in the visceral adipose tissue of DIO mice. Indeed, in eAT of obese mice, the methylation percentage at specific CpG sites at the *Ankrd26* promoter and the binding of *de novo* DNMT3a and DNMT3b to this same promoter region were increased together with an increase of MBD2 binding and a decrease in bound RNA Pol II. All these changes were followed by down-regulation of *Ankrd26* expression in the eAT, demonstrating that the long-term HFD exposure simultaneously changes DNA methylation and expression of *Ankrd26* genes. The transcriptional repression accompanying the epigenetic dysregulation of *Ankrd26* may have been, at least in part, caused by the saturated fat enrichment of the diet rather than representing a consequence of obesity, as it can be mimicked by exposing 3T3-L1 adipocytes to palmitate. It remains possible, however, that obesity *per se* or specific obesity-associated traits further contribute to *Ankrd26* dysregulation.

The evidence that the specific cytosine hyper-methylation at the *Ankrd26* promoter appeared in eAT of obese mice after a prolonged HFD feeding, but not at earliest time-point, emphasize the role of chronic exposure to HFD in the epigenetic regulation of *Ankrd26* gene. This time-dependent effect may contribute to the adipose tissue functional changes and remodeling that accompany weight gain determined by HFD exposure. Indeed, eAT, along with other VAT depots, contributes to the inflammatory and metabolic complications in murine obesity [109], and responds to HFD through specific time-dependent changes [30,110]. Upon early HFD exposure (8-12 weeks), eAT expansion is accompanied by a major increase in adipocyte size. Instead, after more prolonged HFD exposure (20 weeks), eAT expansion is mainly sustained by increased adipogenesis and is accompanied by enhanced secretion of inflammatory mediators, including TNF α , IL-6, MCP1 and Rantes [30,31,110]. The mechanisms triggering this compensatory response of eAT have not been clarified yet. However, the present work shows, for the first time, that they may include the HFD-induced *Ankrd26*

down-regulation.

Along with its role in the control of feeding behavior and body fat accumulation [92-94], *Ankrd26* has been identified as a regulator of adipogenesis *in vitro* [95,96]. Firstly, adipogenesis of 3T3-L1 cells is enhanced by selective silencing of the *Ankrd26* gene with an *Ankrd26*-specific shRNA [95]. Secondly, Mouse Embryonic Fibroblasts from *Ankrd26* mutant mice (MEFs *Ankrd26*^{-/-}) have a higher rate of adipocyte differentiation. The expression of the master regulator genes of differentiation process, CCAAT enhancer-binding protein α (*C/ebpa*), and Peroxisome proliferator-activated receptor γ (*Ppar γ*), are up-regulated in MEFs *Ankrd26*^{-/-}, indicating that this gene is involved in regulating both the pre-adipocyte commitment and differentiation [96]. In addition, in this work, the enhanced expression and/or secretion of the pro-inflammatory mediators Eotaxin, MCP1, KC/IL-8, and Rantes by 3T3-L1 adipocytes, whose *Ankrd26* expression was silenced to levels similar to those occurring in response to HFD, has been further demonstrated. Since secretion of Eotaxin, MCP1, KC/IL-8, and Rantes by eAT increases upon prolonged exposure to HFD [30,110], these findings suggest the involvement of *Ankrd26* down-regulation in raising and/or sustaining the low-grade inflammatory response, that occurs in the eAT after long-term HFD feeding and is implicated in the development of insulin resistance and T2D [30,110,111]. The epigenetic regulation of *Ankrd26* gene in VAT might represent a mechanism by which environmental cues are integrated at specific genomic loci, contributing to the metabolic disorder.

The relevance of these observations to humans is supported by further findings in normal glucose tolerant obese subjects, revealing that the reduction of *ANKRD26* expression in VAT is associated with increased serum concentrations of inflammatory markers and pro-inflammatory chemokines, which are related to obesity development in humans [112] and predict occurrence of T2D [111,113-116]. It is still unclear which is the mechanism accounting for the *Ankrd26*-mediated pro-inflammatory response of VAT, upon metabolic alterations. However, *Cardamone et al.* [117] have recently shown the relevance of cytosolic function of the GPS2 (G protein pathway suppressor 2), an interactor of *Ankrd26* protein [95], to the prevention of uncontrolled activation of inflammatory programs in human adipose tissue [117]. Thus, even though this issue deserves further mechanistic investigation, an intriguing hypothesis is that *Ankrd26* might work as intracellular regulator of pro-inflammatory signaling pathways, at least in part, by facilitating the cytoplasmic localization of its interacting partner GPS2 [95,117]. Therefore, *ANKRD26* down-regulation might represent an early event triggering chronic low-grade inflammation in human adipose tissue.

Detailed mechanistic analysis of specific methylation of -436 and -431 CpG dinucleotides at the *Ankrd26* promoter, both *in vitro* and *in vivo*, have provided evidence that these two cytosine residues play a functional role in the HFD-induced epigenetic repression of *Ankrd26* gene. Current findings support a role for epigenetic changes in the regulation of metabolic diseases, and, in some cases, as in this study, it has been well demonstrated that small DNA methylation changes

are associated with gene expression variability and significant effects on the phenotype [104,118,119]. For instance, in support of this concept, *Barrès et al.* [104] have shown that hyper-methylation of the Peroxisome proliferator-activated receptor γ coactivator 1 α (*PGC1 α*) promoter modulates *PGC1 α* expression, implying a mechanism for decreased mitochondrial content in skeletal muscle from T2D patients. Also, using a gene reporter assay, these authors have demonstrated that the *in vitro* methylation of a single cytosine residue at the *PGC1 α* promoter is responsible for the reduction of gene activity [104]. DNA methylation generally affects transcription directly, by blocking the binding of transcriptional activators [120,121], or indirectly, by recruiting DNA-binding proteins and co-repressor complexes that occupy the methylated promoters and facilitate the formation of heterochromatin [122]. In this study, it has been further demonstrated that *i.*, *in vitro*, the histone acetyltransferase/transcriptional co-activator p300 directly binds the consensus sequence at the *Ankrd26* promoter, containing the methylation sensitive-436 and -431 cytosine residues; *ii.*, the hyper-methylation of these two GpG dinucleotides affects p300 binding and activity both *in vivo* and *in vitro*.

p300 regulates gene expression by acetylating both histones and transcriptional factors and plays a key role in modulating chromatin structure and function [41,106]. This work has provided evidence that prolonged HFD exposure reduces histone H4 acetylation and increases nucleosome occupancy at the *Ankrd26* promoter, and impairs RNA Pol II binding at the *Ankrd26* TSS, suggesting that the HFD-dependent p300 displacement from the *Ankrd26* promoter initiates the epigenetic silencing *Ankrd26* gene. These findings are consistent with recent studies demonstrating that CpG methylation suppresses transcription of several genes by direct inhibition of p300 binding to their promoter sequences [123]. In conjunction with the inhibition of p300 binding, HFD induced the binding of MBD2 to the *Ankrd26* promoter in mice. MBD2 is a methyl-CpG binding protein that induces the silencing of target genes by recruiting histone deacetylase at their methylated promoters [122,124]. Accordingly, all these observations suggest that the specific CpG methylation at the *Ankrd26* promoter lead to HFD-induced epigenetic silencing of *Ankrd26* by triggering a cascade of events which involves DNA-associated regulatory proteins, such as p300 and MBD2, and that changes in chromatin structure.

The relevance of the presented findings to humans is supported by very recent computational data from a genome-wide DNA methylation analysis of human adipose tissue, revealing that *ANKRD26* mRNA expression is negatively correlated with DNA methylation at its promoter and with BMI [88]. This evidence supports the hypothesis that epigenetic regulation of *ANKRD26* gene may occur in humans as well.

6. CONCLUSION

This work has identified the impact of the environment on the regulation of *Ankrd26* gene. The results have revealed that the chronic administration of a high fat diet in mice is able to affect *Ankrd26* expression in eAT, through epigenetic repression of transcriptional gene activity. A schematic model of the epigenetic mechanisms underlying *Ankrd26* gene expression is shown in Figure 27. The degree of methylation of specific CpG dinucleotides at *Ankrd26* promoter changes with development of obesity and regulates the gene expression. The promoter methylation by *de novo* DNMTs is increased together with MBD2 binding. Furthermore, the acetylation of histone H4 and RNA Pol II at *Ankrd26* promoter is concomitantly reduced.

Furthermore, this study provides new insight regarding the physio-pathological role of epigenetic silencing of *Ankrd26* gene in pro-inflammatory response of visceral adipose tissue, following unhealthy dieting. Since evidence linking specific environmental cues and metabolic disorders are still limited, elucidating the mechanisms through which environmental factors can alter metabolic homeostasis remain a challenge.

Therefore, highlighting how environmental cues impact on *Ankrd26* expression and function may provide a good-model to understand more general epigenetic mechanisms by which nutrition interacts with the genome thereby influencing metabolic health.

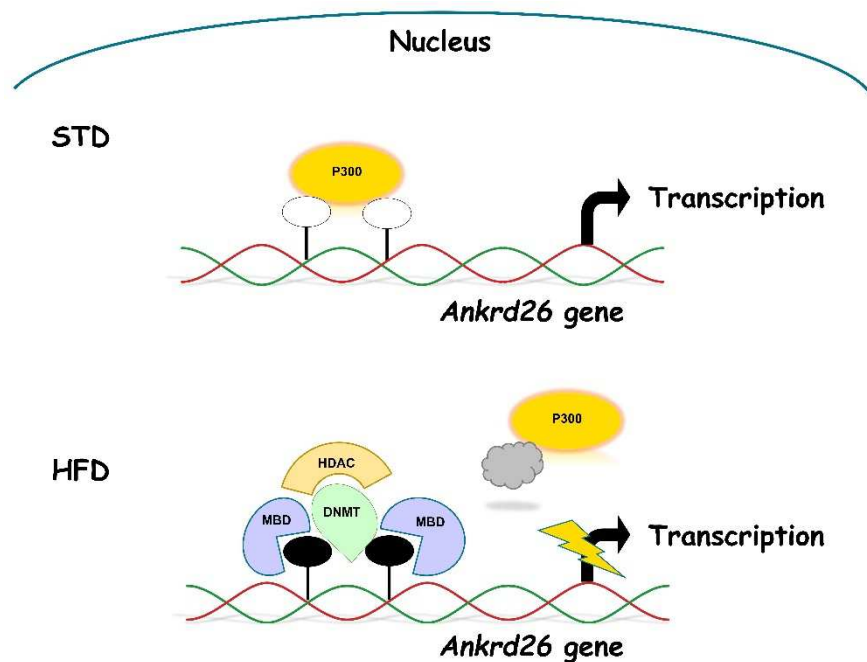


Figure 27. A schematic model of the epigenetic mechanisms underlying *Ankrd26* gene expression in obesity.

7. REFERENCES

1. NCD Risk Factor Collaboration (NCD-RisC). Trends in adult body-mass index in 200 countries from 1975 to 2014: a pooled analysis of 1698 population-based measurement studies with 19.2 million participants. *Lancet*. 2016; 387:1377–1396.
2. González-Muniesa P, Martínez-González MA, Hu FB *et al*. Obesity. *Nat Rev Dis Primers*. 2017; 3:17034.
3. World Health Organization. Obesity and overweight. WHO <http://www.who.int/mediacentre/factsheets/fs311/en/> (2015).
4. Prospective Studies Collaboration, Whitlock G, Lewington S, Sherliker P *et al*. Body-mass index and cause-specific mortality in 900 000 adults: collaborative analyses of 57 prospective studies. *Lancet*. 2009; 373(9669):1083–96.
5. Jackson-Leach J, Mhurchu Ni, Shayeghi K, *et al*. In: Majid Ezzati, Lopez, Rodgers and Murray editors. *Comparative Quantification of Health Risks*. Global and Regional Burden of Disease Attributable to Selected Major Risk Factors. 2004; volume 1.
6. Toubal A, Treuter E, Clément K, *et al*. Genomic and epigenomic regulation of adipose tissue inflammation in obesity. *Trends Endocrinol Metab*. 2013; 24(12):625–34.
7. Galgani J, Ravussin E. Energy metabolism, fuel selection and body weight regulation. *Int J Obes (Lond)*. 2008; 32 Suppl 7:109–19.
8. Yang L, Colditz GA. Prevalence of overweight and obesity in the United States, 2007–2012. *JAMA Intern. Med*. 2015; 175:1412–1413.
9. Nazare JA, Smith JD, Borel AL, *et al*. Ethnic influences on the relations between abdominal subcutaneous and visceral adiposity, liver fat, and cardiometabolic risk profile: the International Study of Prediction of Intra-Abdominal Adiposity and Its Relationship With Cardiometabolic Risk/Intra-Abdominal Adiposity. *Am J Clin Nutr*. 2012; 96(4):714–26.
10. Félix-Redondo FJ, Grau M, Baena-Díez JM, *et al*. Prevalence of obesity and associated cardiovascular risk: the DARIOS study. *BMC Public Health*. 2013; 13:542.
11. Hanley B, Dijane J, Fewtrell M, *et al*. Metabolic imprinting, programming and epigenetics - a review of present priorities and future opportunities. *Br J Nutr*. 2010; 104 Suppl 1:1–25.
12. Eriksson, J. G. Developmental origins of health and disease - from a small body size at birth to epigenetics. *Ann. Med*. 2016; 48:456–467.
13. Chen LW, Aris IM, Bernard JY, *et al*. Associations of maternal macronutrient intake during pregnancy with infant BMI peak characteristics and childhood BMI. *Am J Clin Nutr*. 2017; 105(3):705–713.
14. Arenz S, Ruckerl R, Koletzko B, *et al*. Breast-feeding and childhood obesity - a systematic review. *Int. J. Obes. Relat. Metab. Disord*. 2004; 28:1247–

1256.

15. Péneau S, González-Carrascosa R, Gusto G, *et al.* Age at adiposity rebound: determinants and association with nutritional status and the metabolic syndrome at adulthood. *Int J Obes (Lond)*. 2016; 40(7):1150-6.
16. Vandevijvere S, Chow CC, Hall KD, *et al.* Increased food energy supply as a major driver of the obesity epidemic: a global analysis. *Bull. World Health Organ*. 2015; 93:446–456.
17. Ludwig DS. Lifespan Weighed Down by Diet. *JAMA*. 2016; 315(21):2269-70.
18. Martinez JA, Navas-Carretero S, Saris WH, *et al.* Personalized weight loss strategies - the role of macronutrient distribution. *Nat. Rev. Endocrinol*. 2014; 10:749–760.
19. Mozaffarian, D. Food and weight gain: time to end our fear of fat. *Lancet Diabetes Endocrinol*. 2016; 4:633–635.
20. Tobias DK, Chen M, Manson JE, *et al.* Effect of low-fat diet interventions versus other diet interventions on long-term weight change in adults: a systematic review and meta-analysis. *Lancet Diabetes Endocrinol*. 2015; 3(12):968-79.
21. Bray GA, Fruhbeck G, Ryan DH *et al.* Management of obesity. *Lancet*. 2016; 387:947-1956.
22. Sjostrom L. Review of the key results from the Swedish Obese Subjects (SOS) trial - a prospective controlled intervention study of bariatric surgery. *J. Intern. Med*. 2013; 273:219–234.
23. Rosen ED, Spiegelman BM. What we talk about when we talk about fat. *Cell*. 2014; 156(1-2):20-44.
24. Giralt M, Villarroya F. White, brown, beige/brite: different adipose cells for different functions? *Endocrinology*. 2013; 154:2992–3000.
25. Sacks H, Symonds ME. Anatomical locations of human brown adipose tissue functional relevance and implications in obesity and type 2 diabetes. *Diabetes*. 2013; 62:1783-1790.
26. Matsuzawa Y. The metabolic syndrome and adipocytokines. *FEBS Lett*. 2006; 580:2917–2921.
27. Vegiopoulos A, Rohm M, Herzig S. Adipose tissue: between the extremes. *EMBO J*. 2017; 36(14):1999-2017.
28. Crujeiras AB, Diaz-Lagares A, Moreno-Navarrete JM, *et al.* Genome-wide DNA methylation pattern in visceral adipose tissue differentiates insulin-resistant from insulin-sensitive obese subjects. *Transl Res*. 2016; 178:13-24.e5.
29. Tran TT, Yamamoto Y, Gesta S, *et al.* Beneficial effects of subcutaneous fat transplantation on metabolism. *Cell Metab*. 2008; 7:410-420.
30. Strissel K, Stancheva Z, Miyoshi H, *et al.* Adipocyte death, adipose tissue remodeling, and obesity complications. *Diabetes*. 2007; 56:2910–2918.
31. Strissel KJ, DeFuria J, Shaul ME, *et al.* T-cell recruitment and Th1 polarization in adipose tissue during diet-induced obesity in C57BL/6 mice. *Obesity*. 2010; 18:1918-1925.
32. Shulman GI. Ectopic fat in insulin resistance, dyslipidemia, and

- cardiometabolic disease. *N. Engl. J. Med.* 2014; 371:1131–1141.
33. Arner P, Andersson DP, Thorne A, *et al.* Variations in the size of the major omentum are primarily determined by fat cell number. *J Clin Endocrinol Metab.* 2013; 98:E897–E901.
 34. Spalding KL, Arner E, Westermark PO, *et al.* Dynamics of fat cell turnover in humans. *Nature.* 2008; 453:783-787.
 35. Karpe F, Pinnick KE. Biology of upper-body and lower-body adipose tissue - link to whole-body phenotypes. *Nat. Rev. Endocrinol.* 2015; 11:90–100.
 36. Lotta LA, Gulati P, Day FR, *et al.* Integrative genomic analysis implicates limited peripheral adipose storage capacity in the pathogenesis of human insulin resistance. *Nat Genet.* 2017; 49:17-26.
 37. González-Muniesa P, Garcia-Gerique L, Quintero P, *et al.* Effects of Hyperoxia on Oxygen-Related Inflammation with a Focus on Obesity. *Oxid Med Cell Longev.* 2015; 2015:8957827.
 38. Macartney-Coxson D, Benton MC, Blick R, *et al.* Genome-wide DNA methylation analysis reveals loci that distinguish different types of adipose tissue in obese individuals. *Clin Epigenetics.* 2017; 9:48.
 39. Lu Y, Loos RJ. Obesity genomics: assessing the transferability of susceptibility loci across diverse populations. *Genome Med.* 2013;5(6):55.
 40. Locke AE, Kahali B, Berndt SI, *et al.* Genetic studies of body mass index yield new insights for obesity biology. *Nature.* 2015; 518(7538):197-206.
 41. Drong AW, Lindgren CM, McCarthy MI. The genetic and epigenetic basis of type 2 diabetes and obesity. *Clin Pharmacol Ther.* 2012; 92(6):707-15.
 42. Galton F. Natural Inheritance. Macmillan. 1894.
 43. Pigeyre M, Yazdi FT, Kaur Y, *et al.* Recent progress in genetics, epigenetics and metagenomics unveils the pathophysiology of human obesity. *Clin Sci (Lond).* 2016; 130(12):943-86.
 44. Hainer V, Stunkard A, Kunesova M, *et al.* A twin study of weight loss and metabolic efficiency. *Int. J. Obes.Relat. Metab. Disord.* 2001; 25:533–53.
 45. Brown JM, Witman GB. Cilia and diseases. *Bioscience.* 2014; 64:1126–1137.
 46. Albuquerque D, Stice E, Rodríguez-López R, *et al.* Current review of genetics of human obesity: from molecular mechanisms to an evolutionary perspective. *Mol Genet Genomics.* 2015; 290(4):1191-221.
 47. Yang J, Loos RJ, Powell JE, *et al.* FTO genotype is associated with phenotypic variability of body mass index. *Nature.* 2012; 490(7419):267-72.
 48. Milagro FI, Moreno-Aliaga MJ, Martinez JA. FTO obesity variant and adipocyte browning in humans. *N. Engl. J. Med.* 2016; 374:190–191.
 49. Hagg S, Ganna A, Van Der Laan SW, *et al.* Gene-based meta-analysis of genome-wide association studies implicates new loci involved in obesity. *Hum. Mol. Genet.* 2015; 24:6849–6860.
 50. van der Klaauw AA, Farooqi IS. The hunger genes: pathways to obesity. *Cell.* 2015; 161(1):119-32.
 51. Mitchell JA, Hakonarson H, Rebbeck TR, *et al.* Obesity-susceptibility loci

- and the tails of the pediatric BMI distribution. *Obesity*. 2013; 21:1256–1260.
52. van Dijk SJ, Molloy PL, Varinli H, *et al*. Epigenetics and human obesity. *Int J Obes (Lond)*. 2015; 39(1):85-97.
 53. Zimmet PZ. Diabetes and its drivers: the largest epidemic in human history? *Clin Diabetes Endocrinol*. 2017; 3:1.
 54. Morgan HD, Sutherland HG, Martin DI, *et al*. Epigenetic inheritance at the agouti locus in the mouse. *Nat. Genet*. 1999; 23, 314-318.
 55. Tobi EW, Lumey LH, Talens RP, *et al*. DNA methylation differences after exposure to prenatal famine are common and timing- and sex-specific. *Hum Mol Genet*. 2009; 18(21):4046-53.
 56. Fraga MF, Ballestar E, Paz MF, *et al*. Epigenetic differences arise during the lifetime of monozygotic twins. *Proc Natl Acad Sci U S A*. 2005; 102(30):10604-9.
 57. Margueron R, Reinberg D. Chromatin structure and the inheritance of epigenetic information. *Nat Rev Genet*. 2010; 11(4):285-96.
 58. Desiderio A, Spinelli R, Ciccarelli M, *et al*. Epigenetics: spotlight on type 2 diabetes and obesity. *J Endocrinol Invest*. 2016; 39(10):1095-103.
 59. Jaenisch R, Bird A. Epigenetic regulation of gene expression: how the genome integrates intrinsic and environmental signals. *Nature genetics*. 2003; 33: 245-254.
 60. Tan Q, Frost M, Heijmans BT, *et al*. Epigenetic signature of birth weight discordance in adult twins. *BMC Genomics*. 2014; 15:1062.
 61. Bird A. DNA methylation patterns and epigenetic memory. *Genes Dev*. 2002; 16(1):6-21.
 62. Rassoulzadegan M, Grandjean V, Gounon P, *et al*. RNA-mediated non-mendelian inheritance of an epigenetic change in the mouse. *Nature*. 2006; 441: 469-474.
 63. Zaidi SK, Young DW, Montecino M, *et al*. Bookmarking the genome: maintenance of epigenetic information. *J Biol Chem*. 2011; 286(21):18355-61.
 64. Kawaji H, Nakamura M, Takahashi Y, *et al*. Hidden layers of human small RNAs. *BMC genomics*. 2008; 9:157.
 65. Kouzarides T. Chromatin modifications and their function. *Cell*. 2007; 128:693-705.
 66. Latham JA, Dent SY. Cross-regulation of histone modifications. *Nature structural & molecular biology*. 2007; 14:1017-1024.
 67. Smith ZD, Meissner A. DNA methylation: Roles in mammalian development. *Nat Rev Genet*. 2013; 14(3):204-20.
 68. Deaton AM, Bird A. CpG islands and the regulation of transcription. *Genes Dev*. 2011; 25(10):1010-22.
 69. Jaenisch R, Bird A. Epigenetic regulation of gene expression: How the genome integrates intrinsic and environmental signals. *Nat Genet*. 2003; 33 Suppl:245-54.
 70. Klose RJ, Bird AP. Genomic DNA methylation: The mark and its mediators. *Trends Biochem Sci*. 2006; 31(2):89-97.

71. Thomson JP, Skene PJ, Selfridge J, *et al.* CpG islands influence chromatin structure via the CpG-binding protein Cfp1. *Nature*. 2010; 464(7291):1082-6.
72. Thompson RF, Fazzari MJ, Greally JM. Experimental approaches to the study of epigenomic dysregulation in ageing. *Exp Gerontol*. 2010; 45(4):255-68.
73. Stoger R. Epigenetics and obesity. *Pharmacogenomics*. 2008; 9(12):1851-60.
74. Hackett JA, Sengupta R, Zyllicz JJ, *et al.* Germline DNA demethylation dynamics and imprint erasure through 5-hydroxymethylcytosine. *Science* 2013; 339(6118):448-52.
75. McRae AF, Powell JE, Henders AK, *et al.* Contribution of genetic variation to transgenerational inheritance of DNA methylation. *Genome Biol*. 2014; 15(5):R73.
76. Bell JT, Tsai PC, Yang TP, *et al.* Epigenome-wide scans identify differentially methylated regions for age and age-related phenotypes in a healthy ageing population. *PLoS Genet*. 2012; 8(4):e1002629.
77. Desai M, Jellyman JK, Han G, *et al.* Mechanism of programmed obesity in intrauterine growth restricted newborns: epigenetic mediated early induction of adipocyte differentiation contributes to enhanced adipogenesis. *J Dev Orig Health Dis*. 2013; 2.
78. Parrillo L, Costa V, Raciti GA, *et al.* Hoxa5 undergoes dynamic DNA methylation and transcriptional repression in the adipose tissue of mice exposed to high-fat diet. *Int J Obes (Lond)*. 2016;40(6):929-37.
79. Raciti GA, Spinelli R, Desiderio A, *et al.* Specific CpG hyper-methylation leads to Ankrd26 gene down-regulation in white adipose tissue of a mouse model of diet-induced obesity. *Sci Rep*. 2017; 7:43526.
80. Plagemann A, Harder T, Brunn M, *et al.* Hypothalamic proopiomelanocortin promoter methylation becomes altered by early overfeeding: an epigenetic model of obesity and the metabolic syndrome. *J Physiol*. 2009; 587:4963-76.
81. Stevens A, Begum G, Cook A, *et al.* Epigenetic changes in the hypothalamic proopiomelanocortin and glucocorticoid receptor genes in the ovine fetus after periconceptional undernutrition. *Endocrinology*. 2010; 151(8):3652-64.
82. Shen W, Wang C, Xia L, *et al.* Epigenetic modification of the leptin promoter in diet-induced obese mice and the effects of N-3 polyunsaturated fatty acids. *Sci Rep*. 2014; 4:5282.
83. van Dijk SJ, Molloy PL, Varinli H, *et al.* Epigenetics and human obesity. *Int J Obes (Lond)*. 2015;39(1):85-97.
84. Kuehnen P, Mischke M, Wiegand S, *et al.* An Alu element-associated hypermethylation variant of the POMC gene is associated with childhood obesity. *PLoS Genet*. 2012; 8: e1002543.
85. Godfrey KM, Sheppard A, Gluckman PD, *et al.* Epigenetic gene promoter methylation at birth is associated with child's later adiposity. *Diabetes*. 2011; 60: 1528–1534.
86. Cooper WN, Khulan B, Owens S, *et al.* DNA methylation profiling at

imprinted loci after periconceptional micronutrient supplementation in humans: results of a pilot randomized controlled trial. *FASEB J.* 2012; 26: 1782–1790.

87. Dick KJ, Nelson CP, Tsaprouni L, *et al.* DNA methylation and body-mass index: A genome-wide analysis. *Lancet.* 2014; 383(9933):1990-8.

88. Ronn T, Volkov P, Gillberg L, *et al.* Impact of age, BMI and HbA1c levels on the genome-wide DNA methylation and mRNA expression patterns in human adipose tissue and identification of epigenetic biomarkers in blood. *Hum. Mol. Genet.* 2015; 24:3792–3813.

89. Benton MC, Johnstone A, Eccles D, *et al.* An analysis of DNA methylation in human adipose tissue reveals differential modification of obesity genes before and after gastric bypass and weight loss. *Genome Biol.* 2015; 16, 8.

90. Huang YT, Maccani JZ, Hawley NL, *et al.* Epigenetic patterns in successful weight loss maintainers: a pilot study. *Int. J. Obes.* 2015; 39:865–868.

91. Crujeiras AB, Diaz-Lagares A, Sandoval J, *et al.* DNA methylation map in circulating leukocytes mirrors subcutaneous adipose tissue methylation pattern: a genome-wide analysis from non-obese and obese patients. *Sci Rep.* 2017; 7:41903.

92. Bera TK, Liu XF, Yamada M, *et al.* A model for obesity and gigantism due to disruption of the Ankrd26 gene. *Proc. Natl. Acad. Sci. U S A.* 2008; 105:270-275.

93. Raciti GA, Bera TK, Gavrilova O, *et al.* Partial inactivation of Ankrd26 causes diabetes with enhanced insulin responsiveness of adipose tissue in mice. *Diabetologia.* 2011; 24:2911-2922.

94. Acs P, Bauer PO, Mayer B, *et al.* A novel form of ciliopathy underlies hyperphagia and obesity in Ankrd26 knockout mice. *Brain Struct. Funct.* 2015; 220:1511-1528.

95. Liu XF, Bera TK, Kahue C, *et al.* ANKRD26 and its interacting partners TRIO, GPS2, HMMR and DIPA regulate adipogenesis in 3T3-L1 cells. *PLoS One.* 2012; 7:e38130.

96. Fei Z, Bera TK, Liu X, *et al.* Ankrd26 gene disruption enhances adipogenesis of mouse embryonic fibroblasts. *J. Biol. Chem.* 2011; 286:27761-27768.

97. Mariman EC, Vink RG, Roumans NJ, *et al.* The cilium: a cellular antenna with an influence on obesity risk. *Br J Nutr.* 2016; 116(4):576-92.

98. Ko MJ, Choi HS, Ahn JI, *et al.* Gene expression profiling in C57BL/6 mice treated with the anorectic drugs Sibutramine and Phendimetrazine and their mechanistic implications. *Genom Informat.* 2008; 6:117–125.

99. He L, Kernogitski Y, Kulminskaya I, *et al.* Pleiotropic Meta-Analyses of Longitudinal Studies Discover Novel Genetic Variants Associated with Age-Related Diseases. *Front Genet.* 2016; 13(7):179.

100. Weber M, Davies JJ, Wittig D, *et al.* Chromosome wide and promoter-specific analyses identify sites of differential DNA methylation in normal and transformed human cells. *Nat Genet.* 2005; 37:853–862.

101. Haim Y, Tarnovscki T, Bashari D *et al.* A chromatin

- immunoprecipitation (ChIP) protocol for use in whole human adipose tissue. *Am. J. Physiol. Endocrinol. Metab.* 2013; 305:E1172-1177.
102. Carey M, Smale ST. Micrococcal Nuclease-Southern Blot Assay: I. MNase and Restriction Digestions. *CSH Protoc.* 2007. pdb.prot4890.
 103. Spector AA. Fatty acid binding to plasma albumin. *J. Lipid. Res.* 1975; 16:165-179.
 104. Barrès R, Osler ME, Yan J, *et al.* Non-CpG methylation of the PGC-1alpha promoter through DNMT3B controls mitochondrial density. *Cell Metab.* 2009; 10(3):189-98.
 105. Kribelbauer JF, Laptenko O, Chen S, *et al.* Quantitative Analysis of the DNA Methylation Sensitivity of Transcription Factor Complexes. *Cell Rep.* 2017; 19(11):2383-2395.
 106. Liu X, Wang L, Zhao K, *et al.* The structural basis of protein acetylation by the p300/CBP transcriptional coactivator. *Nature.* 2008;451(7180):846-50.
 107. Wisse BE. The inflammatory syndrome: the role of adipose tissue cytokines in metabolic disorders linked to obesity. *J Am Soc Nephrol.* 2004; 15(11):2792-800.
 108. Kim AY, Park YJ, Pan X, *et al.* Obesity-induced DNA hypermethylation of the adiponectin gene mediates insulin resistance. *Nat Commun.* 2015; 6:7585.
 109. Berry DC, Stenesen D, Zeve D, *et al.* The developmental origins of adipose tissue. *Development.* 2013; 140(19):3939-49.
 110. Wang QA, Tao C, Gupta RK, *et al.* Tracking adipogenesis during white adipose tissue development, expansion and regeneration. *Nat. Med.* 2013; 19,1338-1344.
 111. Dandona P, Aljada A, Bandyopadhyay A. Inflammation: the link between insulin resistance, obesity and diabetes. *Trends Immunol.* 2004; 25(1):4-7.
 112. Stępień M, Stępień A, Wlazeł RN, *et al.* Obesity indices and inflammatory markers in obese non-diabetic normo- and hypertensive patients: a comparative pilot study. *Lipids Health Dis.* 2014; 13:29.
 113. Barzilay JI, Abraham L, Heckbert SR, *et al.* The relation of markers of inflammation to the development of glucose disorders in the elderly: the Cardiovascular Health Study. *Diabetes.* 2001; 50(10):2384-9.
 114. Pradhan AD, Manson JE, Rifai N, *et al.* C-reactive protein, interleukin 6, and risk of developing type 2 diabetes mellitus. *JAMA.* 2001; 286(3):327-34.
 115. Herder C, Haastert B, Müller-Scholze S, *et al.* Association of systemic chemokine concentrations with impaired glucose tolerance and type 2 diabetes: results from the Cooperative Health Research in the Region of Augsburg Survey S4 (KORA S4). *Diabetes.* 2005; 54 Suppl 2:S11-7.
 116. Herder C, Baumert J, Zierer A, *et al.* Immunological and cardiometabolic risk factors in the prediction of type 2 diabetes and coronary events: MONICA/KORA Augsburg case-cohort study. *PLoS One.* 2011;6(6):e19852.
 117. Cardamone MD, Kronen A, Tanasa B, *et al.* A protective strategy against hyperinflammatory responses requiring the nontranscriptional actions of

- GPS2. *Mol Cell*. 2012; 46(1):91-104.
118. Barres R, Kirchner H, Rasmussen M, *et al*. Weight loss after gastric bypass surgery in human obesity remodels promoter methylation. *Cell Rep*. 2013; 3(4):1020-7.
 119. Gracia A, Elcoroaristizabal X, Fernández-Quintela A, *et al*. Fatty acid synthase methylation levels in adipose tissue: effects of an obesogenic diet and phenol compounds. *Genes Nutr*. 2014; 9(4):411.
 120. Ito T, Ikehara T, Nakagawa T, *et al*. p300-mediated acetylation facilitates the transfer of histone H2A-H2B dimers from nucleosomes to a histone chaperone. *Genes. Dev*. 2000; 14:1899-1907.
 121. Kuroda A, Rauch TA, Todorov I, *et al*. Insulin gene expression is regulated by DNA methylation. *PLoS One*. 2009; 4(9):e6953.
 122. Ballestar E, Wolffe AP. Methyl-CpG-binding proteins. Targeting specific gene repression. *Eur. J. Biochem*. 2001; 268:1-6.
 123. Li HP, Peng CC, Chung IC, *et al*. Aberrantly hypermethylated Homeobox A2 derepresses metalloproteinase-9 through TBP and promotes invasion in Nasopharyngeal carcinoma. *Oncotarget*. 2013; 4:2154-2165.
 124. Voisin S, Almén MS, Moschonis G, *et al*. Dietary fat quality impacts genome-wide DNA methylation patterns in a cross-sectional study of Greek preadolescents. *Eur. J. Hum. Genet*. 2015; 23:654-662.

ACKNOWLEDGEMENTS

I would like to thank Professor Francesco Beguinot for his helpful teaching activity as my tutor during my PhD.

I would like to thank Professor Pietro Formisano and Dr Claudia Miela, which gave me the opportunity to be part of their working group.

I would like to express my gratitude to my direct supervisor, Dr. Gregory Alexander Raciti. He always encouraged and helped me to shape my interest and ideas.

My sincere thanks also goes to Michele Longo, for teaching me so much in so few time.

I am also indebted to the student I had the pleasure to work with. Thanks to Giuseppe, who was involved in this project. He was a great help in running the experiments, He was responsible and cooperative with solving the problems. I would like to thank Francesca Pignalosa, she works with lots of enthusiasm and optimism and remind me.

I sincerely thank Antonella, Federica and Luca, which have also been *friends*, giving me their support when I have needed it the most.

I would also like to thank all the people of the lab, from “Edificio 4” to “Corpi Bassi”, for our exchanges of knowledge, skills, time spent together, and venting of frustration during my graduate program. Particularly, special thanks to Daniela Terracciano, Giuseppe Perruolo, Vittoria D'Esposito, Serena Cabaro, Tonia Liotti, Francesca Fiory, Cecilia Nigro, Paola Mirra, Alessia Leone and Imma Prevenzano, we facilitate a lot of work happiness.

I would also like to thank all my family, in particular: my mother, my father, my sister, my brother and my grandmother for always believing in me, for their continuous love and, above all, for their supports in my decisions.

SCIENTIFIC REPORTS

OPEN

Specific CpG hyper-methylation leads to *Ankrd26* gene down-regulation in white adipose tissue of a mouse model of diet-induced obesity

Received: 02 August 2016
Accepted: 27 January 2017
Published: 07 March 2017

Gregory A. Raciti^{1,2,*}, Rosa Spinelli^{1,2,*}, Antonella Desiderio^{1,2}, Michele Longo^{1,2}, Luca Parrillo^{1,2}, Cecilia Nigro^{1,2}, Vittoria D'Esposito^{1,2}, Paola Mirra^{1,2}, Francesca Fiory^{1,2}, Vincenzo Pilone³, Pietro Forestieri⁴, Pietro Formisano^{1,2}, Ira Pastan⁵, Claudia Miele^{1,2} & Francesco Beguinot^{1,2}

Epigenetic modifications alter transcriptional activity and contribute to the effects of environment on the individual risk of obesity and Type 2 Diabetes (T2D). Here, we have estimated the *in vivo* effect of a fat-enriched diet (HFD) on the expression and the epigenetic regulation of the *Ankyrin repeat domain 26* (*Ankrd26*) gene, which is associated with the onset of these disorders. In visceral adipose tissue (VAT), HFD exposure determined a specific hyper-methylation of *Ankrd26* promoter at the −436 and −431 bp CpG sites (CpGs) and impaired its expression. Methylation of these 2 CpGs impaired binding of the histone acetyltransferase/transcriptional coactivator p300 to this same region, causing hypo-acetylation of histone H4 at the *Ankrd26* promoter and loss of binding of RNA Pol II at the *Ankrd26* Transcription Start Site (TSS). In addition, HFD increased binding of DNA methyl-transferases (DNMTs) 3a and 3b and methyl-CpG-binding domain protein 2 (MBD2) to the *Ankrd26* promoter. More importantly, *Ankrd26* down-regulation enhanced secretion of pro-inflammatory mediators by 3T3-L1 adipocytes as well as in human sera. Thus, in mice, the exposure to HFD induces epigenetic silencing of the *Ankrd26* gene, which contributes to the adipose tissue inflammatory secretion profile induced by high-fat regimens.

Obesity and T2D are two common non-communicable diseases, which are now reaching epidemic proportions globally^{1–3}. Epigenetic processes may contribute to the development of these disorders and mediate the effects of environmental exposure on risk of both diseases. Indeed, studies in humans and animal models support the association between changes in the nutritional status, epigenetic modifications and predisposition to obesity and T2D^{4–7}.

White adipose tissue (WAT) is a major endocrine tissue actively involved in the maintenance of the metabolic homeostasis in response to nutrition and other environmental clues through changes in fat storage, tissue expansion and adipokine secretion⁸. In disease states, the failure of compensatory response results in an impaired endocrine function which leads to insulin resistance and metabolic derangement⁹. In particular, fat stored in VAT strongly correlates with metabolic alterations and has been shown to be an independent risk factor for obesity-associated comorbidities^{10–12}.

¹URT of the Institute of Experimental Endocrinology and Oncology "G. Salvatore", National Council of Research, Naples, 80131, Italy. ²Department of Translational Medical Sciences, University of Naples "Federico II", Naples, 80131, Italy. ³Bariatric and Metabolic Surgery Unit, University of Salerno, Salerno, 84084, Italy. ⁴Department of Clinical Medicine and Surgery, University of Naples "Federico II", Naples, 80131, Italy. ⁵Laboratory of Molecular Biology (LMB), National Cancer Institute (NCI), National Institute of Health (NIH), Bethesda, MD 20892, USA. *These authors contributed equally to this work. Correspondence and requests for materials should be addressed to C.M. (email: c.miele@ieos.cnr.it) or F.B. (email: beguino@unina.it)

Variable	16 week-old		30 week-old	
	STD (n = 12)	HFD (n = 12)	STD (n = 12)	HFD (n = 12)
Body weight (g)	24.7 ± 2.1	34.4 ± 3.2 ^a	26.4 ± 2.8	38.8 ± 3.3 ^{b,c}
Fasting glucose (mmol/l)	5.9 ± 0.9	7.7 ± 1.7 ^a	5.8 ± 1.2	9.1 ± 1.8 ^b
GTT AUC (mmol/l 120 min ⁻¹)	725.7 ± 103.3	1290.7 ± 162.4 ^a	653.6 ± 150.0	1344.2 ± 172.2 ^b
ITT AUCi (mmol/l 120 min ⁻¹)	741.6 ± 127.0	355.7 ± 132.2 ^a	681.0 ± 128.9	312.9 ± 117.6 ^b

Table 1. Metabolic characteristics of HFD- and STD-fed mice. 8-week-old male C57BL/6J mice were fed a high-fat diet (HFD) or a standard chow diet (STD) for 8 and 22 weeks. Body weight, fasting blood glucose, glucose tolerance test (GTT) Area Under the Curve (AUC) and insulin tolerance test (ITT) AUCi were reported. Data are mean ± SD of determinations. ^a $p < 0.001$, 16-week-old HFD vs 16-week-old STD; ^b $p < 0.001$, 30-week-old HFD vs 30-week-old STD; and ^c $p < 0.001$, 30-week-old HFD vs 16-week-old HFD.

Ankrd26 was recently identified as a gene involved in the regulation of the feeding behavior and in the development of both obesity and T2D in mice^{13–15}. *ANKRD26* maps at chromosome 10p12 in humans, a region associated with certain forms of hereditary obesity¹⁶. In mice, *Ankrd26* gene is highly expressed in both the hypothalamus and WAT and its partial inactivation induces marked hyperphagia, severe obesity and diabetes *in vivo*^{13,14}. In addition, *in vitro* evidence indicates *Ankrd26* as a regulator of adipogenesis^{17,18}. A methylome analysis of mouse epididymal WAT (eAT)¹⁹, the largest and easy accessible VAT depots in rodents^{20,21}, has identified promoter hyper-methylation of *Ankrd26* gene in HFD-fed compared to age- and sex-matched chow diet-fed mice, suggesting that *Ankrd26* gene is amenable to nutritionally-induced epigenetic modifications. In this study, we aimed at establishing whether and how HFD modulates *Ankrd26* gene expression in VAT *in vivo* through epigenetic processes.

Results

HFD affects body weight, glucose homeostasis and insulin sensitivity in mice. HFD-fed mice were heavier than standard chow diet (STD)-fed mice and reached a 50% increase of body weight compared with controls after 22 weeks of diet regimens (Table 1). These mice also exhibited increased fasting blood glucose levels, impaired glucose tolerance upon glucose loading and reduced insulin sensitivity after insulin injection compared with control mice (Supplementary Fig. S1).

HFD impairs *Ankrd26* expression in mice. To establish whether HFD modulates *in vivo* *Ankrd26* expression, mRNA and protein levels were measured in eAT. Treatment with HFD for 22 weeks led to a significant decrease in both *Ankrd26* mRNA ($p < 0.001$) and protein ($p < 0.01$) levels in obese mice compared with controls (Fig. 1a and b). Similarly, HFD lowered *Ankrd26* mRNA levels in mesenteric VAT (Supplementary Fig. S2). HFD treatment for 4 additional weeks did not elicit any further decrease in *Ankrd26* mRNA expression in the HFD-fed mice (34 week-old STD, *Ankrd26* mRNA: $2.29 \times 10^{-3} \pm 0.11 \times 10^{-3}$ AU; 34 week-old HFD, *Ankrd26* mRNA: $1.36 \times 10^{-3} \pm 0.19 \times 10^{-3}$ AU; $p < 0.001$). Differently from the long-term treatment, both *Ankrd26* mRNA and protein levels showed no differences between HFD- and STD-fed mice upon 8 weeks of diet regimens (Supplementary Fig. S3a and b). Next, the *Ankrd26* gene expression was assessed *in vitro* by exposing 3T3-L1 adipocytes to either palmitate or oleate, representing saturated and unsaturated fatty acid species, which are abundant in the HFD, or alternatively to leptin, whose levels raise through obesity development²². Quantitative real-time PCR (qPCR) analysis showed that palmitate, but not oleate or leptin, reduced *Ankrd26* expression by about 25% (Supplementary Fig. S4a and b), suggesting that, at least in part, excess of saturated fats accounts for HFD-induced *Ankrd26* gene repression.

HFD induces DNA methylation at the *Ankrd26* promoter in mice. To discover whether HFD induces DNA methylation changes at the *Ankrd26* promoter and 5'-untranslated region (5' UTR), we performed Methylated DNA Immunoprecipitation (MeDIP) assay on pooled eAT genomic DNA from STD- and HFD-fed mice. This analysis revealed a 2-fold increase in DNA methylation at a segment of the promoter region (S1; −462 bp/−193 bp) in HFD-fed mice, while no DNA methylation enrichment was observed in a second segment (S2; −158 bp/+140 bp; Fig. 1c). Consistently, palmitate but not oleate or leptin, enhanced S1 DNA methylation at the *Ankrd26* promoter in 3T3-L1 adipocytes (Supplementary Fig. S4c and d), as showed by MeDIP assay. To further determine the specific HFD-induced DNA methylation profile occurring at 9 CpGs located at −436 and −221 bp from the *Ankrd26* TSS, we adopted bisulfite sequencing analysis. High CpG methylation density was detected in obese mice compared with controls in 2 close cytosine residues at −436 and −431 bp from the *Ankrd26* TSS (Fig. 1d). The combined percentage of methylation at these sites was inversely related to the amount of *Ankrd26* mRNA (Fig. 1e). In parallel with mRNA expression, mice fed HFD or STD for 8 weeks showed no difference in the *Ankrd26* DNA methylation state (Supplementary Fig. S3c). In addition, in 16 week-old and 30 week-old STD-fed mice, no difference in both *Ankrd26* mRNA levels (16 week-old STD, *Ankrd26* mRNA: $2.10 \times 10^{-3} \pm 0.20 \times 10^{-3}$ AU; 30 week-old STD, *Ankrd26* mRNA: $1.96 \times 10^{-3} \pm 0.23 \times 10^{-3}$ AU; $p = 0.126$) and DNA methylation (16 week-old STD, DNA methylation: $51.7 \pm 2.9\%$; 30 week-old STD, DNA methylation: $51.3 \pm 4.8\%$; $p = 0.900$) were observed. All together, these data indicate that the long-term exposure to calorie overload, rather than aging, affects eAT *Ankrd26* expression and DNA methylation in mice.

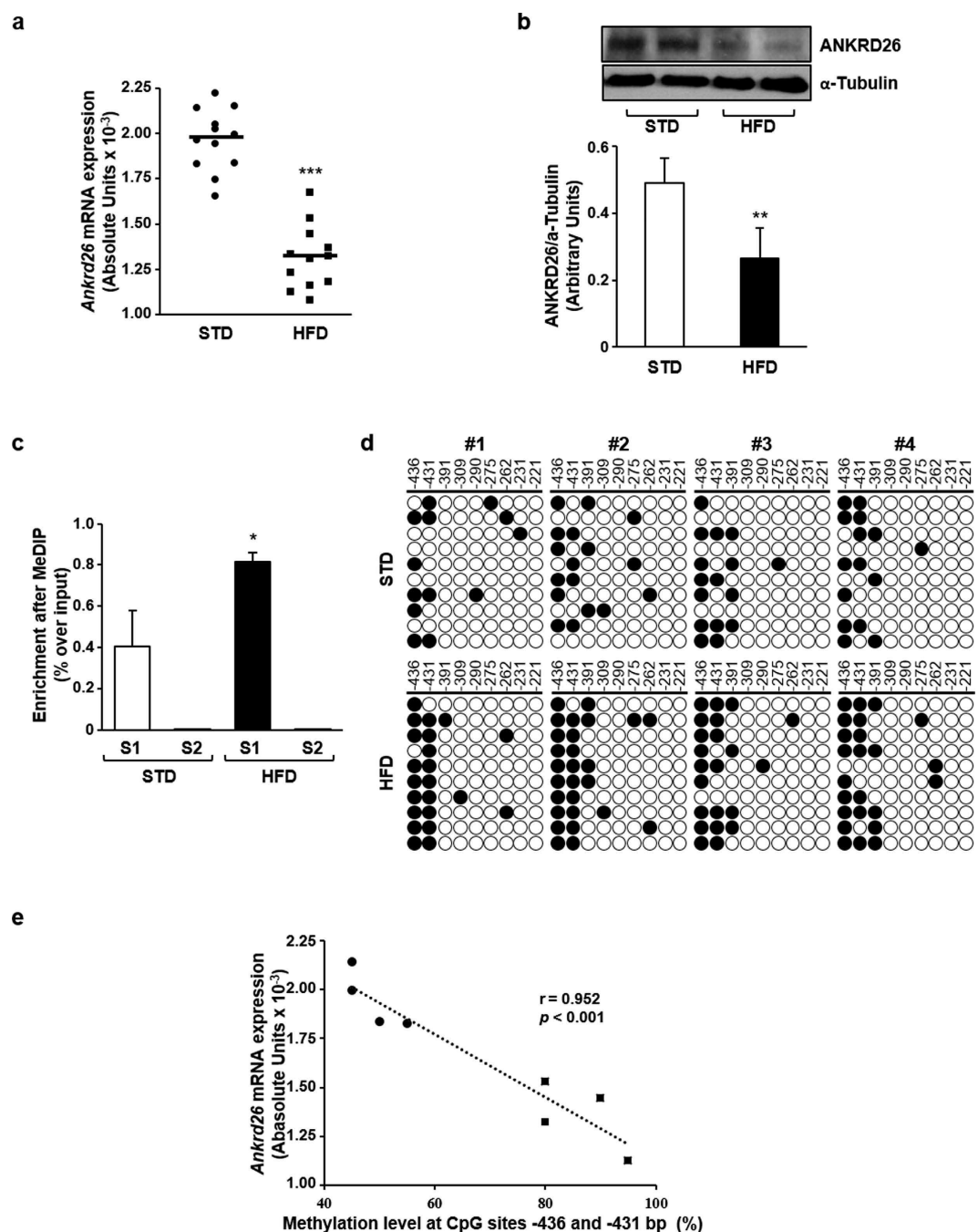


Figure 1. *Ankrd26* expression and DNA methylation in eAT from mice upon 22 weeks of HFD or STD treatments. **(a)** qPCR of *Ankrd26* mRNA for HFD- ($n = 12$) and STD-fed ($n = 12$) mice. mRNA levels are expressed in absolute units (AU). **(b)** Representative western blot for ANKRD26 and α -Tubulin. Uncut western blot images are in the Supplementary Fig. S5. **(c)** MeDIP-qPCR of segment 1 (S1; -462 bp/ -193 bp) and segment 2 (S2; -158 bp/ $+140$ bp) of *Ankrd26* promoter region. **(d)** Bisulfite sequencing of *Ankrd26* promoter region (-436 bp/ -221 bp) in HFD- ($n = 4$) and STD-fed ($n = 4$) mice. Each row indicates sequencing results of ten independent clones. White circles, un-methylated CpGs; black circles, methylated CpGs. CpG position relative to *Ankrd26* TSS is shown above each column. **(e)** Correlation between DNA methylation percentage at CpGs -436 and -431 bp and *Ankrd26* mRNA levels. r and p values are indicated on graph. **(b,c)** Results are mean \pm SD from three independent experiments. **(a-c)**, $*p < 0.05$, $**p < 0.01$, and $***p < 0.001$ vs STD.

Methylation at the CpGs -436 and -431 bp modulates *Ankrd26* promoter activity. To evaluate the causal relationship between the promoter DNA methylation and transcription of *Ankrd26* gene, a luciferase assay was performed in NIH-3T3 cells transfected with *in vitro* methylated (me) or un-methylated (unme) pCpG-*Ankrd26* luciferase reporter vectors, in which a selected region of the *Ankrd26* promoter was cloned,

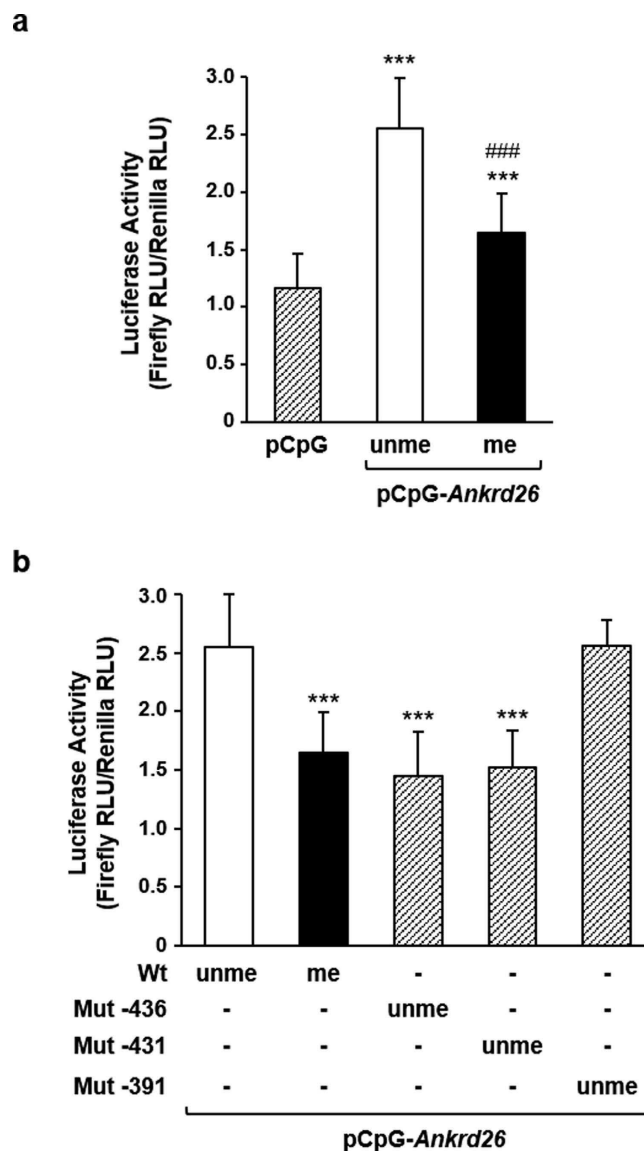


Figure 2. *Ankrd26* promoter activity in NIH-3T3 cells. (a) Luciferase activity of pCpG-*Ankrd26* constructs *in vitro* methylated (me) or un-methylated (unme) and of pCpG empty vector. Firefly luciferase activity was normalized to Renilla luciferase activity. Luciferase activity was measured in relative light units (RLU). *** $p < 0.001$ vs pCpG; ### $p < 0.001$ vs pCpG-*Ankrd26*unme. (b) Luciferase activity of unme mutagenized vectors, pCpG-*Ankrd26*-436, pCpG-*Ankrd26*-431 and pCpG-*Ankrd26*-391. Firefly luciferase activity was normalized to Renilla luciferase activity. Luciferase activity was measured in relative light units (RLU). *** $p < 0.001$ vs Wt unme. (a,b) results are mean \pm SD from three independent experiments.

containing the CpGs -436, -431 and -391 bp. The un-methylated *Ankrd26* promoter induced a 2.5-fold increase in the luciferase activity compared with the empty vector (Fig. 2a), indicating that this selected fragment is sufficient to mediate promoter activity. In addition, methylation of the *Ankrd26* promoter caused a 35% decrease of luciferase activity compared with the un-methylated *Ankrd26* promoter (Fig. 2a), indicating that methylation of this region has a negative impact on *Ankrd26* gene expression. Next, to define whether the CpGs -436 or -431 bp or both is/are responsible for the regulation of the *Ankrd26* promoter activity, luciferase assays were performed in NIH-3T3 cells transfected with un-methylated site-specific mutagenized vectors. The un-methylated *Ankrd26* promoter mutagenized at the -436 bp CpG site (*Ankrd26*-436unme), similarly to the wild type (Wt) methylated *Ankrd26* promoter, showed a 40% reduction of the luciferase activity compared with the un-methylated *Ankrd26* Wt fragment (Fig. 2b). Similar data were obtained when the *Ankrd26* promoter was mutagenized at the -431 bp CpG site (Fig. 2b). Conversely, when the *Ankrd26* promoter was mutagenized at the -391 bp CpG site, the luciferase activity of the un-methylated *Ankrd26*-391 promoter was comparable to the un-methylated Wt promoter (Fig. 2b). Thus, specific methylation at the -436 and -431 bp CpGs in the *Ankrd26* promoter modulates *Ankrd26* gene expression *in vitro*.

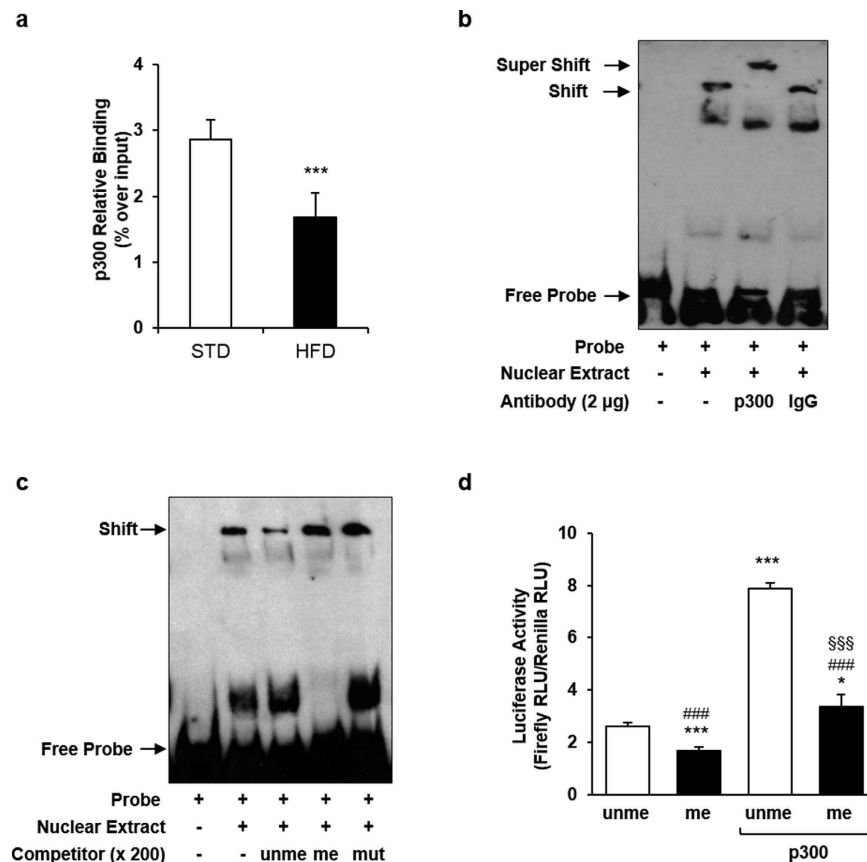


Figure 3. p300 binding and activity on *Ankrd26* promoter. (a) ChIP of p300 binding on *Ankrd26* promoter in eAT from HFD- (n = 3) and STD-fed (n = 3) mice, upon 22 weeks of diet regimens. ChIP enrichment is relative to Input chromatin. *** $p < 0.001$ vs STD. (b,c) Representative EMSA for double-stranded biotinylated *Ankrd26* probe with Nuclear Extract (NE) from NIH-3T3 cells. Uncut gel images are in the Supplementary Fig. S5. (b) EMSA super-shift assay with an anti-p300 antibody (lane 3) or a rabbit IgG (lane 4). (c) EMSA competition assay with 200-fold molar excess of un-labeled un-methylated (unme; lane 3), methylated (me; lane 4) or mutagenized (mut; lane 5) competitor. (d) Luciferase activity of *in vitro* methylated (me) or un-methylated (unme) pCpG-*Ankrd26* vector in NIH-3T3 cells co-transfected with pCl.p300 vector. Firefly luciferase activity was normalized to Renilla luciferase activity. Luciferase activity was measured in relative light units (RLU). *** $p < 0.001$ vs pCpG-*Ankrd26* unme; ### $p < 0.001$ vs pCpG-*Ankrd26* unme + pCl.p300; §§§ $p < 0.001$ vs pCpG-*Ankrd26* me. (a and d), results are mean \pm SD from three independent experiments.

Methylation at the CpGs -436 and -431 bp impairs p300 binding to the *Ankrd26* promoter.

DNA methylation often induces gene silencing by inhibiting transcriptional activator binding to promoters²³. TFBIND analysis of the *Ankrd26* promoter region spanning the CpGs -436 and -431 bp, predicted a consensus sequence (-442 bp/-429 bp) for the histone acetyltransferase/transcriptional coactivator p300^{24,25}. The recruitment of p300 to this putative binding site and its relevance to the regulation of the *Ankrd26* gene expression was therefore investigated. Chromatin Immunoprecipitation (ChIP) analysis showed a 40% decrease in p300 binding to the *Ankrd26* promoter in eAT of obese compared with lean mice (Fig. 3a). In addition, Electrophoretic Mobility Shift Assay (EMSA) with a double-stranded labeled probe containing the p300 consensus sequence on the *Ankrd26* promoter revealed that the addition of p300 antibody to the probe/Nuclear Extract (NE) mix super-shifted one of the complexes formed by interaction of the probe with the NE proteins (Fig. 3b). Also, the presence of an un-methylated competitor to the probe/NE mix effectively displaced p300 binding to the probe, while the probe/p300 complex was not affected by the addition of both a methylated or a mutagenized competitor (Fig. 3c). The *in vitro* over-expression of p300 in NIH-3T3 cells caused a 3-fold increase of the un-methylated *Ankrd26* promoter activity (Fig. 3d). At variance, when p300 was over-expressed, the luciferase activity of the methylated *Ankrd26* promoter was 60% lower compared with the un-methylated *Ankrd26* promoter (Fig. 3d). All together, these data indicate that p300 binding to *Ankrd26* promoter regulates *Ankrd26* gene expression and is dependent on the methylation state of the CpGs -436 and -431 bp.

HFD induces hyper-methylation of the *Ankrd26* promoter through DNMT3a and DNMT3b in mice. The molecular events upstream and downstream methylation-induced displacement of p300 binding to the *Ankrd26* promoter were subsequently analyzed. ChIP analysis revealed that binding of DNMT3a and DNMT3b, but not of DNMT1, to the *Ankrd26* promoter was increased in HFD-fed mice compared to controls

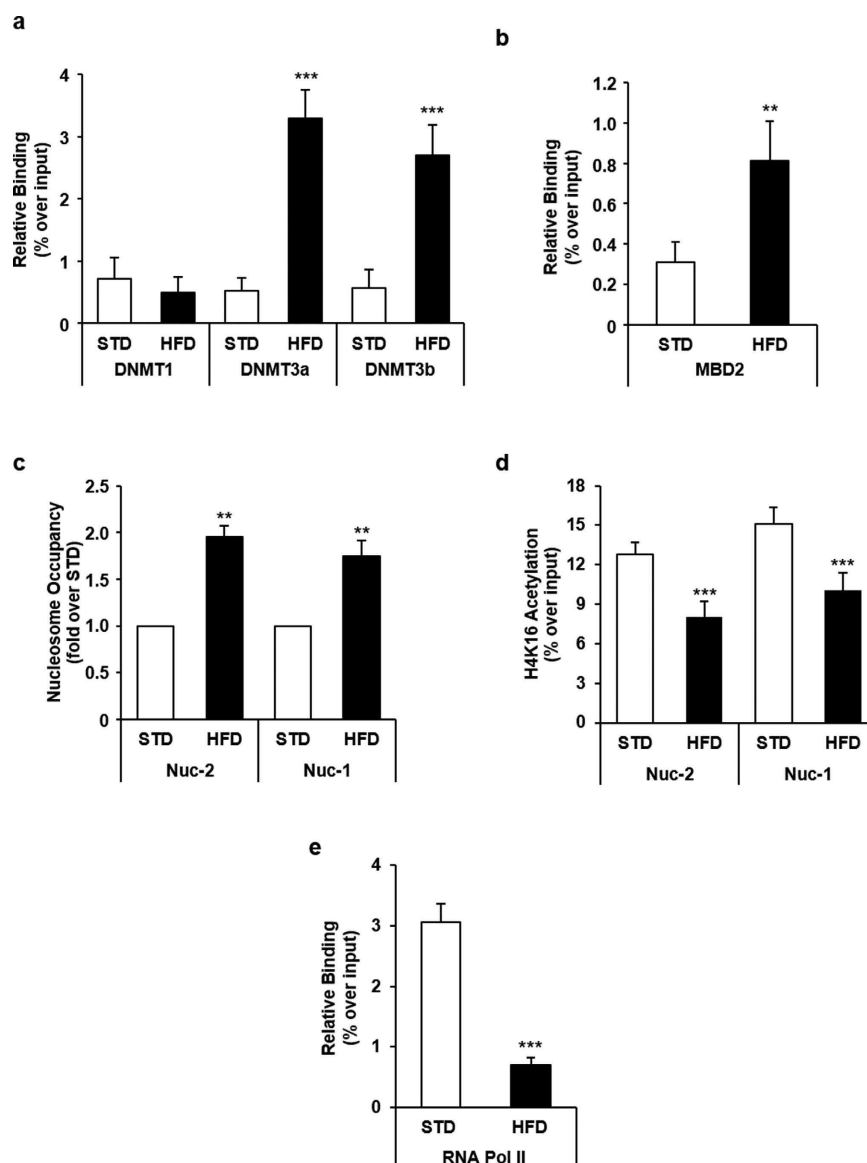


Figure 4. Epigenetic changes and protein binding at *Ankrd26* promoter in eAT from mice upon 22 weeks of HFD. ChIP of DNMT1, DNMT3a, DNMT3b (a) and MBD2 (b) binding at *Ankrd26* promoter region (−553 bp/−348 bp). (c) MNase for Nuc-2 (−257 bp/−198 bp) and Nuc-1 (−84 bp/−25 bp) occupancy at *Ankrd26* promoter. (d) ChIP for acetyl-H4 enrichment at Nuc-2 and Nuc-1. (e) ChIP of RNA Pol II binding at *Ankrd26* TSS (+16 bp/+159 bp). (a,b) and (d,e), ChIP enrichment is relative to Input chromatin. (a–e), results are mean ± SD from three independent experiments. ** $p < 0.01$ and *** $p < 0.001$ vs STD.

(Fig. 4a). Interestingly, HFD increased the binding of methylation-dependent transcriptional repressor MBD2 as well (Fig. 4b)²³.

HFD affects histone acetylation, nucleosome positioning and RNA Pol II binding at the *Ankrd26* promoter in mice. Further analysis of the *Ankrd26* promoter using the NuPoP software predicted 2 nucleosomes (Nuc), Nuc-2 (−288 bp/−132 bp) and Nuc-1 (−105 bp/+41 bp), positioned between the p300 consensus sequence and the *Ankrd26* TSS. Micrococcal Nuclease (MNase) treatment of eAT chromatin from HFD- and STD-fed mice followed by qPCR revealed that HFD rendered the *Ankrd26* promoter less sensitive to nuclease digestion, increasing Nuc-2 and Nuc-1 positioning (Fig. 4c). Consistently, ChIP analysis showed that HFD feeding significantly lowered histone H4 acetylation at both nucleosomes in the HFD- compared to STD-fed mice ($p < 0.001$; Fig. 4d). The RNA Pol II binding to the *Ankrd26* TSS was also significantly lower in HFD-fed mice ($p < 0.001$; Fig. 4e). All together, these data indicate that methylation at the CpGs −436 and −431 bp and the subsequent p300 displacement from this region silenced *Ankrd26* expression through nucleosome remodeling at the *Ankrd26* promoter.

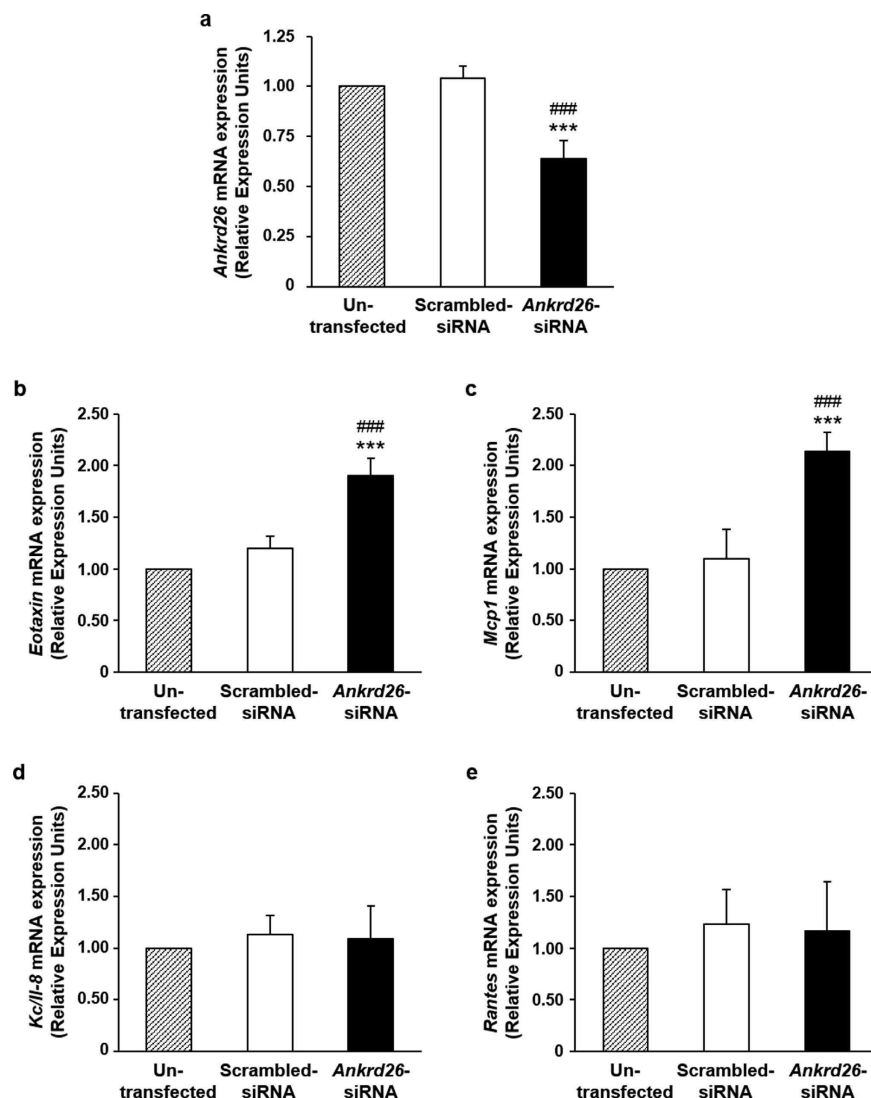


Figure 5. *Ankrd26* mRNA expression in *Ankrd26*-silenced mature adipocytes. 3T3-L1 mature adipocytes were silenced with 25 nmol/l of scrambled-siRNA or *Ankrd26*-siRNA for 48 h. Un-transfected cells were used to exclude transfection interference on mRNA expression. *Ankrd26* (a), *Eotaxin* (b), *Mcp1* (c), *Kc/Il-8* (d) and *Rantes* (e) mRNA levels were evaluated at the end of the experiment and expressed in Relative Expression Units (REU). Data are mean \pm SD of determinations from three independent experiments. *** $p < 0.001$, vs Un-transfected; ### $p < 0.001$, vs Scrambled-siRNA.

***Ankrd26* silencing promotes secretion of pro-inflammatory chemokines by cultured adipocytes.** To assess the functional consequences of the HFD-induced epigenetic silencing of the *Ankrd26* gene, *Ankrd26* mRNA was reduced by about 35% by transfecting *Ankrd26*-specific siRNA in 3T3-L1 adipocytes (Fig. 5a). Silenced adipocytes showed enhanced secretion of the pro-inflammatory chemokines, Keratinocyte-derived Cytokine/Interleukine 8 (KC/IL-8), Eotaxin, Monocyte chemotactic protein 1 (MCP1) and Rantes (Table 2). These changes were accompanied by increased mRNA levels of *Eotaxin* and *Mcp1* with no change in *Kc/Il-8* and *Rantes* mRNAs (Fig. 5b,c,d and e). It appeared therefore that *Ankrd26* physiologically controls the adipocyte pro-inflammatory secretion profile through effects occurring at different levels.

***ANKRD26* expression negatively correlates with Body Mass Index (BMI) and inflammation markers in humans.** mRNA expression of *ANKRD26* in VAT was further examined in human obese subjects (Supplementary Table S1) in relation to BMI and inflammatory parameters. Interestingly, in obese subjects with normal glucose tolerance (NGT), *ANKRD26* expression in VAT was found to negatively correlate with BMI (Fig. 6a), with serum levels of the pro-inflammatory chemokines, IL-8 and RANTES and with serum levels of the inflammatory markers, IL-6 and C-reactive protein (CRP) (Fig. 6b,c,d and e). Altogether, these data indicate that, in obese humans, the reduction of *ANKRD26* gene expression is associated with increased body weight and with a pro-inflammatory status.

Variable	3T3-L1 Adipocytes		
	Un-transfected	Scrambled-siRNA	<i>Ankrd26</i> -siRNA
Eotaxin (pg/ml)	514.34 ± 73.25	521.16 ± 82.90	705.92 ± 98.99 ^{b,d}
G-CSF (pg/ml)	6.45 ± 0.96	7.11 ± 0.22	7.14 ± 0.90
IL-4 (pg/ml)	3.41 ± 0.32	3.21 ± 0.44	3.81 ± 0.51
IL-5 (pg/ml)	0.88 ± 0.14	0.79 ± 0.16	0.83 ± 0.33
KC/IL-8 (pg/ml)	565.39 ± 15.32	588.67 ± 30.86	702.58 ± 34.08 ^{a,c}
IL-17 (pg/ml)	1.44 ± 0.62	1.72 ± 0.51	1.56 ± 0.42
MCP1 (pg/ml)	1758.04 ± 72.31	1718.77 ± 248.29	2500.31 ± 225.38 ^{b,d}
MIP1β (pg/ml)	1.32 ± 0.75	1.14 ± 0.52	1.17 ± 0.37
Rantes (pg/ml)	27.95 ± 2.74	33.31 ± 8.88	53.45 ± 2.35 ^{b,d}
TNFα (pg/ml)	4.98 ± 1.46	5.29 ± 1.31	5.57 ± 1.81

Table 2. Effect of *Ankrd26* gene silencing on adipocyte-released chemokines/cytokines. 3T3-L1 mature adipocytes were silenced with 25 nmol/l of scrambled-siRNA or *Ankrd26*-siRNA for 48 h. Conditioned media were collected for 24 h in Dulbecco's modified Eagle's medium without serum and with 0.5% BSA. Adipokines were then assayed using the Bio-Plex Pro Mouse Cytokine Immunoassay. Un-transfected cells were also used to exclude transfection interference on adipokine secretion. Detectable adipokines are reported. Data are mean ± SD of determinations from three independent experiments. ^a $p < 0.001$ and ^b $p < 0.01$, vs Un-transfected; ^c $p < 0.001$ and ^d $p < 0.01$, vs Scrambled-siRNA. Granulocyte-colony stimulating factor, G-CSF; Interleukin, IL; Keratinocyte-derived Cytokine/Interleukin 8, KC/IL-8; Monocyte chemotactic protein 1, MCP1; Macrophage inflammatory protein 1 beta, MIP1β; Tumor necrosis factor alpha, TNFα.

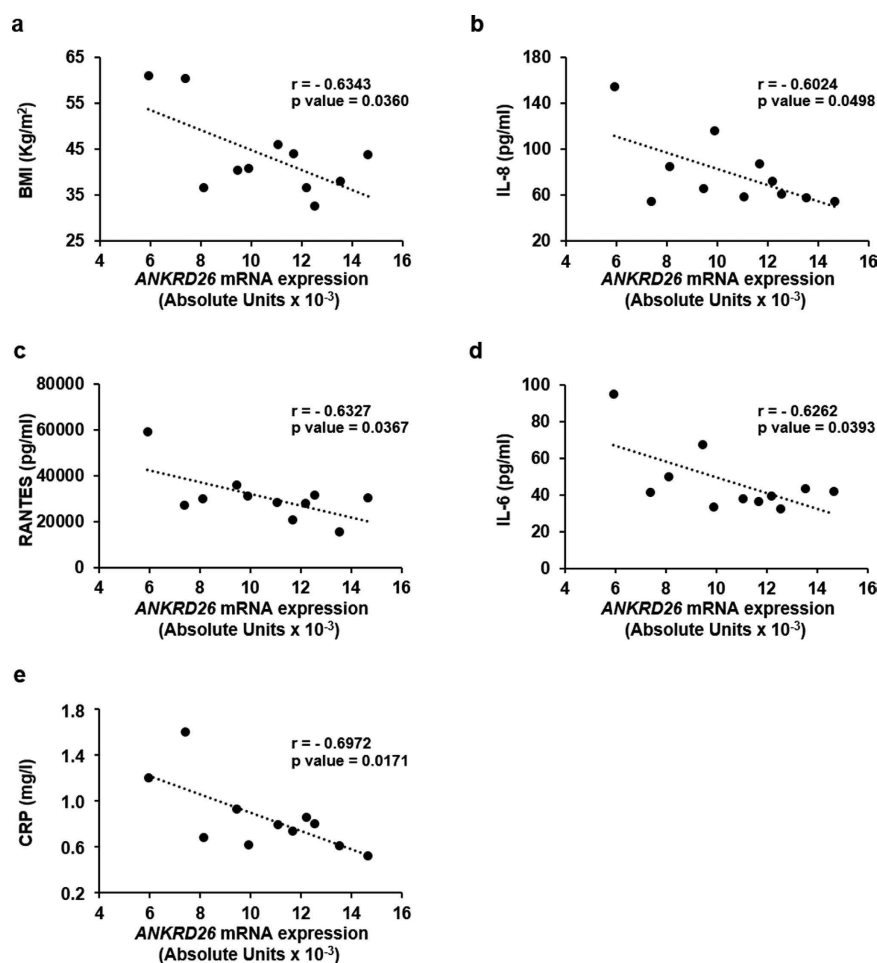


Figure 6. Associations between VAT *ANKRD26* mRNA expression, BMI and systemic inflammatory parameters in humans. Correlations of the human VAT *ANKRD26* mRNA expression with BMI (a) and with serum inflammatory markers, IL-8 (b), RANTES (c), IL-6 (d) and CRP (e) in normal glucose tolerant obese individuals (n = 11; 5 M/6 F). *r*, Pearson's coefficient; $p < 0.05$ were considered statistically significant.

Discussion

Epigenetic modifications represent a common mechanism through which both genetic and environmental exposures impact on the susceptibility to obesity and T2D^{26–28}. Recent evidence has underlined the potential importance of epigenetic regulation of gene expression and function in obesity²⁶. Methylation changes at the promoter of several genes have been identified in both human and rodent obesity²⁹. Additionally, the exposure to high calorie diets, which promotes DNMT expression and enzymatic activities, impacts on DNA methylation profiles both at specific genes and at genome-wide level^{22,30}, suggesting that DNA methylation changes play a role in the responses to fat and high-calorie diets³¹.

Our study revealed HFD-induced methylation of the *Ankrd26* promoter. We have no clue at the moment on the detailed mechanisms causing the increased methylation of *Ankrd26* in HFD-fed mice, but our results indicate that the HFD-induced hyper-methylation at *Ankrd26* promoter was concomitant with enhanced binding of *de novo* DNMT3a and DNMT3b to the same *Ankrd26* promoter region. These changes were followed by down-regulation of *Ankrd26* expression in the eAT. The epigenetic silencing of *Ankrd26* gene in eAT appear to depend, at least in part, on saturated fats, abundant in the HFD. Indeed, we found increased promoter DNA methylation and down-regulation of *Ankrd26* in 3T3-L1 adipocytes upon exposure to palmitate, a major component of the HFD, but not to oleate. At the variance with palmitate, cell exposure to leptin, whose serum concentration increases in relation to obesity²², showed no effect on *Ankrd26* expression and methylation. These findings suggest that specific nutritional components of the HFD may contribute to the epigenetic silencing of *Ankrd26* gene.

The HFD-induced changes in DNA methylation at *Ankrd26* promoter and gene expression result from a long-term diet exposure. Indeed, cytosine hyper-methylation at the *Ankrd26* promoter and gene silencing appeared in eAT from obese mice after a prolonged HFD feeding, while no evident difference was observed at earliest time-point. This time effect was associated with the eAT compensatory remodeling occurring in response to HFD. Indeed, eAT, along with other VAT depots, contributes to the inflammatory and metabolic complications in murine obesity³², and responds to HFD through different time-dependent changes^{33,34}. Early upon HFD exposure (8–12 weeks), eAT expansion is accompanied by a major increase in adipocyte size. Upon more prolonged HFD exposure (20 weeks), however, eAT expansion is mainly sustained by increased adipogenesis and accompanied by enhanced secretion of inflammatory mediators, including Tumor necrosis factor alpha (TNF- α), IL-6, MCP1 and Rantes^{33–35}. The mechanisms triggering this compensatory response in eAT have not been clarified yet but the present work now shows that they may involve HFD-induced *Ankrd26* down-regulation. Along with its role in feeding behavior and body fat accumulation^{13–15}, *Ankrd26* has been identified as a regulator of adipogenesis *in vitro*^{17,18}. Firstly, adipogenesis of 3T3-L1 cells is enhanced by selective silencing of the *Ankrd26* gene with an *Ankrd26*-specific shRNA¹⁸. Secondly, Mouse Embryonic Fibroblasts from *Ankrd26* mutant mice (MEFs *Ankrd26*^{−/−}) have a higher rate of adipocyte differentiation. Indeed, the mRNA expression of the master regulator genes of differentiation process, *CCAAT enhancer-binding protein α* (*C/ebp α*), and *Peroxisome proliferator-activated receptor γ* (*Ppar γ*), are up-regulated in MEFs *Ankrd26*^{−/−}, indicating that this gene is involved in regulating both the pre-adipocyte commitment and differentiation¹⁷.

In this work, we further demonstrated enhanced expression and/or secretion of the pro-inflammatory chemokines Eotaxin, MCP1, KC/IL-8, and Rantes by 3T3-L1 adipocytes whose *Ankrd26* expression was silenced to levels similar to those occurring in response to HFD. These cytokines have been reported to contribute to adipose tissue inflammation^{36,37}. Since secretion of Eotaxin, MCP1, KC/IL-8, and Rantes by the eAT also increases upon prolonged exposure to HFD^{33,34}, our findings suggest the involvement of *Ankrd26* down-regulation in raising and/or sustaining the low-grade inflammatory response which occurs in the eAT after long-term HFD feeding and is implicated in the development of insulin resistance and T2D^{33–35}. This might represent a mechanism by which environmental cues are integrated at specific genomic loci, contributing to the metabolic disorder. The relevance of these observations to humans is supported by our further findings in obese individuals with normal glucose tolerance, revealing that the reduction of *ANKRD26* expression in VAT negatively correlates with the serum concentrations of inflammatory markers and pro-inflammatory chemokines, which are associated to obesity in humans^{38,39} and whose increased levels predict occurrence of T2D^{38–43}. Cardamone *et al.* have recently shown in the adipose tissue the relevance of the cytosolic function of the *Ankrd26* partner GPS2 (G protein pathway suppressor 2) to the prevention of uncontrolled activation of inflammatory programs⁴⁴. Even though this issue deserves further mechanistic investigation, we suggest that *Ankrd26* might work as a molecular regulator of inflammatory signaling pathways, at least in part, by facilitating the cytoplasmic localization of its interacting partner GPS2¹⁸. Therefore, *ANKRD26* down-regulation might represent an early event triggering chronic low-grade inflammatory response in human adipose tissue.

Detailed methylation analysis of the *Ankrd26* promoter showed that HFD induced specific methylations at −436 and −431 bp CpGs, thereby exerting a suppressive effect on *Ankrd26* promoter activity. Similar to DNA methylation, mutagenesis at the *Ankrd26* promoter showed that introduction of C → T mutation at −436 or −431 bp CpGs significantly reduces *Ankrd26* promoter activity. These results provide evidence that *i.*, these cytosine residues have functional significance to the *Ankrd26* gene expression; and *ii.*, the DNA methylation at these specific CpGs plays a functional role in the epigenetic repression of *Ankrd26* gene.

Current evidence supports a role for epigenetic changes in the regulation of metabolic diseases and in some cases, as in our study, it has been demonstrated that small methylation changes are associated with gene expression variability with significant effects on the phenotype^{45–48}. In support of this concept, Barrès *et al.*⁴⁶ have recently shown that hyper-methylation of the *Peroxisome proliferator-activated receptor γ coactivator 1 α* (*PGC1 α*) promoter modulates *PGC1 α* expression, implying a mechanism for decreased mitochondrial content in skeletal muscle from T2D patients. Also, using a gene reporter assay, these same authors have demonstrated that the *in vitro* methylation of a single cytosine residue at the *PGC1 α* promoter is responsible for the reduction of gene activity⁴⁶.

CpG methylation generally affects transcription directly, by blocking the binding of transcriptional activators^{24,49}, or indirectly, by recruiting DNA-binding proteins and co-repressor complexes that occupy the methylated promoters and facilitate the formation of heterochromatin⁵⁰. In this study, we have further demonstrated that *i.*, *in vitro*, the histone acetyltransferase/transcriptional coactivator p300 directly binds the consensus sequence at the *Ankrd26* promoter, containing the methylation sensitive cytosines –436 and –431 bp; *ii.*, hyper-methylation of these sites affects p300 binding and activity *in vivo* and *in vitro*. p300 regulates gene expression by acetylating both histones and transcriptional factors and plays a key role in modulating chromatin structure and function^{25,26}. In this paper, we have also reported that HFD reduces histone H4 acetylation, increases nucleosome occupancy at the *Ankrd26* promoter, and impairs RNA Pol II binding to the *Ankrd26* TSS, suggesting that the HFD-dependent p300 displacement from the *Ankrd26* promoter silences *Ankrd26* gene. These findings are consistent with recent studies demonstrating that CpG methylation suppresses transcription of several genes by direct inhibition of p300 binding to their promoter sequences^{51–53}. In conjunction with the inhibition of p300 binding, HFD induced the binding of MBD2 to the *Ankrd26* promoter in mice. MBD2 is a methyl-CpG binding protein and causes gene silencing by recruiting histone deacetylase at the methylated promoter regions^{31,50}. Accordingly, we propose that the specific CpG methylation at the *Ankrd26* promoter leads to HFD-induced epigenetic gene silencing by triggering a cascade of events which involves DNA-associated regulatory proteins, such as p300 and MBD2, and changes in chromatin structure.

The potential relevance to humans of the findings reported in the present work is supported by our further evidence that VAT *ANKRD26* mRNA levels were negatively correlated with BMI in humans. Consistent with our results, very recent computational data from a genome-wide DNA methylation analysis in human adipose tissue have revealed that *ANKRD26* DNA methylation and mRNA expression correlate with BMI⁵³. Thus, epigenetic regulation of *ANKRD26* gene may occur in humans as well.

In conclusion, our work reveals that the methylation of specific CpGs at the *Ankrd26* promoter occurs in mice during HFD treatment and causes the down-regulation of *Ankrd26* expression, at least in part, by impairing p300 binding to its promoter. We propose that the epigenetic silencing of the *Ankrd26* gene contributes to VAT inflammation following unhealthy dieting.

Methods

Animals, diets and tests. Animal experiments were performed in accordance with the Guide for the Care and Use of Laboratory Animals published by the National Institutes of Health (publication no. 85–23, revised 1996). Protocols were approved by the ethics committee of the “Federico II” University of Naples. Six-week-old C57BL/6J male mice (n = 48) from Charles River Laboratories International, Inc. (Wilmington, MA) were housed in a temperature-controlled (22 °C) room with a 12 h light/dark cycle. Two weeks after arrival, mice were randomly divided into two groups of 12 mice each and were fed either a HFD (60 kcal% fat content; Research Diets formulas D12331; Research Diets, Inc., New Brunswick, NJ) or a standard chow diet (STD; 11 kcal% fat content; Research Diets formulas D12329; Research Diets, Inc.) for 8 and 22 weeks. The composition of these diets is reported in Supplementary Table S2. Body weight was recorded weekly throughout the study. The glucose tolerance test (GTT) and insulin tolerance test (ITT) were performed as described^{14,16}. Blood glucose levels were measured using a glucometer (One Touch Lifescan, Milan, Italy). Mice were killed by cervical dislocation. eAT was collected from each mouse, snap frozen in liquid nitrogen and stored at –80 °C.

Quantitative real-time PCR (qPCR) and western blot analysis. Tissues were homogenized by TissueLyser LT (Qiagen, Hilden, Germany) following manufacturer’s protocol. RNA and DNA were isolated using AllPrep DNA/RNA/miRNA Universal kit (Qiagen). cDNA synthesis and qPCR were performed as described^{19,54}. Immunoblotting was carried out as indicated¹⁴. Antibodies against *ANKRD26* (#SC-82505, Santa Cruz Biotechnology, Inc., Dallas, TX), and α -Tubulin (#MA1-19162, Sigma-Aldrich, St. Louis, MO) were used for protein detection.

Methylated DNA Immunoprecipitation (MeDIP). MeDIP assay was performed as described¹⁹. DNA methylation enrichment was evaluated on genomic DNA isolated from eAT of STD- and HFD-fed mice and from 3T3-L1 adipocytes. Sonicated pooled genomic DNA from eAT or cells was immuno-precipitated using anti-5mCpG (#ab10805, Abcam, Cambridge, MA) or mouse IgG (#I8765, Sigma-Aldrich) with anti-mouse IgG beads (Life Technologies, Carlsbad, CA). DNA methylation enrichment on recovered DNA was evaluated by qPCR. Samples were normalized to their respective input using the $2^{-\Delta\Delta CT}$ method.

Bisulfite sequencing. For bisulfite sequencing analysis, we used genomic DNA isolated from eAT of STD- and HFD-fed mice. Bisulfite conversion of DNA was performed with the EZ DNA Methylation Kit (Zymo Research, Orange, CA), following manufacturer’s instructions. Converted DNA was amplified by PCR. PCR products were cloned into the pGEM T-Easy vector (Promega, Madison, WI) and 10 clones for sample were sequenced on AB 3500 genetic analyzer (Life Technologies). DNA methylation percentage at the –436 and –431 bp CpGs for each mouse was calculated using the formula: DNA methylation % = [methylated CpGs/(methylated CpGs + unmethylated CpGs)]*100.

Cloning strategy, site-direct mutagenesis and *in vitro* methylation. *Ankrd26* promoter (–733 bp/–344 bp) was amplified by PCR. The purified PCR fragment was cloned into the firefly luciferase reporter pCpGfree-promoter-Lucia vector (Invivogen, Toulouse, France). The following site-specific mutated constructs were generated by PCR-based mutagenesis: pCpG-*Ankrd26*-436, pCpG-*Ankrd26*-431, pCpG-*Ankrd26*-391. The wild type (Wt) pCpG-*Ankrd26* vector, used as template, was removed from the PCR reaction by *DpnI* digestion (New England BioLabs, Ipswich, MA). Wt and mutated (mut) vectors were amplified into *E. coli* GT115 cells (Invivogen). Site-specific mutagenesis of each construct was validated by sequencing. *In vitro* methylation

was performed using the *M.SsI* CpG methyltransferase following manufacturer's protocol (New England BioLabs). Un-methylated DNA was obtained in the absence of *M.SsI*. Methylation was confirmed by resistance to *HpyCH4IV* digestion (New England BioLabs).

Luciferase assay. NIH-3T3 cells were transfected with methylated or un-methylated Wt or mutagenized pCpG-*Ankrd26* vector and Renilla control vector (Promega) by lipofectamine (Life Technologies), following manufacturer's instructions. Where indicated, cells were co-transfected with pCL.p300 expression vector (Promega). Firefly luciferase activity of each transfection was normalized for transfection efficiency against Renilla luciferase activity.

Chromatin Immunoprecipitation (ChIP) and Micrococcal Nuclease (MNase) assays. ChIP and MNase assays were performed as described^{55,56}. Briefly, 100 mg of eAT were cross-linked with 1% formaldehyde for 15 min at 37 °C. For ChIP assay, sonicated chromatin was immuno-precipitated with the following antibodies: anti-p300 (#SC-585, Santa Cruz Biotechnology), anti-Ac-H4-K16 (#07-329, Millipore, Temecula, CA), anti-DNMT1 (#NB100-56519) and anti-DNMT3b (#NB300-516) from Novus Biologicals (Littleton, CO), anti-DNMT3a (#ab2850), anti-MBD2 (#ab38646), and anti-RNA Pol II (#ab5408) from Abcam and anti-rabbit IgG (#I8140) and anti-mouse IgG (#I8765) from Sigma-Aldrich. For MNase assay, nuclei were isolated from 100 mg of eAT, suspended in wash buffer (100 mmol/L Tris-HCl, 15 mmol/L NaCl, 60 mmol/L KCl, 1 mmol/L CaCl₂) and treated with 200 U of MNase for 20 min at 37 °C. Cross-link reversal was performed at 65 °C for at least 16 h followed by an RNase and subsequent proteinase K digestion. DNA was purified by phenol–chloroform. Samples were then run on 1% agarose gel and the resulting mononucleosomal DNA fragments (~150 bp) were gel purified. For both assays, relative protein binding and nucleosome occupancy to the *Ankrd26* gene were evaluated on recovered DNA by qPCR. Samples were normalized to their respective input using the $2^{-\Delta\Delta CT}$ method.

Electrophoretic mobility shift assay (EMSA). Protein–DNA complexes were detected using unlabeled or biotin end-labeled double-stranded DNA probes by annealing complementary oligonucleotides. Biotin 3'-end oligonucleotides, spanning the *Ankrd26* promoter sequence from –455 bp to –425 bp relative to the *Ankrd26* TSS, were from Sigma-Aldrich and, where indicated, were synthesized to incorporate methylated cytosines (^mC). Binding reactions, consisting of biotin-labeled probe and NE, were performed using the LightShift kit (Thermo Fisher Scientific, Waltham, MA) following manufacturer's instructions. Biotin-labeled probe (20 fmol) was added and the reaction was allowed to incubate for 20 min at room temperature. In the competition experiments, the nuclear extracts were preincubated with 200 molar excess of unlabeled probes for 20 min on ice. In super-shift experiments, 2 µg of p300 antibody (#SC-585, Santa Cruz Biotechnology) or 2 µg of rabbit IgG (#I8140, Sigma-Aldrich) was preincubated with nuclear extracts for 60 min on ice. Protein–DNA complexes were separated on native polyacrylamide gel, transferred onto nylon membrane and detected by the LightShift Chemiluminescent EMSA kit (Thermo Fisher Scientific) following manufacturer's procedure.

Primer Sequences. The list of oligonucleotides used for PCR, qPCR, MeDIP, bisulfite sequencing, ChIP, MNase, EMSA can be found as Supplementary Table S3.

Fatty Acid/BSA complex solution preparation. Palmitate and oleate have been conjugated to fatty acid-free BSA (2:1 molar ratio Fatty Acid/BSA) as described in ref. 57. Briefly, a stock solution of palmitate (100 nM) was dissolved at 70 °C in 50% ethanol in a shaking water bath. In parallel, a fatty acid-free BSA solution was prepared at 55 °C in NaCl in a shaking water bath. Finally, the palmitate and the fatty acid-free BSA solutions were complexed at 55 °C in a shaking water bath, cooled to room temperature and sterile filtered. Oleate was complexed to the fatty acid-free BSA solutions following the same protocol. For fatty acid cell treatment, control adipocytes were treated with diluent only, corresponding concentrations of BSA and ethanol.

Cell culture and transfection. 3T3-L1 cells were grown and allowed to differentiate in mature adipocytes as described¹⁹. Mature adipocytes were *i.* silenced with 25 nmol/l of scrambled-siRNA or *Ankrd26*-siRNA for 48 h, or *ii.* treated with palmitate (0.250 mM; Sigma-Aldrich), or oleate (0.250 mM; Sigma-Aldrich) or corresponding vehicle (diluent solution with the same concentrations of BSA and ethanol of the Fatty Acid/BSA complex solution) for 96 h, or *iii.* treated with leptin (100 nM; R&D Systems, Minneapolis, CDN) or corresponding vehicle (20 mM Tris-HCl, pH 8.0) for 24 h. Adipokines were assayed in media from silenced cells by Bio-Plex Pro Mouse Cytokine Immunoassay following the manufacturer's protocol (Bio-Rad, Hercules, CA). *Ankrd26* promoter methylation and gene expression were analyzed as previously described in this section.

Patient enrollment and tests. Abdominal VAT biopsies and serum samples were from patients undergoing bariatric surgery. Eleven normal glucose tolerance (NGT) obese subjects were selected. Population characteristics are in Supplementary Table S1. Participants with metabolic and endocrine disorders, inflammatory diseases, previous or current malignancies, and/or treated with drugs able to interfere with the epigenome were excluded. Secreted mediators were assayed in serum samples by Bioplex multiplex Human Cytokine, Chemokine and Growth factor kit (Bio-Rad) following manufacturer's protocol. *ANKRD26* gene expression was analyzed in VAT as previously described in this section.

Ethics statement. This study adhered to the Declaration of Helsinki and has been reviewed and approved by the Ethics Committee of the “Federico II” University of Naples (Ethics Approval Number: No. 225_2013). Informed consent was obtained from all of enrolled individuals.

Statistical procedures. The area under the curve (AUC) was calculated using the trapezoidal rule. Data are expressed as mean \pm SD. Comparison between groups were performed using Student's t-test or the one-way analysis of variance, as appropriate, using GraphPad Software (version 6.00 for Windows, La Jolla, CA). Correlation between two variables was calculated using the parametric Pearson r-test. $p < 0.05$ was considered statistically significant.

References

- Eds Cavan, D., da Rocha Fernandes, J., Makaroff, L., Ogurtsova, K. & Webber, S. Brussels, Belgium: International Diabetes Federation. *International Diabetes Federation. IDF Diabetes Atlas 2015, 7th edition* (pdf available online) Executive summary, 12–19 (Last date of access: 29/11/2016) <http://www.diabetesatlas.org> (2015).
- Hu, F. B. Globalization of diabetes: the role of diet, lifestyle, and genes. *Diabetes Care* **34**, 1249–1257 (2011).
- Ng, M. *et al.* Global, regional, and national prevalence of overweight and obesity in children and adults during 1980–2013: a systematic analysis for the Global Burden of Disease Study 2013. *Lancet* **384**, 766–781 (2014).
- Seki, Y., Williams, L., Vuguin, P. M. & Charron, M. J. Minireview: Epigenetic programming of diabetes and obesity: animal models. *Endocrinology* **153**, 1031–1038 (2012).
- Rakyan, V. K., Down, T. A., Balding, D. J. & Beck, S. Epigenome-wide association studies for common human diseases. *Nat. Rev. Genet.* **12**, 529–541 (2011).
- Toperoff, G. *et al.* Genome-wide survey reveals predisposing diabetes type 2-related DNA methylation variations in human peripheral blood. *Hum. Mol. Genet.* **21**, 371–383 (2012).
- Bell, C. G. *et al.* Integrated genetic and epigenetic analysis identifies haplotype-specific methylation in the FTO type 2 diabetes and obesity susceptibility locus. *PLoS One* **5**, e14040 (2010).
- Virtue, S. & Vidal-Puig, A. Adipose tissue expandability, lipotoxicity and the Metabolic Syndrome—an allostatic perspective. *Biochim. Biophys. Acta*, **1801**, 338–349 (2010).
- Neeland, I. J. *et al.* Dysfunctional adiposity and the risk of prediabetes and type 2 diabetes in obese adults. *JAMA* **308**, 1150–1159 (2012).
- Hayashi, T. *et al.* Visceral adiposity is an independent predictor of incident hypertension in Japanese Americans. *Ann. Intern. Med.* **140**, 992–1000 (2004).
- Boyko, E. J., Fujimoto, W. Y., Leonetti, D. L. & Newell-Morris, L. Visceral adiposity and risk of type 2 diabetes: a prospective study among Japanese Americans. *Diabetes Care* **23**, 465–471 (2000).
- Hayashi, T. *et al.* Visceral adiposity and the risk of impaired glucose tolerance: a prospective study among Japanese Americans. *Diabetes Care* **26**, 650–655 (2003).
- Bera, T. K. *et al.* A model for obesity and gigantism due to disruption of the Ankrd26 gene. *Proc. Natl. Acad. Sci. USA* **105**, 270–275 (2008).
- Raciti, G. A., Bera, T. K., Gavrilova, O. & Pastan, I. Partial inactivation of Ankrd26 causes diabetes with enhanced insulin responsiveness of adipose tissue in mice. *Diabetologia* **54**, 2911–2922 (2011).
- Acs, P. *et al.* A novel form of ciliopathy underlies hyperphagia and obesity in Ankrd26 knockout mice. *Brain Struct. Funct.* **220**, 1511–1528 (2015).
- Dong, C. *et al.* Possible genomic imprinting of three human obesity-related genetic loci. *Am. J. Hum. Genet.* **76**, 427–437 (2005).
- Fei, Z., Bera, T. K., Liu, X., Xiang, L. & Pastan, I. Ankrd26 gene disruption enhances adipogenesis of mouse embryonic fibroblasts. *J. Biol. Chem.* **286**, 27761–27768 (2011).
- Liu, X. F. *et al.* ANKRD26 and its interacting partners TRIO, GPS2, HMMR and DIPA regulate adipogenesis in 3T3-L1 cells. *PLoS One* **7**, e38130 (2012).
- Parrillo, L. *et al.* Hoxa5 undergoes dynamic DNA methylation and transcriptional repression in the adipose tissue of mice exposed to high-fat diet. *Int. J. Obes. (Lond)* **40**, 929–937 (2016).
- Gesta, S. *et al.* Evidence for a role of developmental genes in the origin of obesity and body fat distribution. *Proc. Natl. Acad. Sci. USA* **103**, 6676–6681 (2006).
- Sackmann-Sala, L., Berryman, D. E., Munn, R. D., Lubbers, E. R. & Kopchick, J. J. Heterogeneity among white adipose tissue depots in male C57BL/6J mice. *Obesity* **20**, 101–111 (2012).
- Shen, W. *et al.* Epigenetic modification of the leptin promoter in diet-induced obese mice and the effects of N-3 polyunsaturated fatty acids. *Sci. Rep.* **4**, 5282 (2014).
- Bird, A. DNA methylation patterns and epigenetic memory. *Genes Dev.* **16**, 6–21 (2002).
- Ito, T., Ikehara, T., Nakagawa, T., Kraus, W. L. & Muramatsu, M. p300-mediated acetylation facilitates the transfer of histone H2A–H2B dimers from nucleosomes to a histone chaperone. *Genes. Dev.* **14**, 1899–1907 (2000).
- Liu, X. *et al.* The structural basis of protein acetylation by the p300/CBP transcriptional coactivator. *Nature* **451**, 846–850 (2008).
- Drong, A. W., Lindgren, C. M. & McCarthy, M. I. The genetic and epigenetic basis of type 2 diabetes and obesity. *Clin. Pharmacol. Ther.* **92**, 707–715 (2012).
- Raciti, G. A. *et al.* Understanding type 2 diabetes: from genetics to epigenetics. *Acta Diabetol.* **52**, 821–827 (2015).
- Raciti, G. A. *et al.* Personalized medicine and type 2 diabetes: lesson from epigenetics. *Epigenomics* **6**, 229–238 (2014).
- Desiderio, A. *et al.* Epigenetics: spotlight on Type 2 diabetes and obesity. *J. Endocrinol. Invest.* **10.1007/s40618-016-0473-1** (2016).
- van Dijk, S. J., Molloy, P. L., Varinli, H., Morrison, J. L. & Muhlbauer, B. S. Members of EpiSCOPE. Epigenetics and human obesity. *Int. J. Obes.* **39**, 85–97 (2015).
- Voisin, S. *et al.* Dietary fat quality impacts genome-wide DNA methylation patterns in a cross-sectional study of Greek preadolescents. *Eur. J. Hum. Genet.* **23**, 654–662 (2015).
- Berry, D. C., Stenesen, D., Zeve, D. & Graff, J. M. The developmental origins of adipose tissue. *Development* **140**, 3939–3949 (2013).
- Strissel, K. J. *et al.* Adipocyte death, adipose tissue remodeling, and obesity complications. *Diabetes* **56**, 2910–2918 (2007).
- Wang, Q. A., Tao, C., Gupta, R. K. & Scherer, P. E. Tracking adipogenesis during white adipose tissue development, expansion and regeneration. *Nat. Med.* **19**, 1338–1344 (2013).
- Strissel, K. J. *et al.* T-cell recruitment and Th1 polarization in adipose tissue during diet-induced obesity in C57BL/6 mice. *Obesity* **18**, 1918–1925 (2010).
- Kim, H. J. *et al.* Expression of eotaxin in 3T3-L1 adipocytes and the effects of weight loss in high-fat diet induced obese mice. *Nutr. Res. Pract.* **5**, 11–19 (2011).
- Huber, J. *et al.* CC chemokine and CC chemokine receptor profiles in visceral and subcutaneous adipose tissue are altered in human obesity. *J. Clin. Endocrinol. Metab.* **93**, 3215–3221 (2008).
- Stepień, M. *et al.* Obesity indices and inflammatory markers in obese non-diabetic normo- and hypertensive patients: a comparative pilot study. *Lipids Health Dis.* **13**, 29 (2014).
- Dandona, P., Aljada, A. & Bandyopadhyay, A. Inflammation: the link between insulin resistance, obesity and diabetes. *Trends Immunol.* **25**, 4–7 (2004).
- Barzilay, J. I. *et al.* The relation of markers of inflammation to the development of glucose disorders in the elderly: the Cardiovascular Health Study. *Diabetes* **50**, 2384–2390 (2001).
- Pradhan, A. D. *et al.* C-reactive protein, interleukin 6, and risk of developing type 2 Diabetes mellitus. *JAMA*. **286**, 327–34 (2001).

42. Herder, C. *et al.* Association of systemic chemokine concentrations with impaired glucose tolerance and type 2 diabetes: results from the Cooperative Health Research in the Region of Augsburg Survey S4 (KORA S4). *Diabetes*. **54**, Suppl 2 S11–7 (2005).
43. Herder, C. *et al.* Immunological and cardiometabolic risk factors in the prediction of type 2 diabetes and coronary events: MONICA/KORA Augsburg case-cohort study. *PLoS One*. **6**, e19852 (2011).
44. Cardamone, M. D. *et al.* A protective strategy against hyperinflammatory responses requiring the non-transcriptional actions of GPS2. *Mol. Cell*. **46**, 91–104 (2012).
45. Gracia, A. *et al.* Fatty acid synthase methylation levels in adipose tissue: effects of an obesogenic diet and phenol compounds. *Genes Nutr*. **9**, 411 (2014).
46. Barrès, R. *et al.* Non-CpG methylation of the PGC-1 α promoter through DNMT3B controls mitochondrial density. *Cell Metab*. **10**, 189–198 (2009).
47. Barrès, R. *et al.* Weight loss after gastric bypass surgery in human obesity remodels promoter methylation. *Cell Rep*. **3**, 1020–1027 (2013).
48. Paternain, L. *et al.* Transcriptomic and epigenetic changes in the hypothalamus are involved in an increased susceptibility to a high-fat-sucrose diet in prenatally stressed female rats. *Neuroendocrinology* **96**, 249–260 (2012).
49. Kuroda, A. *et al.* Insulin gene expression is regulated by DNA methylation. *PLoS One* **4**, e6953 (2009).
50. Ballestar, E. & Wolffe, A. P. Methyl-CpG-binding proteins. Targeting specific gene repression. *Eur. J. Biochem*. **268**, 1–6 (2001).
51. Li, H. P. *et al.* Aberrantly hypermethylated Homeobox A2 derepresses metalloproteinase-9 through TBP and promotes invasion in Nasopharyngeal carcinoma. *Oncotarget* **4**, 2154–2165 (2013).
52. Rönn, T. *et al.* Impact of age, BMI and HbA1c levels on the genome-wide DNA methylation and mRNA expression patterns in human adipose tissue and identification of epigenetic biomarkers in blood. *Hum Mol Genet* **24**, 3792–3813 (2015).
53. Raciti, G. A. *et al.* Glucosamine-induced endoplasmic reticulum stress affects GLUT4 expression via activating transcription factor 6 in rat and human skeletal muscle cells. *Diabetologia* **53**, 955–965 (2010).
54. Haim, Y., Tarnowski, T., Bashari, D. & Rudich, A. A chromatin immunoprecipitation (ChIP) protocol for use in whole human adipose tissue. *Am. J. Physiol. Endocrinol. Metab*. **305**, E1172–1177 (2013).
55. Carey, M. & Smale, S. T. Micrococcal Nuclease-Southern Blot Assay: I. MNase and Restriction Digestions. *CSH Protoc.* pdb.prot4890 (2007).
56. Spector, A. A. Fatty acid binding to plasma albumin. *J. Lipid. Res*. **16**, 165–179 (1975).
57. Kuehnen, P. *et al.* An Alu element-associated hypermethylation variant of the POMC gene is associated with childhood obesity. *PLoS Genet*. **8**, e1002543 (2012).

Acknowledgements

This study was funded by the European Foundation for the Study of Diabetes (EFS), by the Ministero dell'Istruzione, Università e della Ricerca Scientifica (grants PRIN and FIRB-MERIT, and PON 01_02460) and by the Società Italiana di Diabetologia (SID-FO.DI.RI). This work was further supported by the P.O.R. Campania FSE 2007–2013, Project CREME.

Author Contributions

G.A.R. conceived, designed and supervised the experiments, analysed data and wrote the paper. RS researched and analysed data and wrote the discussion. A.D., M.L., L.P., C.N., V.D.E., P.M. and F.F. collected the data. V.P. and P.FORE. contributed to the clinical study, acquisition of adipose tissue biopsies and human blood samples. P.FORM. and I.P. analysed and interpreted the data. C.M. and F.B. are the guarantors of this work and, as such, have full access to all the data in the study and take responsibility for the integrity of the data and the accuracy of the data analysis. All authors critically revised and approved the final version the manuscript.

Additional Information

Supplementary information accompanies this paper at <http://www.nature.com/srep>

Competing Interests: The authors declare no competing financial interests.

How to cite this article: Raciti, G. A. *et al.* Specific CpG hyper-methylation leads to *Ankrd26* gene down-regulation in white adipose tissue of a mouse model of diet-induced obesity. *Sci. Rep.* **7**, 43526; doi: 10.1038/srep43526 (2017).

Publisher's note: Springer Nature remains neutral with regard to jurisdictional claims in published maps and institutional affiliations.



This work is licensed under a Creative Commons Attribution 4.0 International License. The images or other third party material in this article are included in the article's Creative Commons license, unless indicated otherwise in the credit line; if the material is not included under the Creative Commons license, users will need to obtain permission from the license holder to reproduce the material. To view a copy of this license, visit <http://creativecommons.org/licenses/by/4.0/>

© The Author(s) 2017

REVIEW

Epigenetics: spotlight on type 2 diabetes and obesity

A. Desiderio^{1,2} · R. Spinelli^{1,2} · M. Ciccarelli^{1,2} · C. Nigro^{1,2} · C. Miele^{1,2} ·
F. Beguinot^{1,2} · G. A. Raciti^{1,2}

Received: 10 March 2016 / Accepted: 18 April 2016 / Published online: 14 May 2016
© Italian Society of Endocrinology (SIE) 2016

Abstract Type 2 diabetes (T2D) and obesity are the major public health problems. Substantial efforts have been made to define loci and variants contributing to the individual risk of these disorders. However, the overall risk explained by genetic variation is very modest. Epigenetics is one of the fastest growing research areas in biomedicine as changes in the epigenome are involved in many biological processes, impact on the risk for several complex diseases including diabetes and may explain susceptibility. In this review, we focus on the role of DNA methylation in contributing to the risk of T2D and obesity.

Keywords Epigenetics · DNA methylation · Type 2 diabetes · Obesity

Epigenetics: current status of knowledge

It is now well recognized that environmental factors including diet, physical activity, drugs and smoking, affect the phenotype and provide a major contribution to susceptibility to most chronic non communicable diseases [1]. Epigenetics acts at the interface between the genome and environmental factors, and might be broadly defined as the sum of all the mechanisms necessary to unfold the genetic program into development [2]. In the early 1940 s, Conrad Waddington linked genetics and developmental biology coining the term epigenetics. He

defined epigenetics as “the branch of biology which studies the causal interactions between genes and their products which bring the phenotype into being” [3]. However, the meaning of the word has gradually changed over the following years, and epigenetics is known today as “the study of changes in gene function that are mitotically and/or meiotically heritable and that do not entail a change in DNA sequence” [4]. Differently from traditional genetics, based on cell lineages and clonal inheritance, epigenetic changes often occur in groups of cells while some epigenetic events are clonal. In addition, genetic changes are, almost by definition, stable, whereas epigenetic changes are plastic events [2]. An example of the latter concept is provided by genomic imprinting, where DNA methylation may be lost during development, or when persisting, it is erased and re-setted during gametogenesis [5]. Epigenetic mechanisms are plastic genomic processes that change genome function under endogenous and exogenous influences [6, 7], and may propagate modifications of gene activity from one cell generation to the next [8]. These mechanisms imply chemical modification of DNA, such as DNA methylation, post-translational changes in histone proteins altering chromatin conformation, and transcriptional gene silencing mediated by non-coding RNAs (ncRNAs) [9] (Fig. 1). Abnormalities in one or more of these mechanisms can lead to inappropriate expression or silencing of genes, resulting in imbalance of the epigenetic network and may result in metabolic disorders such as T2D and obesity [10, 11].

✉ F. Beguinot
beguino@unina.it

¹ URT of the Institute of Experimental Endocrinology and Oncology “G. Salvatore”, National Council of Research, Naples, Italy

² Department of Translational Medical Sciences, University of Naples “Federico II”, Via Pansini 5, 80131 Naples, Italy

Epigenetic mechanisms and gene function

DNA methylation

DNA methylation is a covalent modification of DNA that occurs at position 5 of the cytosine pyrimidine ring [12].

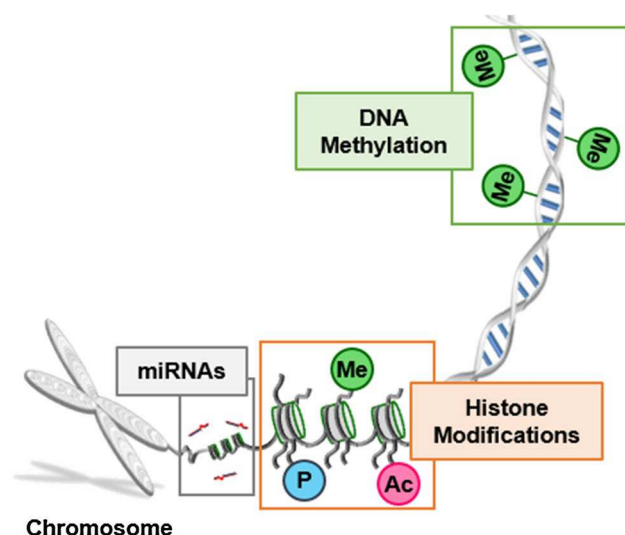


Fig. 1 Schematic representation of epigenetic modifications. Epigenetic modifications include DNA methylation, histone modifications and miRNAs. DNA methylation preferentially occurs at CpG di-nucleotides and is generally recognized as an epigenetic silencing mechanism. Histone modifications, instead, influence gene expression by directly altering the chromatin conformation through the passage from a condensed transcriptionally silent heterochromatin to transcriptionally active euchromatin and vice versa. Different types of modifications are known and include acetylation (Ac), methylation (Me), and phosphorylation (P) of histones tails. Finally, miRNAs act at post-transcriptional level by suppressing target gene expression or, through a non-perfect complementarity between miRNA and target mRNA that causes translation inhibition of the target or through near-perfect complementarity which results in the degradation of the target mRNA

Nearly four decades ago, DNA methylation was identified as hotspot for spontaneous base substitutions [13]. Indeed, while spontaneous deamination of cytosine produces uracil, a nitrogenous base that does not belong to DNA and that is immediately recognized and corrected by the system of DNA repair; deamination of 5-methyl cytosine produces thymine, causes C:G to T:A transitions, and creates a mismatch that the system of DNA repair does not always preserve [10, 14]. DNA methylation is the better characterized epigenetic mark. In mammals, it is essential during development and is involved in a variety of biological processes, including genomic imprinting and X chromosome inactivation [15]. DNA methylation is established during embryogenesis by de-methylation and de novo methylation events that can be inherited and maintained clonally by the action of specific enzymes termed DNA methyltransferases (DNMTs) [15, 16]. DNMT1 faithfully and symmetrically propagates cytosine methylation through recognition of methylated cytosines from an existing DNA strand to its novel partner upon replication and is primarily responsible for the maintenance of DNA methylation in cells. DNMT3A and DNMT3B are mainly involved in

de novo methylation and establish new methylation patterns [4]. DNA methylation has long been recognized as an epigenetic silencing mechanism [17] which preferentially occurs at CpG di-nucleotides that are usually clustered in the CpG islands (CGIs) [18]. Quite often, un-methylated CpG sites at gene promoters create a transcriptionally permissive chromatin state by destabilizing nucleosomes and facilitating the recruitment of transcription factors [19]. On the other hand, dense DNA methylation of CpGs mediates stable long-term gene silencing by direct inhibition of transcription factors binding or by a combination of events mediated by methyl-CpG binding domain proteins (MBDs) which recruit methylated DNA mediators of chromatin remodeling, such as histone deacetylases (HDACs), or other repressors of gene expression (Table 1) [17, 20, 21].

Histone modifications

In eukaryotic cells, nucleosomes are the repeating and functional structural units of chromatin. They are composed of DNA wrapped around eight histone proteins, two homo-dimers histones H3 and H4, and two hetero-dimers histones H2A/H2B. Nucleosomes are mutually connected among themselves by the stretches of variable length of DNA linker conveyed by histone H1 [22, 23]. Histone modifications, such as acetylation, methylation, phosphorylation, ubiquitination, sumoylation and ADP ribosylation, are reversible epigenetic modifications, occurring at the histone tails. These modifications regulate gene expression by dynamically altering chromatin conformation causing electrostatic change and/or modulating binding proteins to chromatin [22, 24]. Even more extensively than other types of modifications, acetylation and methylation mediate formation of the condensed transcriptionally silent heterochromatin and of the transcriptionally active euchromatin. In mammalian cells, heterochromatin prevails and is generally characterized by high levels of DNA methylation and histone de-acetylation, and is enriched in tri-methylation of H3-Lys9, H3-Lys27, and H4-Lys20 [25, 26]. On the other hand, euchromatin exhibits lower levels of DNA methylation, and is typically enriched in acetylation of lysine residues at histones H3 and H4 and in mono- and tri-methylation of H3-Lys4 (Table 1) [27, 28].

NcRNAs

Findings over the past ten years have progressively revealed the relevance of ncRNAs in most epigenetically controlled events including modulation of gene transcription, transposon activity and silencing, X-chromosome inactivation and paramutation [29]. NcRNAs include multiple classes of RNA transcripts that do not encode proteins but rather regulate gene expression at the post-transcriptional level

Table 1 Epigenetic modifications

Epigenetic modifications	Enzymes	Type of modification	Effect on gene expression	References
DNA Methylation	DNMT1	Methylation maintenance	Suppression	[17]
	DNMT3A, DNMT3B	de novo methylation	Suppression	
Histone modifications	TET family	De-methylation	Activation	[16]
	HATs	Acetylation	Activation e.g., H3K9, H3K14, H3K18, H3K56, H4K5, H4K8, H4K12, H4K16.	[25–28]
	HDACs	De-Acetylation	Repression	[25–28]
	HMTs	Methylation	Activation e.g., H3K4me2, H3K4me3, H3K36me3, H3K79me2 Repression e.g., H3K9me3, H3K27me3, H4K20me3.	[25–28]
	HDMs	De-methylation	Activation or repression based on the lysine residue	[25–28]
	MSK1	Phosphorilation	Activation e.g., H3S28	[26]
		Non-perfect complementarity	Inhibition of the mRNA target translation	[35]
		Perfect complementarity	Degradation of the mRNA target	[35]

Overview of the epigenetic modifications and of the different classes of enzymes involved in these processes

DNMTs DNA methyltransferases, *TET* ten–eleven translocation enzymes family, *HATs* histone acetyltransferases, *HDACs* histone deacetylases, *HMTs* histone *N*-methyl transferases, *HDMs* histone demethylases, *MSK1* mitogen-and-stress activated protein kinase-1, *H3* histone 3, *H4* histone 4, *K* lysine residue, *S* serine residue, *Me2* di-methylation, *Me3* tri-methylation

[30]. The most extensively studied ncRNAs are the miRNAs, small RNA molecules (21–25 nucleotides in length) often implicated in cell- and tissue-specific differentiation and development and associated to different disorders [31]. In the human genome, the exact number of reported sequences coding for these regulatory molecules continues to rise. In 2015, an analysis of 13 human cell types has revealed the existence of 3707 novel miRNA sequences, in addition to the 1900 sequences previously described [32]. miRNAs in the human genome are transcribed from both introns and exons of non-coding genes and from introns of protein coding genes as well [33]. In addition, some mammalian miRNAs derived from various transposons and processed pseudogenes [34]. miRNAs are critical regulators of post-transcriptional gene expression. In particular, suppression of the target gene expression mediated by miRNAs occurs based on the degree of complementarity of the miRNA with the 3' Untranslated Region (3'UTR) of the target mRNA. Non-perfect complementarity between miRNA and target RNA, generally due to a pairing of only six to eight nucleotides, causes translation inhibition of the target mRNA, while near-perfect complementarity results in the degradation of the target mRNA by the RNA-induced silencing complex (Table 1) [35]. Interestingly, miRNAs are also susceptible to epigenetic modulation. Aberrant DNA methylation of miRNA gene promoters frequently occurs in human cancer and results in miRNAs expression down-regulation [36]. On the other hand, miRNAs are

able to regulate both DNA methylation and histone modifications. Indeed, miRNAs may control the expression of important epigenetic regulators including DNMTs and HDACs thereby impacting on the entire gene expression profile [37].

Epigenetics in T2D and obesity

T2D and obesity are common metabolic disorders, which have reached epidemic proportions globally [38, 39]. Population and family (including twins) studies have extensively documented the familial aggregation of these diseases [40–45] with more than 175 genetic loci conclusively associated [46, 47]. Nevertheless, the impact of these loci, even in combination, on risk is very modest (5–10 % for T2D and ~2% for body mass index, BMI), leaving the heritability issue unsolved [48]. Technical limitations might, in part, account for this situation [49]. More likely, inheritance may be explained by epigenetics. Indeed, familial aggregation may reflect not only genetic influences, but also represent the effects of a shared family environment and thus of common environmentally induced epigenetic modifications [48]. In addition, while not been proved in humans yet, in rodents, certain environmentally induced epigenetic modifications can be trans-generationally transmitted to the offspring [50–52]. Environmentally induced epigenetic modifications may further explain the global epidemics of

Table 2 DNA methylation in T2D and Obesity

Genes	Regions	Epigenetic modification	Phenotypes	Tissues/cells	References
<i>PGC1α</i>	Promoter	↑ DNA Methylation	T2D	Pancreatic islets, Skeletal muscle	[58] [59]
<i>PDX-1</i>	Promoter	↑ DNA Methylation	T2D	Pancreatic islets	[63]
<i>FTO</i>	Intron 1	↓ DNA Methylation	T2D	PBLs	[64]
<i>POMC</i>	Intron 2-Exon 3	↑ DNA Methylation	Obesity	PBLs	[72]
<i>RXRA</i>	Promoter	↑ DNA Methylation	Obesity	Umbilical cord	[74]

Examples of epigenetically modulated genes in T2D and obesity

T2D type 2 diabetes, PBLs peripheral blood lymphocytes, *PGC1α* peroxisome proliferator activated receptor gamma coactivator-1 alpha, *PDX-1* pancreatic duodenal homeobox 1, *FTO* fat mass and obesity-associated, *POMC* pre-proopiomelanocortin, *RXRA* retinoid X receptor-alpha

T2D and obesity, whose exponential rise in the past decades have been related to rapid cultural and social changes, such as socio-economic status, dietary changes, physical inactivity and unhealthy behaviors, all of which tend to cluster in family groups [38, 53]. Finally, epigenetics may help to understand the identical twin discordance for obesity and T2D [54, 55]. For example, the concordance rates for T2D among monozygotic twins are only ~ 70 % [56]. In these metabolic disorders, the incomplete concordance may be in part due to stochastic or environmentally determined epigenetic modifications that change over the lifetime and is responsible for the phenotypic differences and susceptibility to disease. Epigenetic processes may, therefore, contribute to the development of T2D and obesity and mediate the effects of environmental exposure on risk [9, 57]. In the following paragraphs, examples from our own as well as other investigators will be presented supporting the evidence linking epigenetic modifications, in particular DNA methylation, to T2D and obesity in both humans and rodents.

T2D and DNA methylation

T2D is a metabolic abnormality characterized by elevated plasma glucose levels. T2D typically occurs when insulin secretion fails to keep pace with reduced sensitivity to the action of circulating insulin [38]. There is now substantial evidence indicating that environmentally induced epigenetic changes contribute to diabetes prevalence (Table 2). Ling et al. have recently demonstrated that the promoter of the transcriptional co-activator *Peroxisome proliferator activated receptor gamma coactivator-1 alpha* (*PGC1-α*) gene, mainly involved in mitochondrial function, is highly methylated in pancreatic islets obtained from diabetic patients compared with non-diabetic controls [58]. Additionally, Barrès et al. have shown that the hyper-methylation of the *PGC1-α* promoter occurs even in the skeletal muscle from type 2 diabetic subjects compared with

normal glucose-tolerant (NGT) individuals. Hyper-methylation negatively correlates with *PGC1-α* mRNA expression in these subjects [59]. In addition, the exposure of primary human skeletal muscle cells from NGT individuals to external factors, such as free fatty acids and tumor necrosis factor-α (TNF-α) directly and acutely alters the methylation status of *PGC1-α* promoter. These findings illustrate how alterations in the extracellular milieu may predispose to T2D by inducing DNA methylation changes [59]. Also, a genome-wide DNA methylation analysis of skeletal muscle from obese subjects before and after bariatric surgery provides evidence that the promoter methylation of *PGC1-α* is altered by obesity and restored after weight loss. DNA methylation inversely correlates to BMI, leptin, triglyceride and insulin levels in these subjects, which supports the role of DNA methylation in the physiological control of *PGC1-α* gene transcription [60]. The *Pancreatic duodenal homeobox 1* (*PDX-1*) promoter is also methylated. *PDX-1* is a homeodomain-containing transcription factor that plays a key role in pancreas development and function. In humans, mutations of *PDX-1* cause maturity onset diabetes of the young 4 (MODY4) [61], while *Pdx-1* silencing in pancreatic β-cells causes diabetes in mice [62]. In humans pancreatic islets, Yang et al. have shown that 10 CpG sites in the *PDX-1* promoter and enhancer regions are hyper-methylated in type 2 diabetics compared with healthy individuals and that glycosylated hemoglobin (HbA1c) negatively correlates with mRNA expression of *PDX-1* and positively correlates with DNA methylation, suggesting a role of chronic hyperglycemia in the modulation of *PDX-1* expression through epigenetic events [63]. In support of this concept, these authors also found an increased DNA methylation of the *Pdx-1* gene in clonal rat β-cells exposed to high levels of glucose associated to increased mRNA expression and binding of the Dnmt1 on *Pdx-1* promoter [63]. More recently, a genome-wide analysis of differentially methylated sites in genomic regions associated to T2D has recently revealed that the *Fat mass and Obesity-associated*

(*FTO*) gene is hypo-methylated in a CpG site within the first intron in type 2 diabetics compared with control subjects in human peripheral blood. The T2D predictive power of this mark is significantly greater than all genetic variants so far described [64]. In the same investigation Toperoff et al. have also prospectively established, that, in an independent cohort hypo-methylation at the *FTO* intron is observed in young subjects that later progress to T2D. This further finding provides evidence that methylation changes predispose to T2D and deserve to be considered further investigated as T2D markers.

Obesity and DNA methylation

Obesity is a complex disorder resulting in an abnormal accumulation of fat in the organism due to alterations in energy homeostasis in terms of balance among energy intake, expenditure and storage [65]. It has been extensively documented in both humans and animal models that a relationship exists between obesity and the epigenetic regulation of genes involved in the control of food intake (Table 2) [51, 66–70]. In this context, the epigenetic modulation of the *Agouti* gene is a paradigmatic example of this association in mice. The *Agouti* gene encodes the paracrine-signaling molecule “Agouti signalling peptide” (ASIP), which antagonizes the melanocortin 1 receptor (MC1R) and leads melanocytes to produce yellow rather than black coat pigments. Additionally, ASIP acts as antagonist of the hypothalamic MC4R, inhibiting the anorexigenic neuropeptide alpha-melanocyte-stimulating hormone (α -MSH) signaling, thereby promoting the activation of orexigenic pathways which make mice hyperphagic and prone to develop obesity and diabetes [67]. It is now known that the *Agouti* gene is sensitive to cytosine methylation [69]. When its promoter is un-methylated, the *Agouti* gene is in an “ON” state, ASIP protein is abundant and mice show the typical agouti yellow coat and a tendency to develop obesity and diabetes [70]. On the contrary, when the promoter is heavily methylated, the *Agouti* gene is in an “OFF” state, ASIP levels are low resulting in mice that are lean and exhibit black coat. Interestingly, the *Agouti* gene is sensitive to environmental stimuli [51, 68, 71]. Nutrients and environmental pollutants impact on *Agouti* gene expression altering disease susceptibility through epigenetic modifications. *Agouti* pregnant mice fed diets supplemented with the methyl donors folic acid, vitamin B12 or choline generate lean brown offspring which show increased DNA methylation on the *Agouti* gene promoter and decreased ASIP protein levels [71]. In addition, the effects on coat color induced by maternal methyl-donor supplemented diet are also inherited in the F2 generation, indicating a germline propagation of the epigenetic modifications [51]. On the other hand, maternal exposure to the environmental pollutant bisphenol A, which

is commonly present in many items such as food and plastic beverage containers and baby bottles, shifted the coat color of the offspring toward yellow by decreasing DNA methylation of CpG sites within the *Agouti* promoter [68]. Maternal supplementation with methyl donors abolished the bisphenol A-induced hypo-methylation of the *Agouti* gene in the offspring, demonstrating the potential protective effect of simple dietary interventions against effect of an unhealthy environment effects on the fetal epigenome [68]. In humans, DNA methylation of the *Pre-proopiomelanocortin* (*POMC*) gene which encodes the anorexigenic hormone α -MSH produced by hypothalamic arcuate nucleus neurons has been associated with the individual risk of childhood obesity [72]. In particular, using peripheral blood cells, Kuenen et al. have found hyper-methylation at the Intron 2/Exon 3 boundary of the *POMC* gene in obese compared with normal weight children. In particular, in these obese children, the *Alu* elements, which are known to influence methylation in their genomic proximity at the Intron 2, trigger a default state methylation at the Intron 2/Exon 3 boundary, interfering with binding of the histone acetyltransferase/transcriptional coactivator p300 and reducing *POMC* expression [72]. In addition, several studies suggest a critical role of epigenetic marks also as predictors of susceptibility to obesity and metabolic disease in humans and animal models [73, 74]. A further example of this concept in humans has been provided by studies on the *Retinoid X receptor-alpha* (*RXRA*) gene. Godfrey et al., designed a perinatal epigenetic analysis of the methylation status of CpG sites at the promoters of 78 selected candidate genes in DNA from umbilical cord tissue of children who were assessed for adiposity at age 6 and 9 years. These authors have established that the variation of adiposity and the onset of obesity in pre-pubertal children were associated with the specific hyper-methylation of a CpG site at the *RXRA* chr9:136355885+ at birth [74]. Furthermore, in the same population, it was demonstrated that this neonatal epigenetic mark was associated with lower maternal carbohydrate intake in pregnancy first trimester, providing a further example of how epigenetic processes may link the early prenatal life with the predisposition to obesity and other phenotypic outcomes [74]. In the future, perinatal identification of individuals that present DNA methylation changes at specific genes may help in preventing later obesity. In accordance to this concept, a recent bioinformatic analysis, performed to search for epigenetic obesity biomarkers, has established potential regions of interest which have a high density of CGIs in the promoter of several obesity-related genes (epiobesigenes), such as *Leptin*, *Phosphatase and tensin homolog* (*PTEN*), and *Fibroblast growth factor 2* (*FGF2*) or genes implicated in adipogenesis, such as *Peroxisome proliferator-activated receptor gamma* (*PPARG*), in inflammation, such as *Suppressors of*

cytokine signaling 1 and 3 (SOCS1/SOCS3), and insulin signaling, like *Lipoprotein lipase (LPL)*, *Fatty acid binding protein 4 (FABP4)*, and *Insulin-like growth factor binding protein-3 (IGFBP3)* [75].

Epigenetics and nutrition: lessons from recent studies

Nutritional epigenetics has become an attractive field of study since it associates nutrients and bioactive food components with epigenetic modifications of gene function. As reported in this review, a variety of evidence, in both humans and animal models, supports the association between changes in nutritional status, epigenetic modifications and predisposition to T2D and obesity [76]. Shen et al. have demonstrated that high fat diet (HFD) feeding impacts on the *Leptin* gene by inducing promoter CGI hyper-methylation in murine white adipose tissue (AT) [66]. Consistent with this observation, data obtained by our own group have further highlighted the role of over-nutrition in contributing to the gene function de-regulations occurring in obesity through epigenetic modification. By methylated DNA immuno-precipitation sequencing (MeDIP-seq), we have recently revealed that, HFD triggers a massive DNA methylation reprogramming in AT [77]. In particular, about 14.8×10^3 regions were found to be differentially methylated (DMRs) in mice fed a HFD. Interestingly, we have demonstrated that prolonged HFD regimen promotes a specific DMR distribution in mice [77]. DMR occurrence was increased in the gene-associated elements, particularly introns, and in the CGIs, while the number of DMRs identified in genomic repeat elements including long terminal repeats (LTRs) and long interspersed elements (LINEs) was decreased in obese compared with lean mice. Gene ontology analysis indicates that HFD feeding promotes DMRs enrichment in genes involved in developmental, metabolic and transcriptional processes in mice. In this same study, it has also been revealed that, among several differentially methylated pathways, the *Hox* family of transcription factors was highly enriched in differentially methylated genes in HFD-fed compared with STD-fed mice. In particular, the *Hoxa5* gene, which is implicated in fat tissue differentiation and remodeling [78, 79], was highly methylated at its 5'UTR and transcriptionally repressed in AT from obese compared with lean mice. In addition, the exposure of murine 3T3-L1 adipocytes to palmitate, a major component of the HFD, enhances methylation at the *Hoxa5* 5'UTR and causes *Hoxa5* mRNA down-regulation, suggesting that in AT the epigenetic silencing of *Hoxa5* gene may be dependent, at least in part, on the effect of saturated fats rather than on obesity per se [79].

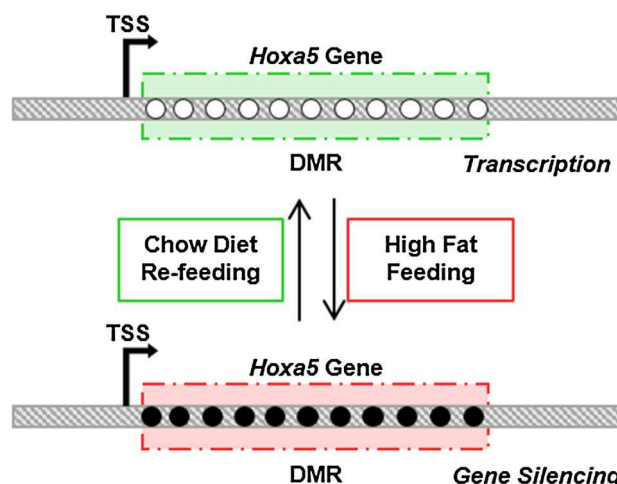


Fig. 2 High fat feeding: DNA methylation at the *Hoxa5* gene in vivo. DNA methylation analysis performed on the AT from mice fed chow diet or high fat diet reveals the presence of a DMR relative to the *Hoxa5* locus among high fat fed- and chow diet fed-mice. This event is associated with a strong reduction of the *Hoxa5* mRNA expression levels in obese mice compared with lean mice. Interestingly, re-feeding obese mice a chow diet for 2 further months reverted the *Hoxa5* DNA methylation and its expression to levels similar to those in lean control fed a standard chow diet

Interestingly, when obese mice exposed to chronic HFD treatment were returned to standard chow diet for two further months, *Hoxa5* DNA methylation and expression levels returned to values similar to those of mice maintained under STD, emphasizing the plasticity of these epigenetic events [79] (Fig. 2).

This same MeDIP-seq approach has also identified the *Ankyrin repeat domain 26 (Ankrd26)* as a gene sensitive to nutrition-induced epigenetic changes. *ANKRD26*, a gene highly expressed in different areas of the hypothalamus, has been related to specific forms of hereditary obesity in humans [80] and was demonstrated to be involved in the regulation of feeding behavior and in the development of both obesity and diabetes in mice [81–83]. Mice with a partial inactivation of this gene show an obese phenotype which results from a marked hyperphagia rather than a reduction of the energy expenditure and activity [81]. When deleted at its C-terminus, *Ankrd26* leads to excessive food intake and obesity due to severe region-specific changes in primary cilia in the brain [83]. In addition to its function in appetite control, the *Ankrd26* gene has a role in the regulation of adipocyte differentiation in mouse embryonic fibroblasts and in 3T3-L1 cells [84, 85]. We have demonstrated that hyper-methylation of the *Ankrd26* promoter occurs in obese mouse AT upon prolonged HFD feeding compared to age- and sex-matched STD-fed mice and directly interferes with the binding of the histone acetyltransferase/transcriptional coactivator p300 to

this same region. These events result in the down regulation of the *Ankrd26* gene expression [unpublished observations]. We have further revealed that *Ankrd26* silencing alters secretion of pro-inflammatory adipokines in vitro. These findings indicate that the epigenetic silencing of the *Ankrd26* gene might be one of the mechanisms responsible for AT inflammation in response to HFD [unpublished observations]. In humans, computational data from a genome-wide DNA methylation analysis in subcutaneous white AT revealed that *ANKRD26* gene is included in a list of 2825 genes where both DNA methylation and mRNA expression levels significantly correlate with BMI [86]. According to these findings, our preliminary data in human peripheral blood leukocytes underline a negative correlation between *ANKRD26* mRNA expression levels and BMI, supporting the hypothesis that an epigenetic regulation of *ANKRD26* gene may occur in humans, as well as in mice, and represent a pathogenic mechanism by which environmental exposures to nutrients contribute to disease susceptibility through epigenetic modifications.

Conclusions and future perspectives

The epigenome undergoes continuous transformations throughout our own lifetime leading to changes in genome function. The epigenetic hypothesis argues that, in addition to genetic variation, epigenetics provides an additional set of mechanisms mediating the relationship between genotype and the external environment and potentially contributing to the individual susceptibility to different disorders. During the past decades, the study of epigenetic modifications has been one of the most emerging and novel areas in fundamental as well as in clinical research and currently represents a very productive field of study, which has already provided a framework for the search of etiological factors in environment-associated diseases such as T2D and obesity. It is, indeed, clear that genetic variability only marginally contributes to the pathogenesis and family risk of these disorders. In this review, we have presented important acquisitions on the epigenetic network in T2D and obesity, mostly focusing on changes of the DNA methylation status of specific genes. However, understanding of the epigenetics of these two complex diseases is still limited. Further work is needed to clarify the molecular mechanisms responsible for the epigenetic control of gene activity and their interactions and alterations, and to establish the role of epigenetics in the risk stratification of these diseases. In the near future, further hints on how epigenetic changes are involved in the etiopathogenesis of T2D and obesity will be attained from studies accomplished on other epigenetic modifications, such as histone modifications and ncRNAs, which may selectively affect the expression of specific

genes, and from epigenome-wide analysis extended to specific human cell types, e.g., stem, precursor and differentiated cells, or to particular tissues, e.g., fat, skeletal muscle, liver and pancreatic islets. It is expected that these studies will pave the way to novel and more effective strategies aimed at diabetes and obesity prevention and at personalized epigenetic treatment. Indeed, it becomes clear that getting a full picture of the epigenetic events involved in these two diseases will (1) represent a powerful tool for predicting and preventing future disease onset in the population; (2) provide additional stimuli for the development of clinical epigenetic biomarkers, which will generate novel relevant information for diagnosis, prognosis and therapy optimization; and (3) drive advancement in epigenetic drug discovery with the generation of more effective epi-drugs, selective for specific epi-targets, which in the forthcoming future might be used in combination with conventional therapeutics and/or might get the opportunity to develop epigenetic treatment personalized to the patient's epigenetic traits.

Compliance with ethical standards

Funding This study was funded by the European Foundation for the Study of Diabetes (EFS), by the Ministero dell'Università e della Ricerca Scientifica (grants PRIN and FIRB-MERIT, and PON 01_02460) and by the Società Italiana di Diabetologia (SID-FO. DIRI). This work was further supported by the P.O.R. Campania FSE 2007-2013, Project CREMe.

Conflict of interest The authors declare that they have no conflict of interest.

Ethical approval This article does not contain any studies with human participants or animals performed by any of the authors.

Informed consent For this type of study informed consent is not required.

References

1. Rappaport SM, Smith MT (2010) Epidemiology. Environment and disease risks. *Science* 330:460–461
2. Holliday R (2006) Epigenetics: a historical overview. *Epigenetics* 1:76–80
3. Waddington CH (1942) The epigenotype. *Endeavour* 1:18–20
4. Dupont C, Armand DR, Brenner CA (2009) Epigenetics: definition, mechanisms and clinical perspective. *Semin Reprod Med* 27:351–357
5. Davis TL, Yang GJ, McCarrey JR, Bartolomei MS (2000) The H19 methylation imprint is erased and re-established differentially on the parental alleles during male germ cell development. *Hum Mol Genet* 9:2885–2894
6. Bollati V, Baccarelli A (2010) Environmental epigenetics. *Heredity* 105(1):105–112
7. Tyson FL, Heindel J (2005) Environmental Influences on Epigenetic Regulation. *Environ Health Perspect* 113:A839

8. Jaenisch R, Bird A (2003) Epigenetic regulation of gene expression: how the genome integrates intrinsic and environmental signals. *Nat Genet* 33(Suppl):245–254
9. Raciti GA, Nigro C, Longo M et al (2014) Personalized medicine and type 2 diabetes: lesson from epigenetics. *Epigenomics* 6:229–238
10. Egger G, Liang G, Aparicio A, Jones PA (2004) Epigenetics in human disease and prospects for epigenetic therapy. *Nature* 429:457–463
11. Sun C, Burgner DP, Ponsonby AL et al (2013) Effects of early-life environment and epigenetics on cardiovascular disease risk in children: highlighting the role of twin studies. *Pediatr Res* 73:523–530
12. Esteller M (2008) Epigenetics in cancer. *N Engl J Med* 358:1148–1159
13. Coulondre C, Miller JH, Farabaugh PJ, Gilbert W (1978) Molecular basis of base substitution hotspots in *Escherichia coli*. *Nature* 274:775–780
14. Gonzalgo ML, Jones PA (1997) Mutagenic and epigenetic effects of DNA methylation. *Mutat Res* 386:107–118
15. Li E (2002) Chromatin modification and epigenetic reprogramming in mammalian development. *Nat Rev Genet* 3:662–673
16. Reik W, Dean W, Walter J (2001) Epigenetic reprogramming in mammalian development. *Science* 293:1089–1093
17. Klose RJ, Bird AP (2006) Genomic DNA methylation: the mark and its mediators. *Trends Biochem Sci* 31:89–97
18. Smith ZD, Meissner A (2013) DNA methylation: roles in mammalian development. *Nat Rev Genet* 14:204–220
19. Deaton AM, Bird A (2011) CpG islands and the regulation of transcription. *Genes Dev* 25:1010–1022
20. Mohn F, Weber M, Rebhan M et al (2008) Lineage-specific polycomb targets and de novo DNA methylation define restriction and potential of neuronal progenitors. *Mol Cell* 30:755–766
21. Payer B, Lee JT (2008) X chromosome dosage compensation: how mammals keep the balance. *Annu Rev Genet* 42:733–772
22. Luger K (2001). Nucleosomes: Structure and Function. *Encyclopedia of Life Sciences* 1–8
23. Cooper GM (2000) *The Cell: A Molecular Approach*. 2nd edition. Sunderland (MA): Sinauer Associates. Chromosomes and Chromatin. Available from: <http://www.ncbi.nlm.nih.gov/books/NBK9863/>
24. Ma J (2005) Crossing the line between activation and repression. *Trends Genet* 21:54–59
25. Richards EJ, Elgin SC (2002) Epigenetic codes for heterochromatin formation and silencing: rounding up the usual suspects. *Cell* 108:489–500
26. Kouzarides T (2007) Chromatin modifications and their function. *Cell* 128:693–705
27. Tamaru H (2010) Confining euchromatin/heterochromatin territory: jumongji crosses the line. *Genes Dev* 24:1465–1478
28. Seol JH, Kim HJ, Yang YJ et al (2006) Different roles of histone H3 lysine 4 methylation in chromatin maintenance. *Biochem Biophys Res Commun* 349:463–470
29. Costa FF (2008) Non-coding RNAs, epigenetics and complexity. *Gene* 410:9–17
30. Mattick JS, Makunin IV (2006) Non-coding RNA. *Hum Mol Genet* 15 Spec No 1:R17–29
31. Bartel DP (2004) MicroRNAs: genomics, biogenesis, mechanism, and function. *Cell* 116:281–297
32. Londin E, Loher P, Telonis AG et al (2015) Analysis of 13 cell types reveals evidence for the expression of numerous novel primate- and tissue-specific microRNAs. *Proc Natl Acad Sci USA* 112:E1106–E1115
33. Mattick JS, Makunin IV (2005) Small regulatory RNAs in mammals. *Hum Mol Genet* 14 Spec No 1:R121–132
34. Guo X, Zhang Z, Gerstein MB, Zheng D (2009) Small RNAs originated from pseudogenes: cis- or trans-acting? *PLoS Comput Biol* 5:e1000449
35. Wienholds E, Plasterk RH (2005) MicroRNA function in animal development. *FEBS Lett* 579:5911–5922
36. Vrba L, Muñoz-Rodríguez JL, Stampfer MR, Futscher BW (2013) miRNA gene promoters are frequent targets of aberrant DNA methylation in human breast cancer. *PLoS One* 8:e54398
37. Sato F, Tsuchiya S, Meltzer SJ, Shimizu K (2011) MicroRNAs and epigenetics. *FEBS J* 278:1598–1609
38. International Diabetes Federation. *Diabetes Atlas* 6th ed, 2013 Brussels, Belgium: International Diabetes Federation, 2014
39. Ng M, Fleming T, Robinson M et al (2014) Global, regional, and national prevalence of overweight and obesity in children and adults during 1980–2013: a systematic analysis for the Global Burden of Disease Study 2013. *Lancet* 384:766–781
40. InterAct Consortium et al (2013) The link between family history and risk of type 2 diabetes is not explained by anthropometric, lifestyle or genetic risk factors: the EPIC-InterAct study. *Diabetologia* 56:60–69
41. Meigs JB, Cupples LA, Wilson PW (2000) Parental transmission of type 2 diabetes: the Framingham Offspring Study. *Diabetes* 49:2201–2207
42. Klein BE, Klein R, Moss SE, Cruickshanks KJ (1996) Parental history of diabetes in a population-based study. *Diabetes Care* 19:827–830
43. Stunkard AJ, Harris JR, Pedersen NL, McClearn GE (1990) The body-mass index of twins who have been reared apart. *N Engl J Med* 322:1483–1487
44. Rice T, Pérusse L, Bouchard C, Rao DC (1999) Familial aggregation of body mass index and subcutaneous fat measures in the longitudinal Québec family study. *Genet Epidemiol* 16:316–334
45. Segal NL, Allison DB (2002) Twins and virtual twins: bases of relative body weight revisited. *Int J Obes Relat Metab Disord* 26:437–441
46. Grarup N, Sandholt CH, Hansen T, Pedersen O (2014) Genetic susceptibility to type 2 diabetes and obesity: from genome-wide association studies to rare variants and beyond. *Diabetologia* 57:1528–1541
47. Al-Azzam SI, Khabour OF, Alzoubi KH, Alzayadeen RN (2014) The effect of leptin promoter and leptin receptor gene polymorphisms on lipid profile among the diabetic population: modulations by atorvastatin treatment and environmental factors. *J Endocrinol Invest* 37(9):835–842
48. Drong AW, Lindgren CM, McCarthy MI (2012) The genetic and epigenetic basis of type 2 diabetes and obesity. *Clin Pharmacol Ther* 92:707–715
49. Bloom JS, Ehrenreich IM, Loo WT, Lite TL, Kruglyak L (2013) Finding the sources of missing heritability in a yeast cross. *Nature* 494(7436):234–237
50. Jirtle RL, Skinner MK (2007) Environmental epigenomics and disease susceptibility. *Nat Rev Genet* 8:253–262
51. Cropley JE, Suter CM, Beckman KB, Martin DI (2006) Germ-line epigenetic modification of the murine A_{vy} allele by nutritional supplementation. *Proc Natl Acad Sci U S A* 103:17308–17312
52. Saad MI, Abdelkhalek TM, Haiba MM, Saleh MM, Hanafi MY, Tawfik SH, Kamel MA (2016) Maternal obesity and malnourishment exacerbate perinatal oxidative stress resulting in diabetogenic programming in F1 offspring. *J Endocrinol Invest* 39(6):643–655
53. Speakman JR, O’Rahilly S (2012) Fat: an evolving issue. *Dis Model Mech* 5:569–573
54. Castillo-Fernandez JE, Spector TD, Bell JT (2014) Epigenetics of discordant monozygotic twins: implications for disease. *Genome Med* 6:60

55. Poulsen P, Esteller M, Vaag A, Fraga MF (2007) The epigenetic basis of twin discordance in age-related diseases. *Pediatr Res* 61:38R–42R
56. Lyssenko V, Laakso M (2015) Genetic Screening for the Risk of Type 2 Diabetes: worthless or valuable? *Diabetes Care* 36:S120–S126
57. Raciti GA, Longo M, Parrillo L et al (2015) Understanding type 2 diabetes: from genetics to epigenetics. *Acta Diabetol* 52(5):821–827
58. Ling C, Del Guerra S, Lupi R et al (2008) Epigenetic regulation of PPARGC1A in human type 2 diabetic islets and effect on insulin secretion. *Diabetologia* 51:615–622
59. Barrès R, Osler ME, Yan J et al (2009) Non-CpG methylation of the PGC-1 α promoter through DNMT3B controls mitochondrial density. *Cell Metab* 10:189–198
60. Barres R, Kirchner H, Rasmussen M et al (2013) Weight loss after gastric bypass surgery in human obesity remodels promoter methylation. *Cell Rep* 3:1020–1027
61. Velho G, Robert JJ (2002) Maturity-onset diabetes of the young (MODY): genetic and clinical characteristics. *Horm Res* 57(Suppl 1):29–33
62. Ahlgren U, Jonsson J, Jonsson L, Simu K, Edlund H (1998) beta-cell-specific inactivation of the mouse *Ipfl/Pdx1* gene results in loss of the beta-cell phenotype and maturity onset diabetes. *Genes Dev* 12:1763–1768
63. Yang BT, Dayeh TA, Volkov PA et al (2012) Increased DNA methylation and decreased expression of PDX-1 in pancreatic islets from patients with type 2 diabetes. *Mol Endocrinol* 26:1203–1212
64. Toperoff G, Aran D, Kark JD et al (2012) Genome-wide survey reveals predisposing diabetes type 2-related DNA methylation variations in human peripheral blood. *Hum Mol Genet* 21:371–383
65. Jung UJ, Choi MS (2014) Obesity and its metabolic complications: the role of adipokines and the relationship between obesity, inflammation, insulin resistance, dyslipidemia and nonalcoholic fatty liver disease. *Int J Mol Sci* 15(4):6184–6223
66. Shen W, Wang C, Xia L et al (2014) Epigenetic modification of the leptin promoter in diet-induced obese mice and the effects of N-3 polyunsaturated fatty acids. *Sci Rep* 4:5282
67. Cifani C, Micioni Di Bonaventura MV et al (2015) Regulation of hypothalamic neuropeptides gene expression in diet induced obesity resistant rats: possible targets for obesity prediction? *Front Neurosci* 9:187
68. Dolinoy DC (2008) The agouti mouse model: an epigenetic biosensor for nutritional and environmental alterations on the fetal epigenome. *Nutr Rev* 66(Suppl 1):S7–11
69. Cooney CA, Dave AA, Wolff GL (2002) Maternal methyl supplements in mice affect epigenetic variation and DNA methylation of offspring. *J Nutr* 132:2393S–2400S
70. Wolff GL, Kodell RL, Moore SR, Cooney CA (1998) Maternal epigenetics and methyl supplements affect agouti gene expression in *Avy/a* mice. *FASEB J* 12:949–957
71. Ling C, Groop L (2009) Epigenetics: a molecular link between environmental factors and type 2 diabetes. *Diabetes* 58:2718–2725
72. Kuehnen P, Mischke M, Wiegand S et al (2012) An Alu element-associated hypermethylation variant of the POMC gene is associated with childhood obesity. *PLoS Genet* 8:e1002543
73. Reddy MA, Natarajan R (2015) Recent developments in epigenetics of acute and chronic kidney diseases. *Kidney Int* 88:250–261
74. Godfrey KM, Sheppard A, Gluckman PD et al (2011) Epigenetic gene promoter methylation at birth is associated with child's later adiposity. *Diabetes* 60(5):1528–1534
75. Campión J, Milagro FI, Martínez JA (2009) Individuality and epigenetics in obesity. *Obes Rev* 10:383–392
76. Seki Y, Williams L, Vuguin PM, Charron MJ (2012) Minireview: epigenetic programming of diabetes and obesity: animal models. *Endocrinology* 153:1031–1038
77. Parrillo L, Costa V, Raciti GA, et al (2016) *Hoxa5* undergoes dynamic DNA methylation and transcriptional repression in the adipose tissue of mice exposed to high-fat diet. *Int J obesity*. (in press)
78. Cowherd RM, Lyle RE, Miller CP, McGehee RE Jr (1997) Developmental profile of homeobox gene expression during 3T3-L1 adipogenesis. *Biochem Biophys Res Commun* 237:470–475
79. Charlier C, Segers K, Karim L et al (2001) The callipyge mutation enhances the expression of coregulated imprinted genes in cis without affecting their imprinting status. *Nat Genet* 27:367–369
80. Dong C, Li WD, Geller F et al (2005) Possible genomic imprinting of three human obesity-related genetic loci. *Am J Hum Genet* 76:427–437
81. Bera TK, Liu XF, Yamada M et al (2008) A model for obesity and gigantism due to disruption of the *Ankrd26* gene. *Proc Natl Acad Sci USA* 105:270–275
82. Raciti GA, Bera TK, Gavrilova O, Pastan I (2011) Partial inactivation of *Ankrd26* causes diabetes with enhanced insulin responsiveness of adipose tissue in mice. *Diabetologia* 54:2911–2922
83. Acs P, Bauer PO, Mayer B et al (2015) A novel form of ciliopathy underlies hyperphagia and obesity in *Ankrd26* knockout mice. *Brain Struct Funct* 220:1511–1528
84. Fei Z, Bera TK, Liu X, Xiang L, Pastan I (2011) *Ankrd26* gene disruption enhances adipogenesis of mouse embryonic fibroblasts. *J Biol Chem* 286:27761–27768
85. Liu XF, Bera TK, Kahue C et al (2012) *ANKRD26* and its interacting partners *TRIO*, *GPS2*, *HMMR* and *DIPA* regulate adipogenesis in 3T3-L1 cells. *PLoS ONE* 7:e38130
86. Rönn T, Volkov P, Gillberg L et al (2015) Impact of age, BMI and HbA1c levels on the genome-wide DNA methylation and mRNA expression patterns in human adipose tissue and identification of epigenetic biomarkers in blood. *Hum Mol Genet* 24:3792–3813

ORIGINAL ARTICLE

Hoxa5 undergoes dynamic DNA methylation and transcriptional repression in the adipose tissue of mice exposed to high-fat diet

L Parrillo^{1,2}, V Costa^{3,5}, GA Raciti^{1,2,5}, M Longo^{1,2}, R Spinelli^{1,2}, R Esposito³, C Nigro^{1,2}, V Vastolo^{1,2}, A Desiderio^{1,2}, F Zatterale^{1,2}, A Ciccociola^{3,4}, P Formisano^{1,2}, C Miele^{1,2} and F Beguinot^{1,2}

BACKGROUND/OBJECTIVES: The genomic bases of the adipose tissue abnormalities induced by chronic positive calorie excess have been only partially elucidated. We adopted a genome-wide approach to directly test whether long-term high-fat diet (HFD) exposure affects the DNA methylation profile of the mouse adipose tissue and to identify the functional consequences of these changes.

SUBJECTS/METHODS: We have used epididymal fat of mice fed either high-fat (HFD) or regular chow (STD) diet for 5 months and performed genome-wide DNA methylation analyses by methylated DNA immunoprecipitation sequencing (MeDIP-seq). Mouse Homeobox (*Hox*) Gene DNA Methylation PCR, RT-qPCR and bisulphite sequencing analyses were then performed.

RESULTS: Mice fed the HFD progressively expanded their adipose mass accompanied by a significant decrease in glucose tolerance ($P < 0.001$) and insulin sensitivity ($P < 0.05$). MeDIP-seq data analysis revealed a uniform distribution of differentially methylated regions (DMR) through the entire adipocyte genome, with a higher number of hypermethylated regions in HFD mice ($P < 0.005$). This different methylation profile was accompanied by increased expression of the *Dnmt3a* DNA methyltransferase (*Dnmt*; $P < 0.05$) and the methyl-CpG-binding domain protein *Mbd3* ($P < 0.05$) genes in HFD mice. Gene ontology analysis revealed that, in the HFD-treated mice, the *Hox* family of development genes was highly enriched in differentially methylated genes ($P = 0.008$). To validate this finding, *Hoxa5*, which is implicated in fat tissue differentiation and remodeling, has been selected and analyzed by bisulphite sequencing, confirming hypermethylation in the adipose tissue from the HFD mice. *Hoxa5* hypermethylation was associated with downregulation of *Hoxa5* mRNA and protein expression. Feeding animals previously exposed to the HFD with a standard chow diet for two further months improved the metabolic phenotype of the animals, accompanied by return of *Hoxa5* methylation and expression levels ($P < 0.05$) to values similar to those of the control mice maintained under standard chow.

CONCLUSIONS: HFD induces adipose tissue abnormalities accompanied by epigenetic changes at the *Hoxa5* adipose tissue remodeling gene.

International Journal of Obesity (2016) 40, 929–937; doi:10.1038/ijo.2016.36

INTRODUCTION

Through the second half of the past century, obesity established as an increasingly prevalent response to the unhealthy environment and nutrition, both in the developed and in developing countries.¹ Obesity is associated with increased risk of a number of different metabolic complications, and with increased mortality.² In part, the excess morbidity accompanying obesity is determined by dysfunctional adipose tissue.³

While most caloric excess is stored in the subcutaneous adipose tissue, chronically positive caloric balance may induce ectopic storage of lipids and involve intra-abdominal, pericardial, perivascular and intramuscular adipose tissue (visceral adipose tissue). Increased visceral adipose tissue is well recognized as an independent risk factor for most obesity-associated comorbidities, with the distribution of adipose tissue, their anatomical, cellular and molecular features determining their occurrence.⁴ However, it

has been proposed that visceral adiposity represents a surrogate marker for global body fat dysfunction.³

Recent genome-wide association studies in humans led to the identification of >100 common gene variants determining individual propensity to adiposity. Most of them have an unknown function at the present.⁵ In addition, the effect size of these variants is small compared with the large effect of unhealthy nutrition on the development of obesity.⁶ Even in the case of this effect, however, the genomic bases of the visceral fat abnormalities induced by chronically positive calorie excess have been only partially elucidated.

It has become progressively clearer that environmental factors, including the quality of nutrition, may affect individual phenotypes by causing epigenetic modifications of the DNA.^{7,8} These occur in the absence of DNA sequence alterations and include variations in the methylation status at specific regions of the genome, as well as posttranslational histone changes and

¹Dipartimento di Scienze Mediche e Traslazionali dell'Università di Napoli 'Federico II', Naples, Italy; ²URT dell'Istituto di Endocrinologia e Oncologia Sperimentale 'Gaetano Salvatore', Consiglio Nazionale delle Ricerche, Naples, Italy; ³Institute of Genetics and Biophysics 'Adriano Buzzati-Traverso', National Research Council, Naples, Italy and ⁴DiST, Department of Science and Technology, 'Parthenope' University of Naples, Centro Direzionale, Naples, Italy. Correspondence: Professor F Beguinot, Dipartimento di Scienze Mediche e Traslazionali, Università di Napoli 'Federico II', Naples 80131, Italy.

E-mail: beguinot@unina.it

⁵These authors equally contributed to this work.

Received 27 July 2015; revised 28 December 2015; accepted 24 January 2016; accepted article preview online 16 March 2016; advance online publication, 12 April 2016

differential miRNA expression.^{9,10} Studies in humans have also revealed that specific epigenotypes have a very large effect on adiposity variance. Godfrey and co-workers¹¹ reported a positive correlation between the degree of *RXRα* methylation at one specific site in the promoter and childhood body adiposity at age 6 and 9 years. These findings were replicated in both within-cohort and between-cohort replicates. In contrast to the small effect sizes typically seen with genetic polymorphisms associated with metabolic disease risk, this single site epigenotype accounted for at least 25% of the variance in childhood adiposity. However, genes for which polymorphisms have strong associations with disease risk might be anticipated to have epimutations.¹² One such gene is *FTO*, that acts as a nucleic acid demethylase,¹³ a co-substrate of which is α-ketoglutarate (a product of the Krebs cycle), recently described as a biomarker of obesity-associated non-alcoholic fatty liver disease.¹⁴ The *FTO* gene has been first identified by genome-wide association studies as being involved in the risk of obesity. In a prospective study of nonsymptomatic individuals of a mean age of 30 years, Toperoff et al.¹⁵ showed that those who featured hypomethylation at an intronic CpG site at *FTO* had an increased risk of developing impaired glucose metabolism.

However, the majority of these studies have focused on methylation at specific genes rather than adopting an unbiased approach, although functionally relevant DNA methylation changes may be located in different areas of the genome.^{16,17} Thus, a comprehensive analysis of the genome methylation profile in response to changes in the nutritional status is necessary to interpret the epigenetic mechanisms accompanying diet-induced obesity.

In this work, we have adopted methylated DNA immunoprecipitation sequencing (MeDIP-seq) to identify whole-genome methylation changes occurring in the adipose tissue of mice exposed to a long-term treatment with fat-enriched diet. We have identified and cataloged several differentially methylated genes (DMGs) whose function is modulated by this nutritional regimen. We have further demonstrated that return of the animals to a standard chow diet caused improvement of the metabolic derangement, accompanied by rescue of both the epigenetic modifications and the function of selected genes. Some of them might therefore enable to quantify individual response to lifestyle intervention in humans as well as in mice.

MATERIALS AND METHODS

Animals and diet

Male 5-week-old C57BL/6J mice were obtained from Charles Rivers (Deisenhofen, Germany) and housed in a temperature-controlled room (22 ± 2 °C) with 12-h light-dark cycle. Mice were enabled *ad libitum* access to food and water. Animals were randomly assigned to a standard chow diet (STD about 10% energy as fat) or a high-fat diet (HFD about 60% energy as fat) for 5 months. The composition of these diets is reported in Supplementary Table S1. Body weight was recorded weekly. For insulin tolerance testing, mice were fasted for 4 h and then subjected to intraperitoneal injection with insulin (0.75 mIU g⁻¹ of body weight). Venous blood was subsequently drawn by tail clipping at 0, 15, 30, 45, 60, 90 and 120 min as previously described.¹⁸ For intraperitoneal glucose tolerance testing, mice were fasted overnight and then subjected to intraperitoneal injection with glucose (2.0 g kg⁻¹ of body weight). Venous blood was subsequently drawn by tail clipping at 0, 15, 30, 45, 60, 90 and 120 min as previously described.¹⁸ Blood glucose levels were measured with Accu-Chek glucometers (Roche Applied Science, Penzberg, Germany). The total area under the curve and the inverse area under the curve for glucose response during glucose tolerance testing and insulin tolerance testing were calculated as previously described.¹⁸ At the end of the experiment, the animals were killed; the epididymal white adipose tissue (WAT) was carefully dissected and stored at -80 °C until analyzed. For histology, epididymal WAT was fixed in 10% neutral buffered formalin and embedded in paraffin. Sections of 5 μm were obtained and stained with hematoxylin and eosin. Images captured by an Olympus BX51 microscope

equipped with an Olympus (Shinjuku, Japan) DP-21 digital camera were processed using the ImageJ software.

All the procedures performed were in agreement with the National and Institutional Guidelines of the Animal Care and Use Committee at the University of Naples Medical School.

Fractionation of adipose tissue

WAT was washed and minced in Dulbecco's modified Eagle's medium and then incubated for 1 h at 37 °C with the same medium containing collagenase (1 mg ml⁻¹; Sigma-Aldrich, St Louis, MO, USA). The mixture was passed through a nylon filter (pore size, 250 μm) to remove undigested material. The filtrate was centrifuged for 5 min at 1500 g and floating cells and the pellet were recovered as the mature adipocyte fraction and the stromal vascular fraction, respectively, and were used for RNA extraction.

DNA preparation and MeDIP-Seq

Genomic DNA was isolated from WAT of STD and HFD mice using the AllPrep DNA/RNA Mini Kit (Qiagen, Hilden-Düsseldorf, Germany) according to the manufacturer's instructions. The quality of each DNA sample was analyzed for integrity, purity and concentration on a NanoDrop 2000c Spectrophotometer (Thermo Fisher Scientific Inc., Waltham, MA, USA). Purified DNA (>50 ng per sample) was then sent to Beijing Genomics Institute (BGI at Shenzhen, China) for MeDIP-seq analysis by a Illumina HiSeq 2000 (Illumina Inc., San Diego, CA, USA), and their detailed protocol was published in the study by Li et al.¹⁹ DNA methylation data have been deposited in GEO database under accession number GSE71476.

Reads alignment and pre-processing

Data filtering was applied to remove adapter sequences, contamination and low-quality reads from raw reads. About 73 million of filtered fragments—36.5 million 50 bp paired-end reads—were obtained for each sample from MeDIP-seq experiments.

FastQC (<http://www.bioinformatics.babraham.ac.uk/projects/fastqc/>) was used to assess the quality of sequenced reads. Raw reads were aligned to the reference mouse genome (UCSC mm9) using BWA²⁰ with default parameters for paired-end mapping. Reads alignments in SAM format were converted to BAM for further analyses using SAMtools.²⁰ Statistics of mapping quality was assessed by SAMStat on SAM/BAM input files. Nucleotide composition, length distribution, base quality distribution, mapping statistics, mismatches, insertions/deletions and error profiles were reported in html5 format including unmapped, poorly and accurately mapped reads. Only uniquely mapped reads were extracted from the sam file by a custom shell script and were used for further analyses. BEDtools were used first to convert mapped reads in BED format and then to create files in Bedgraph format (.wiggle). These files were uploaded in UCSC Genome Browser (<http://genome.ucsc.edu>) for visual inspection and for gene-specific analysis.

Peak calling and identification of differentially methylated regions (DMRs)

The distribution of MeDIP-Seq reads on each mm9 chromosome was analyzed. The genome was divided into windows of the arbitrary 10 kb length, and read depth for each window was calculated. Read count within each window was normalized using the following equation: RC*10⁶/UMR (RC = Read count in the 10 kb window; UMR = uniquely mapped reads). Results are shown in Supplementary Figure S1. Reads coverage analysis has been performed using BEDtools²¹ to test the number of CpGs covered by sequenced reads, looking at the depth of coverage. The global distribution of MeDIP-Seq-generated reads on specific genomic elements of mouse genome (CGIs, shores and shelves, exons, introns, CDS, 5' and 3' untranslated regions (UTRs), as well as repeat elements) has been independently evaluated for both samples (Supplementary File S1). Annotations of the genomic elements of interest were downloaded from the Table Browser of UCSC Genome Browser for mm9 genome release. Genomic coordinates of CGIs in mm9 genome release were obtained from Smallwood et al.²² Shores and shelves genomic coordinates were automatically computed from CGIs coordinates of.²² We annotated CpG shores considering a range of ±2 kb from the start and end positions of each CGI, and CpG shelves in the range of ±2 kb from start and end of each CpG shore. MeDIP-Seq datasets from HFD and STD mice groups were independently analyzed with model-based analysis of ChIP-Seq²³ to find

significant methylation peaks in both samples, and with the MEDIPS package²¹ to identify DMRs. For both samples, the P -value $< 10^{-10}$ was used to select significant peaks computed by model-based analysis of ChIP-Seq. Using MEDIPS package, uniquely mapped reads were extended in the sequencing direction to a length of 300 nt. For the identification of DMRs, we used the MEDIPS option that enables to compute differential methylation within fixed genome-wide frames. Mean r.p.m. (reads per million) values were computed for genome-wide 500 bp windows overlapping of 250 bp using MEDIPS ('frame_size=500' and 'step=250' parameters were used). DMRs calculated by the MEDIPS software were converted with custom scripts in BED format and loaded on Genome Browser for immediate visualization. DMRs were mapped to known genes or gene-associated elements (CGIs, shores and shelves, exons, introns, CDS, 5' and 3' UTRs, repeat elements) using SAMtools.²⁰ BED files of each annotated gene (or gene-associated elements) were downloaded from the Table Browser of UCSC. ChipPeakAnno was used to assign each CGIs to RefSeq genes based on the proximity of each gene transcription start site to the nearest CGI. A similar approach was extended to associate all DMRs to the above-mentioned gene-related elements. Protein Analysis Through Evolutionary Relationships (PANTHER) Classification System (<http://www.pantherdb.org>) was used to determine whether hypermethylated CGIs are mostly associated with specific gene pathways and ontology terms. A false discovery rate < 0.05 was considered significant.

Bisulphite sequencing analysis

Genomic DNA bisulphite modification was performed using the EZ DNA Methylation Kit (Zymo Research, Irvine, CA, USA) according to the manufacturer's instruction. The following primer pairs were designed by Methprimer²⁴ to amplify DMR-associated *Hoxa5* locus: sense 5'-TTGGA GTTGTAGGGAGTTTTT-3'; antisense 5'-CCTCTAAAAATCATCAACAA AATTAC-3'. PCR products were purified using Min Elute Gel Extraction Kit (Qiagen) and cloned into the pGEM T-Easy vector (Promega, Fitchburg, WI, USA). Individual clones were grown and plasmids purified using the NucleoSpin Plasmid Kit (Macherey-Nagel, Düren, Germany). For each condition, 10 clones were sequenced using SP6 promoter primer on AB 3500 genetic analyzer (Applied Biosystem, Waltham, MA, USA). The proportion of methylation for each individual was calculated by dividing the total number of methylated sites in all clones by the total number of CG sites.

Methylated DNA immunoprecipitation (MeDIP)

MeDIP assay was performed as described by Weber *et al.*²⁵ Sonicated pooled genomic DNA from WAT was immunoprecipitated using anti-5meCpG (#ab10805, Abcam, Cambridge, MA, USA) or mouse IgG with anti-mouse IgG beads (#10003D, Life Technologies, Waltham, MA, USA). DNA methylation enrichment on recovered DNA was evaluated by qPCR. Samples were normalized to their respective input using the $2^{-\Delta\Delta C_T}$ method. The following primer sequences were used: sense 5'-GTGCTTGATTGTGGCTCGC-3'; anti-sense 5'-TCCACCAACTCCCCATTA-3'.

RNA isolation, reverse transcription and quantitative RT-PCR Analysis

Total RNA was isolated from WAT using AllPrep DNA/RNA Mini Kit (Qiagen). cDNA was synthesized by reverse transcription using Superscript III Reverse Transcriptase (Invitrogen, Waltham, MA, USA), according to the manufacturer's protocol. Real-time RT-qPCR was performed on an iCycler IQ multicolor Real Time PCR Detection System (Bio-Rad Laboratories, Inc., Hercules, CA, USA) using the comparative CT method (2-DDCT) with a Platinum SYBR Green qPCR Super-UDG mix (Bio-Rad Laboratories, Inc.;²⁶). All reactions were performed in triplicate, and the relative mRNA expression levels of target genes were normalized to *cyclophilin A*. The primer sequences used are shown in Supplementary Table S2.

Mouse *Hox* Genes DNA methylation PCR array

The Mouse *Homeobox* (*Hox*) Genes DNA Methylation PCR Array (SABiosciences, Hilden-Düsseldorf, Germany) has been used to profile DNA methylation levels of *Hox* genes ($n=22$). This novel restriction enzyme-based technology was described by Kim *et al.*²⁷ Briefly, genomic DNA is treated with a combination of methylation-sensitive and/or methylation-dependent enzymes. Subsequent RT-qPCR enabled comparison of Ct values between particular enzymatic reactions and thus assessment of DNA methylation levels. PCR reactions were performed using iCycler IQ multicolor Real Time PCR Detection System (Bio-Rad

Laboratories, Inc.). Detailed description of sample preparation and PCR reaction conditions are provided in the manufacturer's protocol.

Western blot analyses

Adipose tissues were lysed in T-PER reagent (#78510, Thermo-Scientific, Waltham, MA, USA) with a protease inhibitor cocktail (#05892791001, Roche) and a phosphatase inhibitor (#04906837001, Roche). Twenty micrograms of protein extracts were separated by sodium dodecyl sulfate-polyacrylamide gel electrophoresis and transferred to polyvinylidene difluoride membranes (Millipore, Billerica, MA, USA). Upon incubation with primary *Hoxa5* (1:1000; #ab82645, Abcam), α -tubulin (1:1000; #SC5546, Santa Cruz, Dallas, TX, USA) and secondary antibodies (Bio-Rad Laboratories, Inc.), immunoreactive bands were detected by enhanced chemiluminescence according to the manufacturer's instructions (Pearce ECL Western Blotting Substrate, # 32106, Thermo-Scientific).

Cell culture, treatments and transfection

3T3-L1 cells were grown and were allowed to differentiate into mature adipocytes as described Bezy *et al.*²⁸ Subsequently, adipocytes were exposed to palmitate (0.25 mM; Sigma-Aldrich) and harvested 96 h later for DNA and RNA extraction. For *Hoxa5* silencing during adipogenesis, 3T3-L1 cells were transfected with 25 nmol l⁻¹ of *Hoxa5* siRNA (OriGene, Rockville, MD, USA), and subsequently induced to differentiate into mature adipocytes. Transfection was repeated as on day -2 every 48 h until day 8. Then, lipid accumulation was assessed by Oil Red O staining as previously described.²⁹

Statistical analysis

Data are expressed as mean \pm s.e.m. Comparison between groups were performed using Student's *t*-test or the one-way analysis of variance followed by Tukey multiple comparison tests, as appropriate, using GraphPad Software (version 6.00 for Windows, San Diego, CA, USA): a P -value ≤ 0.05 was considered significant. Statistical significance of DMRs—in HFD compared with STD mice—in genomic regions was performed with chi-square test.

RESULTS

HFD changes the global DNA methylation profile in adipose tissue from C57BL/6 J mice

Five-week-old male mice were fed either standard chow (STD) or fat-enriched diets (HFD) for 5 months followed by metabolic phenotyping. Despite comparable food intake in the two groups, mice exposed to the HFD exhibited a 37% increase in body weight ($P < 0.001$). Fasting glucose levels were increased in the HFD treated mice ($P < 0.05$). Glucose and insulin tolerance tests revealed, respectively, decreased glucose tolerance ($P < 0.001$) and insulin sensitivity ($P < 0.05$) in these animals (Table 1).

HFD treatment induced an increase in the individual adipose cell size, accompanied by an elevated expression of macrophage marker genes, including *F4/80*, *Cd68* and *Mcp-1*. Moreover, HFD exposure determined an upregulation of *Fabp4* and *Fas* mRNA

Table 1. Metabolic phenotypes of high-fat- and standard chow diet-exposed mice

	STD (n = 16)	HFD (n = 16)	P-value
Body weight	30.78 \pm 0.9	42.18 \pm 1.1	$P < 0.001$
AUC GTT (mg dl ⁻¹ *120 min)	11150 \pm 1463	23686 \pm 1783	$P < 0.001$
AUC inv. ITT (mg dl ⁻¹ *120 min)	10986 \pm 920.12	6702.85 \pm 1136.34	$P < 0.05$
Glucose (mg dl ⁻¹)	106 \pm 12.7	163 \pm 14.1	$P < 0.05$

Abbreviations: AUC, area under the curve; GTT, glucose test tolerance; ITT, insulin test tolerance; HFD, high-fat diet mice; STD, standard diet mice. All values are means \pm s.e.m.

levels, together with a significant reduction of adiponectin mRNA levels, whereas *Ppar2* expression showed no significant variation between HFD- and STD-fed mice, similar as described previously^{29,30} (Supplementary Figure S1).

We have subsequently compared global methylation profiles in epididymal fat from STD- and HFD-treated animals. By immunoprecipitation of methylated DNA followed by massively parallel sequencing (MeDIP-seq^{25,31}), we generated 73 million reads in each condition. Alignment to the mouse genome (mm9) revealed that about 50% of the reads mapped in unique regions (Supplementary Table S3). In addition, these reads were uniformly distributed through the entire mouse genome, as indicated by the detection of methylation events in most chromosomal regions (Supplementary Figure S2), and were found to be mainly located within introns and exons regions of the gene-associated elements (Supplementary Table S4A).

About 17.6×10^4 and 16.7×10^4 methylation peaks were identified, respectively, in HFD- and STD-maintained mice (Bonferroni corrected $P < 0.01$). Most of these peaks (52%) were within the gene bodies, with 36% in intronic regions and 9% in CpG islands (Supplementary Table S4B). Analysis of different repeat types revealed that methylation peaks were abundant in *LTR* and *LINE* classes of the mouse genome (Supplementary Table S4C).

About 14.8×10^3 DMRs were also identified in the genomes from HFD- and STD-exposed mice ($P < 0.005$), about 53% of which were hypermethylated while 47% were hypomethylated in the HFD compared with the STD mice. The highest frequency of DMR occurrence was detected in gene bodies, particularly in the intronic sequences where hypermethylation events were more common (Figure 1a). Significant DMR hypermethylation was also noted in the CpG islands of HFD-fed mice, while no significant difference was observed in the CpG shores and shelves

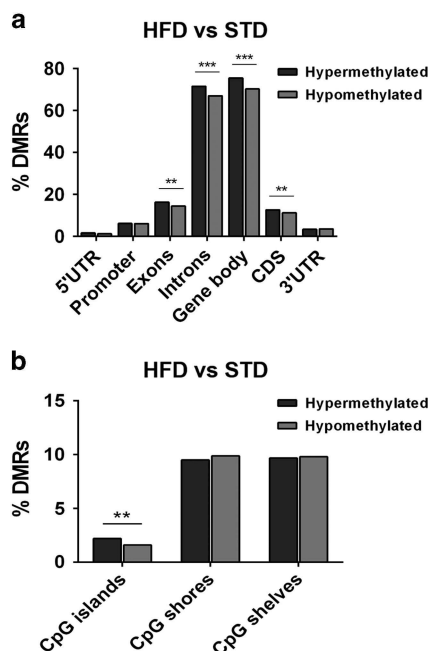


Figure 1. DMR distribution in mice subjected to HFD feeding. Distribution of hypermethylated and hypomethylated DMRs (a) across different gene elements (promoter, 5-UTR, exons, cds, introns, 3-UTR and gene body) and (b) CpG-Island, -Shores and -Shelves. A CpG-Island is defined 200 bp (or larger) fragment of DNA with a C+G content of $> 50\%$ and an observed CpG/expected CpG ratio > 0.6 . Shores: the flanking regions of the CpG-Islands, 0–2000 bp. Shelves: the regions flanking the island shores, i.e., covering 2000–4000 bp distant from the CpG-Island. $**P < 0.005$ and $***P < 0.0005$.

(Figure 1b). At variance with the gene-associated elements, repeat type analysis identified an increased number of hypomethylated DMR in *LTR* and *LINE* classes of the HFD mouse genome (Supplementary Figure S3).

Effect of HFD on expression of DNA-methylating enzymes in adipose tissue

We then sought to explore whether the changes in DNA methylation profile observed in mice exposed to HFD could be attributed to changes in the expression of DNA-methylating enzymes and focused our attention on DNA methyltransferases^{32,33} and methyl-CpG-binding domain proteins (*Mbd*³⁴). Interestingly, quantitative real-time PCR analysis of mRNA from adipose tissue revealed a specific twofold increase in the abundance of *Dnmt3a* transcript in the HFD-fed mice ($P < 0.05$; Figure 2a). The *Mbd3*, but not the *Mbd1*, *Mbd2* or *Mbd4* genes was also significantly overexpressed in the adipose tissue of HFD-fed mice ($P < 0.05$; Figure 2b), suggesting a role *Dnmt3a* and *Mbd3* genes in mediating diet-induced hypermethylation events.

Diet-induced methylation changes affect developmental processes

For the purpose of the present study, genes whose nearest CpG island, shelf and/or shore overlap a DMR were termed differentially methylated genes, which allowed us to identify 1.673×10^3 DMG. To initially address their functional significance, we performed gene set enrichment analysis both for the gene ontology categories and the canonical pathways.

This analysis enabled us to identify the '*Ppar signaling pathway*' as the most significantly enriched pathway among DMG (false discovery rate $< 5\%$; Supplementary Table S5). DMG were also enriched in the '*PI3k-Akt*', '*Insulin resistance*', '*Cytokine-cytokine*

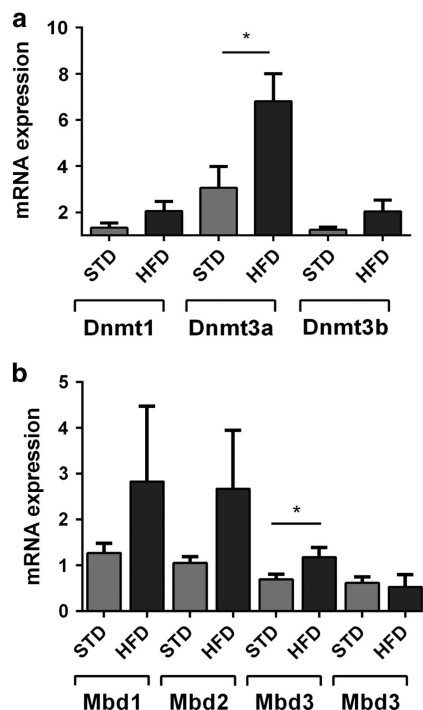


Figure 2. Expression of *Dnmt* and *Mbd* in WAT from HFD-exposed mice. qRT-PCR analysis of mRNA expression levels of WAT *Dnmt1*, *Dnmt3a*, *Dnmt3b* (a), and *Mbd1*, *Mbd2*, *Mbd3* and *Mbd4* (b). All data are expressed as means \pm s.e.m. ($n = 8$ for STD; $n = 8$ for HFD). $*P < 0.05$, HFD vs STD.

we performed RT-qPCR assays. On the basis of this approach, *Hoxc8* mRNA levels in adipose tissue from HFD-exposed mice were found to be significantly higher compared with control mice (Figure 3b). At variance, *Hoxa5* mRNA levels were decreased in the adipose tissue of HFD-fed mice (Figure 3c). To further validate the HFD-induced methylation changes occurring at the *Hoxa5* gene, we have subjected to bisulphite treatment and then directly sequenced the *Hoxa5*-associated DMR, which encompasses a significant portion of the 5'-UTR promoter region of the *Hoxa5* gene. As shown in Figure 3d, this procedure revealed an average 25% increased methylation of the region from HFD compared with STD-exposed mice ($P < 0.01$), validating the MeDIP-seq data. Furthermore, the amounts of the *Hoxa5* protein in WAT were decreased in the HFD-fed mice compared with controls (Figure 3e).

To investigate whether diet-induced obesity or specific fats is responsible for the changes in *Hoxa5* methylation and expression associated to exposure to HFD, we analyzed the effect of different fat components on *Hoxa5* in cultured 3T3-L1 cells. Supplementation of the culture medium with 0.25 mM palmitate, a major component of the HFD, increased *Hoxa5* promoter methylation and decreased the expression of the gene to a similar extent as that observed in WAT from HFD-treated mice (Supplementary Figure S5A and B). Medium supplementation with 0.25 mM oleate did not elicit any significant effect.

Reversibility of HFD effect on *Hoxa5* function

Current evidence indicates that, once established, epigenetic modifications may be persistent.³⁷ We therefore sought to assess the stability of HFD-induced changes in promoter methylation and expression of *Hoxa5*. To this end, we have prolonged the nutritional intervention in animals exposed to HFD by returning them to a STD for a further 2-month period, followed by re-assessment of the metabolic phenotype. This diet change was accompanied by a 50% reduction in the excess weight caused by the previous HFD regimen ($P < 0.01$; Figure 4a). Fasting plasma glucose levels and IP glucose tolerance test were also significantly improved, indicative of improved glucose tolerance (Figures 4b and c). Importantly, *Hoxa5*-associated DMR featured an almost twofold decreased global methylation (Figure 5a). This effect was accompanied by an almost complete rescue of *Hoxa5* mRNA expression in the adipose tissue (Figure 5b).

Expression of *Hoxa5* is modulated during *in vitro* adipogenesis

In HFD-fed mice, *Hoxa5* expression was downregulated in isolated adipocytes but remained unchanged in stromal vascular fraction cells (Supplementary Figure S6A). To investigate the role of *Hoxa5* in WAT biology, we first evaluated *Hoxa5* expression during adipogenesis, and found that *Hoxa5* mRNA was induced in parallel with differentiation in 3T3-L1 preadipocytes (Supplementary Figure S6B). Consistently, the expression of *Hoxa5* mRNA was higher in the adipocyte fraction than in WAT stromal vascular fraction from mice maintained under standard chow diet (Supplementary Figure S6A).

3T3-L1 cells were subsequently transfected with *Hoxa5*-specific siRNA and then induced to differentiate into mature adipocytes (Supplementary Figure S6C). Oil Red O staining revealed a decrease in lipid accumulation in the *Hoxa5*-siRNA treated compared with control cells (Figure 5c). In parallel, the expression of the adipogenic markers *Pparγ2* and *C/ebpα* was reduced in *Hoxa5*-siRNA-treated cells (Figure 5d), suggesting that, at least in the 3T3-L1 cells, *Hoxa5* is important for adipocyte differentiation.

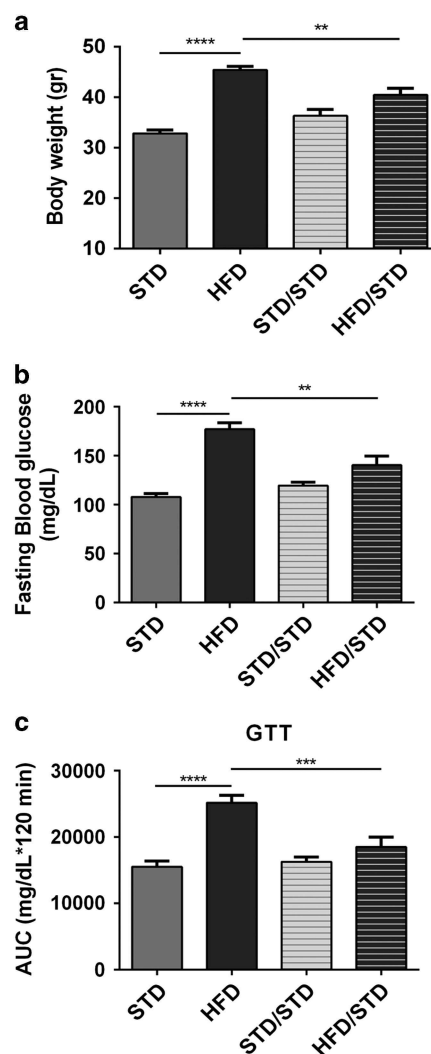


Figure 4. Metabolic parameters of HFD-treated mice upon STD rescue. Mice were either maintained under STD for 7 months (STD/STD) or returned (and maintained for two further months) to a STD after 5-month HFD treatment. Animals maintained under STD or HFD for 5 months (respectively, STD, HFD) are also shown for comparison. (a) Body weight; (b) fasting blood glucose; (c) glucose AUC during GTT. Data are means \pm s.e.m. ($n = 8$ for STD; $n = 8$ for HFD; $n = 8$ for STD/STD; $n = 8$ for HFD/STD). ** $P < 0.01$ *** $P < 0.001$, **** $P < 0.0001$. STD/STD mice maintained on STD diet through the entire protocol; HFD/STD, HFD-treated mice returned to STD; AUC, area under the curve; GTT, glucose tolerance test.

DISCUSSION

We have adopted MeDIP-seq^{25,31} analysis to directly test whether long-term HFD exposure affects the DNA methylation profile of the mouse adipose tissue and to identify the consequences of these changes. We have shown a greater number of hypermethylated compared with hypomethylated regions in the gene elements of the HFD-exposed animals indicating that, in association with obesity, this nutritional regimen induces increased DNA methylation in this part of the genome. Consistent with our finding, human obesity has been shown to be associated with gene element hypermethylation in the skeletal muscle.³⁸ In addition, very recent analysis of global DNA methylation profiles of adipose tissue from severely obese individuals showed increased methylation in the gene bodies and 3' UTRs compared with the same subjects examined upon bariatric surgery and weight loss.³⁹

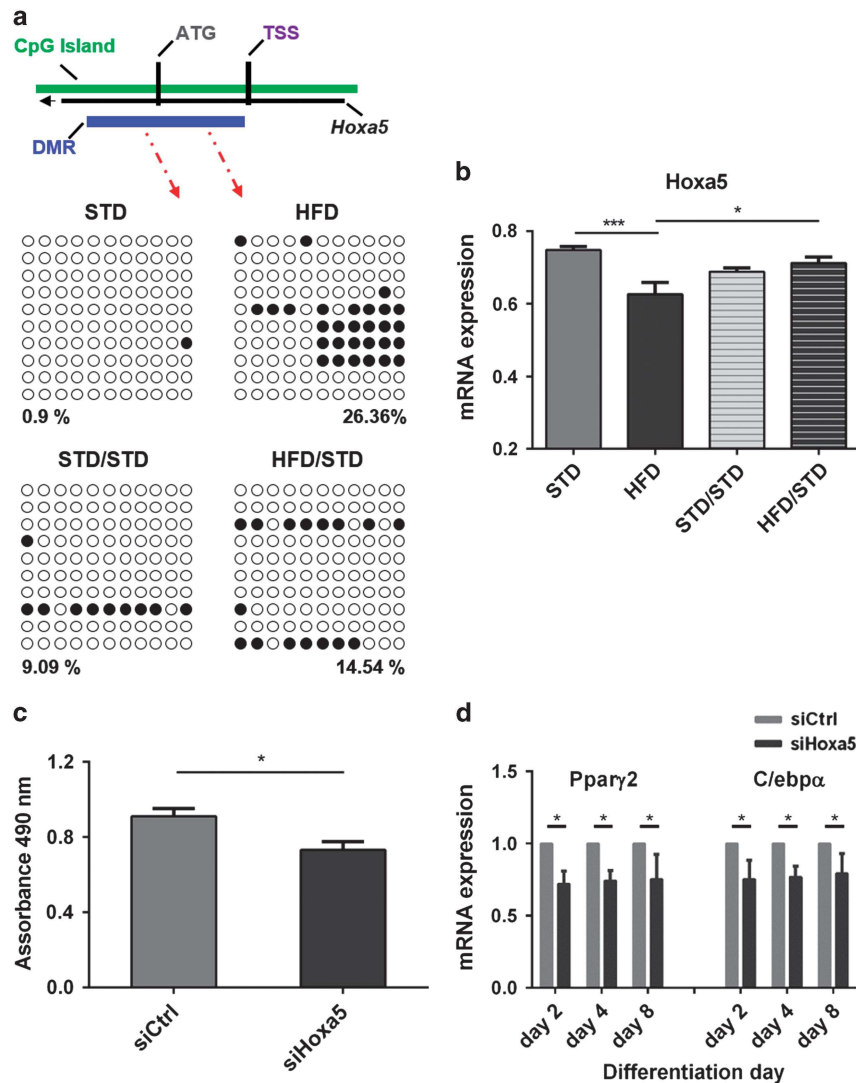


Figure 5. *Hoxa5* DMR methylation status and mRNA levels after STD rescue and the effect of *Hoxa5* silencing on adipogenesis *in vitro*. (a) Graphic representation of bisulphite sequencing of the *Hoxa5*-DMR in WAT from animals maintained under HFD or returned to a standard chow diet (STD). Each horizontal row represents a single clone; the methylation percentages of 10 individual clones are indicated, with unmethylated (○) and methylated (●) CpG sites. The data shown are representative of three mice per group. (b) qRT-PCR analysis of mRNA expression levels of WAT *Hoxa5* after returning the HFD mice to STD. Data are means \pm s.e.m. ($n = 8$ for STD; $n = 8$ for HFD; $n = 8$ for STD/STD; $n = 8$ for HFD/STD). * $P < 0.05$ *** $P < 0.001$. (c) Effect of *Hoxa5* knockdown on the extent of adipocyte differentiation was assessed by Oil Red O staining of intracellular triglyceride, and measuring the extract's absorbance at 490 nm. (d) qRT-PCR analysis of mRNA expression levels of *Pparγ2* and *C/ebpα* in 3T3-L1 treated with *Hoxa5*-specific siRNA and controls, at different time point during differentiation. All data are represented as means \pm s.e.m. of triplicates. * $P < 0.05$.

Maunakea and co-workers^{40,41} have recently reported that, in mammals, methylation occurring in the gene-associated regions mainly involve gene bodies rather than promoter 5' CGI, as $< 3\%$ of promoter-associated CGI are methylated. Similarly, our MeDIP-seq analysis revealed that most methylated sites identified in the mouse adipose tissue falls within the gene bodies, while methylation peaks at the 5'-UTR and gene promoter regions only account for a small fraction of the total number of the genome-wide methylated regions. Our data further revealed that only a small proportion of methylated CGI undergo methylation changes in response to HFD exposure, suggesting that CGI methylation is specifically affected by the nutritional intervention. In addition, despite the important role in gene regulation of the CGI shores and shelves,⁴² our study did not reveal any significant difference in the methylation of these regions in response to HFD, indicating that CGI, rather than their surrounding regions, are involved in mediating the impact of the diet on genome plasticity.

At variance from the gene-associated elements, repeated elements, particularly the *LTR* and *LINE* families, are hypomethylated in the HFD mice. Interestingly, in mice, *LTR* hypomethylation is responsible for the agouti phenotype,⁴³ while in humans, *LINE* hypomethylation in the visceral adipose tissue is associated with increased risk of metabolic syndrome in the presence of obesity.⁴⁴ All together, these findings underline the potential importance of these repetitive elements in determining pathological traits in humans as well as in mouse models.

The level and pattern of DNA methylation are regulated by both DNA methyltransferases (DNMT1, DNMT3A and DNMT3B) and demethylating proteins.⁴⁵ In addition, the effects of DNA methylation on chromatin and gene expression are largely mediated by methylated DNA reader proteins, including Methyl-CpG-binding domain protein 3 (*Mbd3* (ref. 46)). In this study, we report that the increased methylation of several genomic regions in adipose tissue of HFD-exposed mice is accompanied by the

upregulation of *MBD3* and *Dnmt3a*. It is possible that a causal relationship exists between this increased *MBD3* and *Dnmt3a* expression and the observed hypermethylation at specific genes/ gene-associated elements occurring in mice in response to HFD treatment. It is equally possible that the enhanced *MBD3* and *Dnmt3a* function impair the DNA demethylation machinery which is, in turn, responsible for the hypermethylation revealed in the HFD mice. Both mechanisms may also simultaneously occur. Interestingly, however, recent studies by Kohno and co-workers⁴⁷ have provided evidence for an important role of *Dnmt3a* in linking environmental determinants to altered energy homeostasis. Independent investigations have further identified evidence that this methylase is involved both in the development of obesity and in the obesity-related inflammation caused by HFD exposure.⁴⁸ Demethylation events also seemed to affect several genomic regions in the HFD-treated mice. The impact of these changes is presently under investigation in the laboratory, as available evidence indicates that they may well have effects on cell phenotype.⁴⁹

Investigating the functional consequences of the genome-wide changes in DNA methylation accompanying HFD exposure led us to recognize that most DMG that we have identified encode for transcription factors. Interestingly, the class I Homeobox family of transcription factors (*Hox* genes³⁵) revealed a very significant DMG enrichment in mice treated with HFD. In these same mice, a perturbation in the methylation of genes included into the *Ppar* signaling, *PI3K-AKT* and *insulin resistance* pathways was also detected. However, different considerations led us to focus our attention on the *Hox* genes in the context of the present work. First, besides the well-described role in controlling tissue regional development,³⁵ increasing evidence indicates that *Hox* genes are highly expressed in the adipose tissue³⁵ and have an active role in controlling adipocyte functions, including differentiation, and body fat distribution.^{50,51} Second, human studies further revealed that different members of the *HOX* subfamily are upregulated upon the severe weight loss following bariatric surgery, indicating that they respond to changes in body fat mass.^{39,52} Third, current evidence indicates epigenetic control of *Hox* genes during neurogenesis, development and disease.⁵³ Thus, the contribution of diet-induced epigenetic modifications to the control of *Hox* gene function in the adipose tissue deserved to be clarified. Indeed, an aberrant methylation of transcription factor promoters may potentially trigger a completely distinct transcriptional program in the hit tissues, producing a broad spectrum of downstream transcriptional events.

In this work, we have shown that long-term HFD exposure simultaneously changes methylation and expression of several *Hox* genes. Among these genes, *Hoxa5* exhibited the more robust repression in response to diet-induced hypermethylation. The transcriptional repression accompanying the epigenetic dysregulation of *Hoxa5* may have been, at least in part, caused by the saturated fat enrichment of the diet rather than representing a consequence of obesity, as it can be mimicked by exposing 3T3-L1 adipocytes to palmitate. It remains possible, however, that obesity *per se* or specific obesity-associated traits further contribute to *Hoxa5* dysregulation.

The downregulation of *Hoxa5* expression may contribute to the adipose tissue functional changes and remodeling that accompany weight gain determined by HFD exposure. Indeed, *HOXA5* expression increases during differentiation of human primary adipocytes and is differentially regulated in various adipose tissue districts.^{54,55} Consistently, we report that the expression of *Hoxa5* is modulated during *in vitro* adipogenesis in 3T3-L1 and its mRNA levels were higher in the adipocyte fraction than in the stromal vascular fraction of WAT from lean mice. In addition, *Hoxa5* silencing was accompanied by an impaired differentiation, paralleled by an altered adipogenic gene expression and decreased lipid accumulation. These findings, and the crucial role

of the *Hox* genes in developmental processes, highlight the potential role of *Hoxa5* as regulator of differentiation and/or commitment of adipogenic precursor cells.

Previous studies reported that *Hoxa5* inhibits angiogenesis,⁵⁶ while angiogenesis inhibitors improve obesity in animal models.⁵¹ Blood vessels not only supply nutrients and oxygen to individual adipose cells, they also serve as a cellular reservoir to provide adipose precursor and stem cells that control adipose tissue mass and function.⁵⁷ It is possible therefore that HFD-induced downregulation of *Hoxa5* negatively affects recruitment of new adipose cell precursors or contribute to the adipose cell dysfunction that often accompany adipose tissue expansion in response to caloric excess.

HFD-exposed mice returned to a standard chow diet for a further 2-month period underwent simultaneous weight loss and almost complete rescue of *Hoxa5* mRNA levels. Importantly, *Hoxa5* methylation also returned to levels comparable with control animals fed the standard chow diet for an identical period of time. This finding supported the role of diet-induced *Hoxa5* methylation in controlling mRNA expression of this gene. Similar to the HFD-exposed mice, obese human individuals achieving profound weight loss after bariatric surgery treatment also revealed improved *HOXA5* expression in adipose tissue.⁵² Whether quantification of *Hoxa5* expression can be exploited to assess response to caloric restriction in animals and in humans, is presently being investigated in the laboratory.

In conclusion, we have used MeDIP-seq analysis to verify whether the exposure to HFD modifies the DNA methylation profile in mouse adipose tissue and obtain indications on the consequence of these changes on adipocyte function. Our work reveals that the level of *Hoxa5* mRNA expression, whose function is implicated in fat tissue remodeling in response to changes in body fat mass, is repressed in association with the methylation changes caused by the nutritional intervention. Thus, environmental cues may generate adipose tissue dysfunction by inducing epigenetic modifications. Rescue of *Hoxa5* methylation and function in response to standard chow diet indicates that its expression may represent a potential tool to quantify obesity response to nutritional intervention.

CONFLICT OF INTEREST

The authors declare no conflict of interest.

ACKNOWLEDGEMENTS

LP is the recipient of the EFSD/Lilly Research Fellowship 2015. This work has been supported, in part, by the European Foundation for the Study of Diabetes (EFSD), by the Ministero dell'Università e della Ricerca Scientifica (grants PRIN and FIRB-MERIT, and PON 01_02460) and by the Società Italiana di Diabetologia (SID-FO.DI.RI). This work was also supported by the P.O.R. Campania FSE 2007-2013, Project CREMe.

REFERENCES

- Boonchaya-anant P, Apovian CM. Metabolically healthy obesity--does it exist? *Curr Atheroscler Rep* 2014; **16**: 441.
- Bray GA. Medical consequences of obesity. *J Clin Endocrinol Metab* 2004; **89**: 2583-2589.
- Bays H. Central obesity as a clinical marker of adiposopathy; increased visceral adiposity as a surrogate marker for global fat dysfunction. *Curr Opin Endocrinol Diabetes Obes* 2014; **21**: 345-351.
- Walker GE, Marzullo P, Ricotti R, Bona G, Prodam F. The pathophysiology of abdominal adipose tissue depots in health and disease. *Horm Mol Biol Clin Invest* 2014; **19**: 57-74.
- Yazdi FT, Clee SM, Meyre D. Obesity genetics in mouse and human: back and forth, and back again. *PeerJ* 2015; **3**: e856.
- Apalasamy YD, Mohamed Z. Obesity and genomics: role of technology in unraveling the complex genetic architecture of obesity. *Hum Genet* 2015; **134**: 361-374.

- 7 Ng SF, Lin RC, Laybutt DR, Barres R, Owens JA, Morris MJ. Chronic high-fat diet in fathers programs β -cell dysfunction in female rat offspring. *Nature* 2010; **467**: 963–966.
- 8 Dunn GA, Bale TL. Maternal high-fat diet effects on third-generation female body size via the paternal lineage. *Endocrinology* 2011; **152**: 2228–2236.
- 9 Raciti GA, Nigro C, Longo M, Parrillo L, Miele C, Formisano P *et al*. Personalized medicine and type 2 diabetes: lesson from epigenetics. *Epigenomics* 2014; **6**: 229–238.
- 10 Mirra P, Raciti GA, Nigro C, Fiory F, D'Esposito V, Formisano P *et al*. Circulating miRNAs as intercellular messengers, potential biomarkers and therapeutic targets for Type 2 diabetes. *Epigenomics* 2015; **7**: 653–667.
- 11 Godfrey KM, Sheppard A, Gluckman PD, Lillycrop KA, Burdge GC, McLean C *et al*. Epigenetic gene promoter methylation at birth is associated with child's later adiposity. *Diabetes* 2011; **60**: 1528–1534.
- 12 Gluckman PD. Epigenetics and metabolism in 2011: Epigenetics, the life-course and metabolic disease. *Nat Rev Endocrinol* 2011; **8**: 74–76.
- 13 Gerken T, Girard CA, Tung YC, Webby CJ, Saudek V *et al*. The obesity-associated FTO gene encodes a 2-oxoglutarate-dependent nucleic acid demethylase. *Science* 2007; **318**: 1469–1472.
- 14 Rodríguez-Gallego E, Guirro M, Riera-Borrull M, Hernández-Aguilera A, Mariné-Casadó R *et al*. Mapping of the circulating metabolome reveals α -ketoglutarate as a predictor of morbid obesity-associated non-alcoholic fatty liver disease. *Int J Obes (Lond)* 2015; **39**: 279–287.
- 15 Toperoff G, Aran D, Kark JD, Rosenberg M, Dubnikov T, Nissan B *et al*. Genome-wide survey reveals predisposing diabetes type 2-related DNA methylation variations in human peripheral blood. *Hum Mol Genet* 2012; **21**: 371–383.
- 16 Mikeska T, Craig JM. DNA methylation biomarkers: cancer and beyond. *Genes (Basel)* 2014; **5**: 821–864.
- 17 Volkmar M, Dedeurwaerder S, Cunha DA, Ndlovu MN, Defrance M, Deplus R *et al*. DNA methylation profiling identifies epigenetic dysregulation in pancreatic islets from type 2 diabetic patients. *EMBO J* 2012; **31**: 1405–1426.
- 18 Miele C, Raciti GA, Cassese A, Romano C, Giacco F, Oriente F *et al*. PED/PEA-15 regulates glucose-induced insulin secretion by restraining potassium channel expression in pancreatic beta-cells. *Diabetes* 2007; **56**: 622–633.
- 19 Li Q, Li N, Hu X, Li J, Du Z, Chen L *et al*. Genome-wide mapping of DNA methylation in chicken. *PLoS One* 2011; **6**: e19428.
- 20 Li H, Durbin R. Fast and accurate short read alignment with Burrows-Wheeler transform. *Bioinformatics* 2009; **25**: 1754–1760.
- 21 Chavez L, Jozefczuk J, Grimm C, Dietrich J, Timmermann B, Lehrach H *et al*. Computational analysis of genome-wide DNA methylation during the differentiation of human embryonic stem cells along the endodermal lineage. *Genome Res* 2010; **20**: 1441–1450.
- 22 Smallwood SA, Tomizawa S, Krueger F, Ruf N, Carli N, Segonds-Pichon A *et al*. Dynamic CpG island methylation landscape in oocytes and preimplantation embryos. *Nat Genet* 2011; **43**: 811–814.
- 23 Zhang Y, Liu T, Meyer CA, Eeckhoutte J, Johnson DS, Bernstein BE *et al*. Model-based analysis of ChIP-Seq (MACS). *Genome Biol* 2008; **9**: R137.
- 24 Li LC, Dahiya R. MethPrimer: designing primers for methylation PCRs. *Bioinformatics* 2002; **18**: 1427–1431.
- 25 Weber M, Davies JJ, Wittig D, Oakeley EJ, Haase M, Lam WL *et al*. Chromosome-wide and promoter-specific analyses identify sites of differential DNA methylation in normal and transformed human cells. *Nat Genet* 2005; **37**: 853–862.
- 26 Fiory F, Parrillo L, Raciti GA, Zatterale F, Nigro C, Mirra P *et al*. PED/PEA-15 inhibits hydrogen peroxide-induced apoptosis in Ins-1E pancreatic beta-cells via PLD-1. *PLoS One* 2014; **9**: e113655.
- 27 Kim JH, Dhanasekaran SM, Prensner JR, Cao X, Robinson D, Kalyana-Sundaram S *et al*. Deep sequencing reveals distinct patterns of DNA methylation in prostate cancer. *Genome Res* 2011; **21**: 1028–1041.
- 28 Bezy O, Elabd C, Cochet O, Petersen RK, Kristiansen K, Dani C *et al*. Delta-interacting protein A, a new inhibitory partner of CCAAT/enhancer-binding protein beta, implicated in adipocyte differentiation. *J Biol Chem* 2005; **280**: 11432–11438.
- 29 Kim AY, Park YJ, Pan X, Shin KC, Kwak SH, Bassas AF *et al*. Obesity-induced DNA hypermethylation of the adiponectin gene mediates insulin resistance. *Nat Commun* 2015; **6**: 7585.
- 30 Gracia A, Elcoroaristizabal X, Fernández-Quintela A, Miranda J, Bedia NG *et al*. Fatty acid synthase methylation levels in adipose tissue: effects of an obesogenic diet and phenol compounds. *Genes Nutr* 2014; **9**: 411.
- 31 Clark SJ, Harrison J, Frommer M. CpNpG methylation in mammalian cells. *Nat Genet* 1995; **10**: 20–27.
- 32 Barrès R, Osler ME, Yan J, Rune A, Fritz T, Caidahl K *et al*. Non-CpG methylation of the PGC-1 α promoter through DNMT3B controls mitochondrial density. *Cell Metab* 2009; **10**: 189–198.
- 33 Robertson KD, Keyomarsi K, Gonzales FA, Velicescu M, Jones PA. Differential mRNA expression of the human DNA methyltransferases (DNMTs) 1, 3a and 3b during the G0/G1 to S phase transition in normal and tumor cells. *Nucleic Acids Res* 2000; **28**: 2108–2113.
- 34 Guibert S, Weber M. Functions of DNA methylation and hydroxymethylation in mammalian development. *Curr Top Dev Biol* 2013; **104**: 47–83.
- 35 Procino A, Cillo C. The HOX genes network in metabolic diseases. *Cell Biol Int* 2013; **37**: 1145–1148.
- 36 Smith ZD, Meissner A. DNA methylation: roles in mammalian development. *Nat Rev Genet* 2013; **14**: 204–220.
- 37 Dolinoy DC, Weidman JR, Jirtle RL. Epigenetic gene regulation: linking early developmental environment to adult disease. *Reprod Toxicol* 2007; **23**: 297–307.
- 38 Barres R, Kirchner H, Rasmussen M, Yan J, Kantor FR, Krook A *et al*. Weight loss after gastric bypass surgery in human obesity remodels promoter methylation. *Cell Rep* 2013; **3**: 1020–1027.
- 39 Benton MC, Johnstone A, Eccles D, Harmon B, Hayes MT, Lea RA *et al*. An analysis of DNA methylation in human adipose tissue reveals differential modification of obesity genes before and after gastric bypass and weight loss. *Genome Biol* 2015; **16**: 8.
- 40 Maunakea AK, Nagarajan RP, Bilenky M, Ballinger TJ, D'Souza C, Fouse SD *et al*. Conserved role of intragenic DNA methylation in regulating alternative promoters. *Nature* 2010; **466**: 253–257.
- 41 Zhang P, Zhao M, Liang G, Yin G, Huang D, Su F *et al*. Whole-genome DNA methylation in skin lesions from patients with psoriasis vulgaris. *J Autoimmun* 2013; **41**: 17–24.
- 42 Irizarry RA, Ladd-Acosta C, Wen B, Wu Z, Montano C, Onyango P *et al*. The human colon cancer methylome shows similar hypo- and hypermethylation at conserved tissue-specific CpG island shores. *Nat Genet* 2009; **41**: 178–186.
- 43 Jaenisch R, Bird A. Epigenetic regulation of gene expression: how the genome integrates intrinsic and environmental signals. *Nat Genet* 2003; **33**: 245–254.
- 44 Turcot V, Tchernof A, Deshaies Y, Pérusse L, Bélisle A, Marceau S *et al*. LINE-1 methylation in visceral adipose tissue of severely obese individuals is associated with metabolic syndrome status and related phenotypes. *Clin Epigenetics* 2012; **4**: 10.
- 45 Hamidi T, Singh AK, Chen T. Genetic alterations of DNA methylation machinery in human diseases. *Epigenomics* 2015; **7**: 247–265.
- 46 Du Q, Luu PL, Stizaker C, Clark SJ. Methyl-CpG-binding domain proteins: readers of the epigenome. *Epigenomics* 2015; **30**: 1–23.
- 47 Kohno D, Lee S, Harper MJ, Kim KW, Sone H, Sasaki T *et al*. Dnmt3a in Sim1 neurons is necessary for normal energy homeostasis. *J Neurosci* 2014; **34**: 15288–15296.
- 48 Kamei Y, Suganami T, Ehara T, Kanai S, Hayashi K, Yamamoto Y *et al*. Increased expression of DNA methyltransferase 3a in obese adipose tissue: studies with transgenic mice. *Obesity (Silver Spring)* 2010; **18**: 314–321.
- 49 Choi SW, Friso S. Epigenetics: a new bridge between nutrition and health. *Adv Nutr* 2010; **1**: 8–16.
- 50 Cowherd RM, Lyle RE, Miller CP, McGehee RE Jr. Developmental profile of homeobox gene expression during 3T3-L1 adipogenesis. *Biochem Biophys Res Commun* 1997; **237**: 470–475.
- 51 Charlier C, Segers K, Karim L, Shay T, Gyapay G, Cockett N *et al*. The callipyge mutation enhances the expression of coregulated imprinted genes in cis without affecting their imprinting status. *Nat Genet* 2001; **27**: 367–369.
- 52 Dankel SN, Fadnes DJ, Stavrum AK, Stansberg C, Holdhus R, Hoang T *et al*. Switch from stress response to homeobox transcription factors in adipose tissue after profound fat loss. *PLoS One* 2010; **5**: e11033.
- 53 Barber BA, Rastegar M. Epigenetic control of Hox genes during neurogenesis, development, and disease. *Ann Anat* 2010; **192**: 261–274.
- 54 Karastergiou K, Fried SK, Xie H, Lee MJ, Divoux A, Rosencrantz MA *et al*. Distinct developmental signatures of human abdominal and gluteal subcutaneous adipose tissue depots. *J Clin Endocrinol Metab* 2013; **98**: 362–371.
- 55 Gesta S, Blüher M, Yamamoto Y, Norris AW, Berndt J, Kralisch S *et al*. Evidence for a role of developmental genes in the origin of obesity and body fat distribution. *Proc Natl Acad Sci USA* 2006; **103**: 6676–6681.
- 56 Dunn J, Qiu H, Kim S, Jjingo D, Hoffman R, Kim CW *et al*. Flow-dependent epigenetic DNA methylation regulates endothelial gene expression and atherosclerosis. *J Clin Invest* 2014; **124**: 3187–3199.
- 57 Cao Y. Angiogenesis and vascular functions in modulation of obesity, adipose metabolism, and insulin sensitivity. *Cell Metab* 2013; **18**: 478–489.

Supplementary Information accompanies this paper on International Journal of Obesity website (<http://www.nature.com/ijo>)